BIOCHEMICAL CHARACTERIZATION OF AN ASPARTIC PROTEASE INHIBITOR FROM *BACILLUS LICHENIFORMIS:* INTERACTIONS WITH HYDROLYTIC ENZYMES

Thesis submitted to University of Pune

For the degree of

DOCTOR OF PHILOSOPHY

IN

BIOTECHNOLOGY

By

Ajit Kumar

Division of Biochemical Sciences

National Chemical Laboratory

Pune – 411008

India

March 2007

In Fond Memories of My Father…

TABLE OF CONTENTS

ACKNOWLEDGEMENTS

I take this opportunity to express my heart-felt gratitude to my guide, ***Dr. (Mrs.) Mala Rao*** *for her able guidance, unceasing encouragement and sustained interest throughout the course of my work. I consider myself extremely fortunate to have her as my guide. Her integral view on research and her mission for providing 'only high-quality work and not less' has made a deep impression on me. I owe her lots of gratitude for having me shown this right attitude towards research. Her continued interest and involvement in my work and concern for my welfare have greatly motivated me. I am indebted to her for the valuable suggestions, hints and critical comments in all the time of research and writing of this thesis.*

I deeply acknowledge the encouragement and support of ***Dr. Vasanti Deshpande*** *throughout my work. I profoundly thank* ***Prof. Constantinos E. Vorgias*** *(Division of Biochemistry and Molecular Biology, Athens University, Athens, Greece) for providing ChitinaseA during my research. Thanks are due to* ***Dr. M.V. Deshpande and Mahesh Kulye*** *for their help in insect related work. I am highly thankful to* ***Dr. Sushma Gaikwad*** *for her help during the fluorescence spectroscopy experiments and amino acid analysis of the peptide.* ***Dr. Saurav Paul*** *and* ***Akhilesh Tanwar*** *(Physical Chemistry Division) are gratefully acknowledged for their help in structural modeling studies.*

My seniors, ***Drs. Sudeep, CV and Jui*** *have in some or the other way helped in tuning my practical hand in the initial stages of my research work. Thank are due to them too. I am thankful to my lab mates,* ***Aarohi, Anamika, Sharmili, Dr. Rachna, Neha, Anish, Vinod, Gyan, Nitin*** *and* ***Nilesh*** *for maintaining a lively environment in the laboratory during the course of my work.*

I acknowledge ***Ramakantji*** *and* ***Trehan*** *who were always there whenever required.* ***Indira Mohandasan and Mari*** *are duly acknowledged for their support throughout my tenure at N.C.L.*

I am also thankful to my friends ***Atul Thakur, Atul Farenze, Ambrish, Anil, Chetan, Chandrashekar, Feroz, Harish, JP, Manish(s), Nishant, Priyanka, Rohtas, Sagar, Shabab, Shadab, Sajid, Shashidhar, Satya, Sushim, Sameer, Suresh, Santosh, Swati, Kavita, Anil Sharma, Hardev, Kamal, Dharmander, Manas, Jitu Panday,***

Sudheer *and* ***Jitu Cheema*** *for their charming company. I would also like to thank my friends* ***Jaswinder, Jaswant, Sukhwinder, Jarnail, Rajesh Nagpal, Mukesh, Manmohan, Ajay, Bansi, Ramavtar*** *and* ***Vinod.***

Special thanks go to ***Madan Lal*** *who has a great impact in my life. I have learnt a lot from him and cherish the lighter moments we shared. I am grateful to my neighbors in the village who have helped me a lot during my course of study.*

I also express my sincere appreciation to my ***father In-law*** *and Brother In-laws (****Anil, Sunil, Pankaj****) for their efficient and timely Help.*

Words fall short to express my feelings towards my uncles ***Chajju Ram****,* ***Subhash****,* ***Naresh, Ramniwas*** *and* ***Master Mani Ram****. They have made an outstanding contribution towards my outlook to life. They have been always there with me during my ups and downs of life. They always encouraged me and also appreciated my study efforts throughout.*

I am indeed thankful to my mother and my brother ***Rajender,*** *who always kept me tension free and encouraged me to complete my Doctorate.*

I owe my deepest gratitude towards my better half for her eternal support and understanding of my goals and aspirations. Her infallible love and support has always been my strength. Her patience and sacrifice will remain my inspiration throughout my life. Without her help, I would not have been able to complete much of what I have done and become who I am. It would be ungrateful on my part if I thank ***Saroj*** *in these few words. I am thankful to my son* ***Tejasvi*** *for giving me happiness during the last two years of my studies.*

I gratefully acknowledge ***Council of Scientific and Industrial Research****, for providing me financial support and* ***Director, NCL*** *to allow me to carryout my research in this esteemed laboratory.*

Ajit Kumar

CERTIFICATE

Certified that the work incorporated in the thesis entitled: "**Biochemical Characterization of an Aspartic Protease Inhibitor from *Bacillus licheniformis*: Interactions with Hydrolytic Enzymes**", submitted by Mr. Ajit Kumar, for the Degree of ***Doctor of Philosophy***, was carried out by the candidate under my supervision at Division of Biochemical Sciences, National Chemical Laboratory, Pune - 411 008, Maharashtra, India. Material obtained from other sources is duly acknowledged in the thesis.

Dr. Mala Rao
(Research Supervisor)

DECLARATION BY RESEARCH SCHOLAR

I hereby declare that the thesis entitled "**Biochemical Characterization of an Aspartic Protease Inhibitor from *Bacillus licheniformis*: Interactions with Hydrolytic Enzymes**", submitted for the Degree of ***Doctor of Philosophy*** to the University of Pune, has been carried out by me at Division of Biochemical Sciences, National Chemical Laboratory, Pune - 411 008, Maharashtra, India, under the supervision of Dr. Mala Rao. The work is original and has not been submitted in part or full by me for any other degree or diploma to any other University.

Ajit Kumar
(Research Scholar)

ABBREVIATIONS

°C	Degree Celsius
µl	Micro liter
Å	Angstrom
AccQ Fluor Reagent	6-amino quinolyl-N-hydroxysuccinimide carbamate
*Af*ChiB1	Aspergillus fumigatus
AHMHA	(S)-3- amino-5-methylhexane-2-one instead of the C-terminal (3S, 4S)-4-amino-3-hydroxy-6-methylheptanoic acid
AP	Aspartic Protease
APD	N-acetyl-L-phenylalanyl-L-3, 5-diiodotyrosine
API	Aspartic Protease Inhibitor
ATBI	Alkalo-Thermoplic Bacillus Inhibitor
BBTI	Bowman-Birk trypsin inhibitor
BLAST	Basic Local Alignment Search Tool
BSA	bovine serum albumin
CD	Circular dichroism
CH_3CN	acetonitrile
*Ci*Chi	Coccidioides immitis chitinase
Da	Dalton
DANLME	diazoacetylnorleucine methyl ester
DMAB	p-dimethyl amino benzaldehyde
DNA	Deoxyribonucleic acid
dNTP	Deoxy nucleotide triphosphate
E	Eenzyme
E-64	L-trans-epoxysuccinyl-leucyl-amido (4-guanidino)-butane)
EC	enzymes classification
EDTA	Ethylene diamine tetra acetic acid
EI*	Enzyme inhibitor complex
EPNE	1, 2-epox-3-(p-nitrophenoxy) propane
Et	Total enzyme
g	Gram
GlcNAc	N-acetylglucoseamine
h	hours
HCHT	human chitotriosidase
HIV	human immunodeficiency virus
I	Inhibitor

It	Total inhibitor
kDa	Kilo Dalton
Ki	Inhibition constant
K_m	Michaelis Menton Constant
L	liter
LB	Luria Bertani
M	Molar
min	Minutes
ml	Milliliter
mM	Milli molar
NCBI	National Center for Biotechnology Information
nm	Nanometers
OD	Optical density
OPTA	o-phthalaldehyde
PAGE	Polyacrylamide gel electrophoresis
PCR	Polymerase Chain Reaction
pHMB	p-hydroxymercutybenzoic acid
pI	Isoelectric point
p-NP-$(glcNAc)_2$	p-nitrophenyl-N,N'-Diacetyl-β-chitobioside
PxAP	Plutella xylostella aspartic protease
RBV	Ramazol Brilliant Violet
rDNA	Ribosomal Deoxyribonucleic acid
REA	Relative Enzyme Activity
RNAase	Ribonuclease
Rp-HPLC	Reverse phase high performance liquid chromatography
rpm	Revolutions per minute
SDS	Sodium dodecyl sulphate
SDS-PAGE	Sodium dodecyl sulfate polyacrylamide gel electrophoresis
*Sm*ChiA	Saccharomyces cerevisiae chitinaseA
*Sm*ChiB	Saccharomyces cerevisiae chitinaseB
TBE	Tris Borate EDTA
TCA	trichloric acid
TE	Tris-Ethylene diamine tetra acetic acid
TFA	Trifluoroacetate
TLCK	Na-p-tosyl-L-lysine chloromethyl ketone
TPCK	N-tosyl-L-phenyl alanine chloromethyl ketone
V_{max}	Maximum velocity

ABSTRACT

Hydrolytic enzymes (Hydrolases) are the enzymes that catalyze the hydrolysis of various chemical bonds. They are classified as EC 3 in the EC number classification of enzymes. Hydrolases can be further classified into several subclasses, based upon the bonds they act upon. Peptide hydrolases (Peptidases) are the enzymes that catalyze the peptide bonds and are recommended to be further divided into "exopeptidases" that act only near a terminus of a polypeptide chain and "endopeptidases" that act internally in polypeptide chains. The endopeptidases are divided into sub-subclasses on the basis of catalytic mechanism, and specificity is used only to identify individual enzymes within the groups. The sub-subclasses of endopeptidases are aspartic proteases (EC 3.4.23), serine proteases (EC 3.4.21), cysteine proteases (EC 3.4.22), metallo proteases (EC 3.4.24) and threonine proteases (EC 3.4.25).

The aspartic proteases constitute one of the primary classes of proteolytic enzymes utilizing two aspartic acid residues in the active site for the catalytic activity with the direct participation of a water molecule. The study of the kinetic properties of this class of enzymes frequently has been motivated by their involvement in physiological and pathological processes of human, thus their effective regulators, i.e., aspartic protease inhibitors, are tremendously essential for physiological regulations. The enzymatic properties of pepsin, plasma renin, HIV1 protease, plasmepsin, lysosomal cathepsins and chymosins and their significant role in human diseases like Alzheimer's disease, malaria, and candidal infections have evoked considerable interest for investigating the role of inhibitors. Recent developments in the involvement of aspartic proteases in the life cycle of human immunodeficiency virus and in the degradation of

hemoglobin by malarial parasite have generated enormous attention to investigate the interaction between the potent inhibitors and the target enzymes.

The other very important class of hydrolytic enzymes is the Glycoside hydrolases (EC 3.2.1.). They are a group of enzymes that catalyze the hydrolysis of glycosidic linkages. Chitinases (EC 3.2.1.14) are glycoside hydrolases that catalyze the hydrolytic cleavage of β-1, 4-glucosidic linkage of chitin. It has recently been suggested that Chitinases could play an important role in human diseases such as arteriosclerosis, colorectal cancer, Gaucher disease, pneumonia and infections in immune-compromised hosts. Therefore, from the biomedical point, inhibitors of this class of enzymes will have tremendous importance in near future. A number of naturally occurring reversible Chitinase inhibitors like allosamidine have been reported. Specific inhibitors of Chitinases have been proved valuable tools not only to understand about the active site structures and mechanisms of these interesting enzymes but also in generating new therapeutic agents. Determination of the kinetic parameters of the inhibition of aspartic proteases and Chitinases will provide insights into the mechanism of the interaction between the enzyme-inhibitor complexes.

The work carried out has been structured under the following chapters.

1. General introduction

2. Biochemical characterization of an aspartic protease inhibitor from thermo tolerant *Bacillus licheniformis*: Interaction with Pepsin.

(*i)* Isolation and identification of thermo tolerant *Bacillus licheniformis*.

(ii) Purification and characterization of API from thermo tolerant *Bacillus licheniformis*.

(*iii)* Interaction of API with pepsin: Implications in the mechanism of inactivation.

3. Purification and characterization of an aspartic protease from mid gut of *Plutella xylostella*: Inactivation by API.

4. Bifunctional role of API: Structural and mechanistic insights into the inhibition of Chitinase.

5. Aspartic protease inhibitor from alkalo-thermophilic *Bacillus sp.*: In *vivo* and in *vitro* effects on cuticle moulting fluid enzymes of *Helicoverpa armigera*.

Chapter 1. General introduction

This chapter presents the literature survey of the research carried out on aspartic proteases. The study of the kinetic properties of this class of enzymes frequently has been motivated by their involvement in physiological and pathological processes of human, thus their effective regulators, i.e., aspartic protease inhibitors, are tremendously essential for physiological regulations.

Chapter 2. Biochemical characterization of an aspartic protease inhibitor from thermo tolerant *Bacillus licheniformis*: Interaction with Pepsin.

(*i)* Isolation and identification of thermo tolerant *Bacillus licheniformis*.

(ii) Purification and characterization of API from thermo tolerant *Bacillus licheniformis*.

(*iii)* Interaction of API with pepsin: Implications in the mechanism of inactivation.

(i)* Isolation and identification of thermo tolerant *Bacillus licheniformis

The microorganism was isolated in the laboratory from the fruit tomato. The culture was purified by the single colony plating technique. The strain was an aerobic, motile, gram positive, spore forming rod-shaped bacterium. On nutrient agar at 50°C, the colonies were large, irregular, sticky and pale cream colored. The organism was thermo-tolerant with a broad growth range of 28°C-50°C with optimum growth at 50°C and pH

7. The isolated organism was identified to be *Bacillus licheniformis* based on the biochemical characteristics as described in the Bergey's Manual of Determinative Bacteriology and 16S rDNA sequencing.

(ii)* Purification and characterization of API from thermo tolerant *Bacillus licheniformis

The indispensable nature of the aspartic proteases in numerous physiological functions has evoked tremendous response towards isolating new inhibitors from various resources. After extensive screening, a thermo tolerant *Bacillus licheniformis* was isolated, which produces an aspartic protease inhibitor (API). The organism produced API in the peptone beef extract complex media at 50°C and pH 7. The extracellular culture filtrate of *Bacillus licheniformis* was subjected to activated charcoal treatment, ultra filtration and gel filtration to remove the high molecular weight impurities and salts. The gel filtration fractions showing anti pepsin activity were concentrated and loaded in C-8 pre- packed column for rp-HPLC. The anti pepsin activity was associated with the peak A, having a retention time of 5.966 min and other eluted peak B with retention times 7.649, showed no inhibitory activity. Homogeneity of the active fractions was indicated by the single peak as analyzed on rp-HPLC and mass spectrometry (MALDI-TOF) showed Mr 1363 Da. Reverse zymographic SDS-gel electrophoresis showed Mr 1358 Da. The amino acid analysis experiments indicate the presence of 12 amino acid residues having a Mr of 1425 Da, which suggest peptidic nature of API. The amino acid sequence of the purified peptide was found to be Asp-Leu-Tyr-Asp-Gly-Trp-Lys-His-Glu-Ala-Glu-Cys-Ile with a pI value of 4.3. The estimated secondary structure contents from the CD analysis were 7% α-helix, 49% β-sheet, and 44% aperiodic structure. API was stable in a

broad range of pH (2-11) and temperature (37-80°C). API was stable for 2 ½ hours and 30 minutes at 90°C and 100°C respectively. A very low inhibitory activity of API was recorded against other aspartic proteases like HIV1 protease, plasmapsin II and cathapsin D. The inhibitor didn't show any inhibitory activity against other classes of the proteases like trypsin, chymotrypsin, papain and subtilisin.

(*iii)* Interaction of API with pepsin: Implications in the mechanism of inactivation

The Kinetic studies of Pepsin-API interactions reveal that API is a slow-tight binding competitive inhibitor of pepsin with the IC_{50} and K_i values 4.0 nM and (3.83 nM-5.31nM) respectively. The overall inhibition constant K_i* value is 0.107 ± 0.015 nM. The progress curves are time-dependent and consistent with slow-tight binding inhibition: E + I ⇄ (k_4, k_5) EI ⇄ (k_6, k_7) EI*. Rate constant k_6 =2.73 ± 0.32 s^{-1} reveals a fast isomerization of enzyme-inhibitor complex and very slow dissociation as proved by k_7=0.068±0.009s^{-1}. The Rate constants from the intrinsic tryptophanyl fluorescence data is in agreement with those obtained from the kinetic analysis; therefore, the induced conformational changes were correlated to the isomerization of EI to EI*. On the basis of our foregoing results, it is concluded that, concomitant with the kinetic characterization; fluorescence studies will be useful for the evaluation of inhibitor kinetic constants in the absence of enzyme turnover number and the deciphering the inhibition mechanism of aspartic proteases by slow tight binding inhibitors.

3. Purification and characterization of an aspartic protease from mid gut of *Plutella xylostella,* diamond backmoth: Inactivation by Pepstatin A and API.

An aspartic protease from *Plutella xylostella* (PxAP) was purified to homogeneity by ammonium sulphate precipitation; gel filtration and affinity chromatography with 110

fold purification. The enzyme exhibited a Mr. of 46.1 kDa on SDS-PAGE with an optimum pH and temperature of 3.4 and 37°C respectively. The enzyme hydrolyzed hemoglobin with a K_M value of 538 μM. The enzyme properties are consistent with those of aspartic proteases as it was inhibited by a universal inhibitor of aspartic proteases, pepstatin. The enzyme was also inhibited by an aspartic protease inhibitor, API, recently reported from our laboratory. The kinetic analysis of PxAP-API interaction suggested the competitive mode of inhibition with IC_{50} and K_i values of 44.0μM and 55.0 μM respectively.

Chapter 4. Bifunctional role of API: Structural and mechanistic insights into the inhibition of Chitinase.

The inhibition of 1, 4-β-poly-*N*-acetylglucosaminidase (Chitinase A) from *Serratia marcescens* by API is reported in this chapter. ChitinaseA-API kinetic interactions reveal noncompetitive, irreversible and tight binding nature of API with an IC_{50} value 710 nM and K_i value 510-920 nM. The inhibition progress curves show a two step slow tight binding inhibition mechanism where first step involves a rapid equilibrium for formation of reversible enzyme inhibitor complex (*E*I) that isomerizes to a stable complex (*E*I*) in the second step because of inhibitor induced conformational changes in ChitinaseA (ChiA) with rate constant k_6 ($8.74\pm0.1\times10^{-3}s^{-1}$). Slower dissociation rate constant k_7 ($7.3\pm0.6\times10^{-5}$ s^{-1}) for *E*I* to *E*I and overall inhibition constant K_i* (6.3-7.5 nM) indicates the tight binding nature of API. CD-spectra analysis and time dependent Tryptophanyl fluorescence quenching of ChiA incubated with incresing API concentrations indicates malicious changes in secondary and tertiary conformation of ChiA, which is correlated to the isomerization of *E*I to *E*I* and to the

irreversible conformationally locked *E*I** complex. Abolished isoindole fluorescence of *o*-phthalaldehyde (OPTA)-labeled ChiA proves that Asp1 residue of API binds to the Lysine and Histidine residues present near active site of ChiA which disrupt electronic microenvironment and hydrogen-bonding network near the active site of ChiA. For the first time, it is also shown the importance of near active site residues in ChiA and model can be applied to study other enzymes.

Chapter 5. Aspartic protease inhibitor from alkalo-thermophilic *Bacillus sp.*: In *vivo* and in *vitro* effects on cuticle moulting fluid enzymes of *Helicoverpa armigera*.

The inhibition of moulting fluid enzymes from *Helicoverpa armigera* by an aspartic protease inhibitor ATBI (Alkalo-Thermoplic Bacillus Inhibitor) is reported in the present chapter. In vivo and in vitro experiments were carried out to evaluate the effects of ATBI against the development of *H. armigera.* ATBI showed 75% proteolytic and 95% of chitinase enzyme inhibition with the IC_{50} values of 48 μM and 35 μM respectively. The inhibition studies of proteases with the help of specific protease inhibitors and ATBI suggest that one or more aspartic proteases have important roles in insect development. Also, laboratory experiments in vitro showed significant inhibition towards the growth and development of *H. armigera*. The effect of ATBI on insect metamorphosis can be correlated through the inhibition of proteases and chitinase from moulting fluid. The results provide the basis for the selection of non-host inhibitors and present an optimized combination for developing *H. armigera* resistant transgenic plants. It will be a new area of making transgenic plants targeting the insect moulting fluid enzymes.

PUBLICATIONS

1. Ajit Kumar and, Mala Rao (2006). Biochemical characterization of a low molecular weight aspartic protease inhibitor from thermo-tolerant *Bacillus licheniformis*: Kinetic interactions with Pepsin. **Biochimica et Biophysica Acta 1760, 1845–1856.**

2. Ajit Kumar and, Mala Rao (2006). A Novel Bifunctional Aspartic Protease Inhibitor Inhibits 1, 4-β-Poly-N-Acetylglucosaminidase: Conformational Alterations Responsible for Conferring Irreversibility to the Enzyme-Inhibitor Complex **(Manuscript communicated).**

3. Ajit Kumar, Mahesh Kule, Mukund Deshpande and Mala Rao (2006). In *vivo* and in *vitro* effects of an aspartic protease inhibitor on cuticle moulting fluid enzymes of *Helicoverpa armigera* **(Manuscript communicated).**

4. Ajit Kumar and, Mala Rao (2006) Biochemical Characterization of a Novel Aspartic Protease from Midgut of *Plutella xylostella,* Diamondback moth (Lepidoptera: Plutellidae): Inactivation by an Aspartic Protease Inhibitor **(Manuscript communicated).**

CONFERENCES / ABSTRACTS/ POSTERS

1. Participated and poster presented in the **XXXIII National Seminar on Crystallography** during 8-10 January, 2004 held at National Chemical Laboratory, Pune, India.

2. Participated and poster presented in the 2nd National conference of the biotechnology society of India, **Biotech 2004 challenges and opportunities** organized by the Institute of genomics and Integrative Biology, Delhi, held from 13-15 October 2004 at India International Centre, New Delhi, India.

3. Participated and poster presented in the 3rd National conference of the biotechnology society of India, **Biotech 2005 concept to commercialization** organized by the Centre for Biotechnology, Jawaharlal Nehru University, new Delhi, held from 22-24 December 2005 at the Heritage Village, Manesar, Gurgaon (NCR), India.

4. Participated in the 3rd International Symposium on **Current Trends in Drug Discovery Research (CTDDR)** organized by the Central Drug Research Institute Lucknow, India held from 17-21 February 2007 at Central Drug Research Institute, Lucknow, India.

CHAPTER 1

GENERAL INTRODUCTION

Hydrolytic enzymes (Hydrolases) catalyze the hydrolysis of a chemical bond and are classified as EC 3 in the EC number classification of enzymes. Hydrolases can be further classified into several subclasses, based upon the bonds they act upon:

EC 3.1 Acting on ester bonds

EC 3.2 Glycosylases

EC 3.3 Acting on ether bonds

EC 3.4 Acting on Peptide Bonds (Proteases)

EC 3.5 Acting on Carbon-Nitrogen Bonds, other than Peptide Bonds

EC 3.6 Acting on Acid Anhydrides

EC 3.6.3 Acting on acid anhydrides; catalyzing transmembrane movement of substances.

EC 3.7 Acting on Carbon-Carbon Bonds

EC 3.8 Acting on Halide Bonds

EC 3.9 Acting on Phosphorus-Nitrogen Bonds

EC 3.10 Acting on Sulfur-Nitrogen Bonds

EC 3.11 Acting on Carbon-Phosphorus Bonds

EC 3.12 Acting on Sulfur-Sulfur Bonds

EC 3.13 Acting on Carbon-Sulfur Bonds

The Proteases

Proteases (EC 3.4) are one of the largest and most diverse families of enzymes. They catalyze the addition of water across amide (and ester) bonds to affect cleavage using a reaction involving nucleophilic attack on the carbonyl carbon of the scissile bond. Proteases play a critical role in many physiological and pathological processes such as protein catabolism, blood coagulation, cell growth, cell migration, tissue arrangement, morphogenesis in development, inflammation, tumor growth, metastasis and activation of zymogens, release of hormones and transport of secretory proteins across membranes. Their activity, if uncontrolled, would be destructive to the cell or organism and therefore must be precisely regulated. Thus, inhibitors of such proteases are emerging with promising therapeutic uses (Shaw, 1990; Craik et al., 1995; Seife, 1997) in the treatment of diseases such as cancers (Beckett et al., 1996; Johnson et al., 1998; Yan et al., 1998), parasitic, fungal, and viral infections (Wlodawer et al., 1993; Darke and Huff, 1994; Li et

al., 1994; Becker et al., 1995; West and Fairlei, 1995; Abad-Zapatero et al., 1996; Kim et al., 1996; Love et al., 1996; Shieh, 1996; Silva et al., 1996; Brindley et al., 1997; Abad-Zapatero et al., 1998; Gibson and Hall, 1997;), inflammatory, immunological, respiratory, cardiovascular and neurodegenerative disorders (Stubbs and Bode, 1993; Bernstein et al., 1994; Tanaka et al., 1995; Hugli, 1996; Fath et al., 1998; Vassar et al., 1999). The mechanism of cleavage and the active site substituents vary widely among different proteases subtypes and provide the basis for the classification of proteases into the aspartic proteases, serine proteases, cysteine proteases and metallo proteases (Barett et al., 1998). There are a few miscellaneous proteases that do not precisely fit into the standard classification, for example, ATP-dependent proteases, which require ATP for activity (Menon and Goldberg, 1987).

I. The aspartic proteases

Aspartic proteases are a group of proteolytic enzymes of the pepsin family that share the same catalytic mechanism and usually function in acidic conditions. Aspartic proteases have been isolated and studied from a wide range of organisms such as vertebrates, plants, fungi, parasites, retroviruses and bacteria (Hill and Phylip, 1997; James et al., 1998). Thre aspartic proteases like pepsin, gastricsin, and renin documented from the human body are secretory and have well-defined physiological roles. Cathepsin D, is found ubiquitously in the lysosomes of most cells (Saftig et al., 1995), while the Cathepsin E, located within the endoplasmic reticulum/trans-Golgi network/endosomal compartments of cells (Kageyama, 1998). Aspartic proteases have been studied extensively for their structure and functional relationships and have been the topics of several reviews or monographs (Tang, 1977; Tang, 1979; Kay, 1985; James and Sielecki, 1987; Dunn, 1991; Dunn, 1992; Dunn et al., 1995; Fusek et al., 1995; Takahasi, 1995; James, 1998; Rao et al., 1998; Dunn, 2002; Fruton, 2002). Aspartic proteases are directly dependent on aspartic acid residues for their catalytic activity and represent the simplest sub-subclass of proteases comprising the three families, pepsin (A1), retro pepsin (A2) and para retroviruses such as the cauliflower mosaic virus form family A3. Crystallographic studies have shown that the enzymes of the pepsin family are homologous bilobed molecules with the active-site cleft located between the lobes, and each lobe contributes an aspartate residue of the catalytically active diad of aspartates.

These two aspartyl residues are in close geometric proximity in the active molecule and one aspartate is ionized, whereas the second one is unionized at the optimum pH range of 2 to 3 (Blundell et al., 1991; Sielicki et al., 1991). Retropepsins carry only one catalytic aspartate, and thus dimerization is required to form an active enzyme (Miller et al., 1989; Blundell et al., 1991). The nucleophilic attack is achieved by two simultaneous proton transfers, one from a water molecule to the diad of the two-carboxyl groups and a second one from the diad to the carbonyl oxygen of the substrate with the concurrent CO-NH bond cleavage. This general acid-base catalysis, which may be called a "push-pull" mechanism, leads to the formation of a noncovalent neutral tetrahedral intermediate (Holm et al., 1984; Blundell et al., 1991; Veerapandian et al., 1992; Northrop, 2001; Dunn, 2002). In family A1 of pepsin (clan AA), the catalytic Asp residues occur within the motif Asp-Xaa-Gly, in which Xaa can be Ser or Thr. Members of clan AA are all more or less strongly inhibited by pepstatin by a mechanism that is known to be similar at least for families A1 and A2 (Fitzgerald et al., 1990). Leader proteases II (family U11) and thermopsin (family U16) also are sensitive to this inhibitor. Covalently reacting inhibitors of pepsin, namely, diazoacetylnorleucine methyl ester (DANLME), 1,2-epox-3-(*p*-nitrophenoxy) propane (EPNE), and *p*-bromophenacyl bromide, have also been used as diagnostic reagents for aspartic endoproteases.

i) Pepsin family

All members of the pepsin family have been found in eukaryotes like animal digestive tract enzymes, such as pepsin and chymosin, lysosomal enzymes such as cathepsin D and enzymes involved in posttranslational processing such as renin and yeast aspartic proteases. There are also examples from protozoa (e.g., Eimeria, Plasmodium), fungi, and plants. Family A1 contains many enzymes that enter the secretory pathway, and it is probable that all the proteins are synthesized with signal peptides and propeptides. Unusually, barrier pepsin from yeast has a long C-terminal extension that can be excised without affecting enzymatic activity (Mackay et al., 1988).

ii) Retropepsin family

Retropepsin is required for processing of all three viral polyproteins, although cellular enzymes perform initial stages of envelope polyprotein cleavage. Processing occurs at a very late stage in virion assembly, usually after budding of virus particles

from the cell membrane; inactive virions containing only gag polyprotein can be formed. Processing seems to be essential for RNA dimerization within the virion, and hence for infectivity. Therefore, there have been intense research interests in the development of inhibitors of retropepsins as antiretroviral agents (Hellen and Wimmer, 1992). A subset of the retropepsins from oncoviruses and avian retroviruses are larger proteins with N-terminal domain homologous to dUTPases.

iii) Cauliflower mosaic virus proteases family

Cauliflower mosaic virus belongs to a group of plant viruses known as pararetroviruses. Although the viral genome is double-stranded DNA, it contains an open reading frame (ORF V) analogous to the pol gene of retroviruses. ORF V encodes a polyprotein, including a reverse transcriptase that is homologous to that of retroviruses and based on an Asp-Thr-Gly triplet near the N terminus, was suggested to be included as an aspartic proteases as well (Fuetterer and Hohn, 1987). The existence of an endoproteases was confirmed by mutational studies that implicated the involvement of Asp-45 in catalysis. There was also weak inhibition by pepstatin. The proteases are larger than retropepsin, however, because it contains only one Asp-Thr-Gly sequence, it is assumed to be active only as a dimer (Torruella et al., 1989). Other pararetroviruses contain sequences homologous to the cauliflower mosaic virus proteases.

iv) Plant aspartic proteases

Aspartic proteases reported from plants are mostly confined to seeds and are involved in the processing of storage proteins during ripening and germination (Runeberg-Roos et al., 1994; Takahasi, 1995; Hiraiwa et al., 1997; James, 1998; Mutlu et al., 1998). Aspartic proteases in plant seeds have been purified from barley wheat, rice (Doi et al., 1980; Runeberg-Roos., 1991; Asakura et al., 1995), castor bean (Hiraiwa et al., 1997), and buckwheat and their enzymatic properties have been investigated. Many plant aspartic proteases are synthesized as the preproform. cDNA cloning of plant aspartic proteases has demonstrated the presence of an insert of approximately 100 amino acids at the C-terminal region that is not found in animal or microbial aspartic proteases. This plant aspartic proteases-specific insert (PSI) may thus characterize aspartic proteases of plant origin (Runeberg-Roos et al., 1994; Asakura et al., 1995; D'Arcy-Lameta et al., 1996; Verissimo et al., 1996; Faro et al., 1999). Investigations of the crystal structures of

phytepsin (Kervinen et al., 1999) and cardosin A (Frazao et al., 1999) also showed that the PSI should be located in the surface of the molecule, as each of these proAPs binds to the plasma membrane at the PSI site prior to being transported into the vacuole, where the PSI is eventually removed by processing (Kervinen et al., 1999). The gene for cyprosin obtained from the cardoon, *Cyanara cardunculus* was expressed in the yeast *Pischia pastoris*. The resulting protein was shown to be a disulfide-linked dimer, where the unique PSI had been processed out of the sequence (White et al., 1999). It has been reported that the PSI-deletion mutant of cyprosin is not processed by itself, indicating that in the absence of PSI, plant aspartic proteases fail to autolyze from the proform to the mature form.

v) Membrane bound aspartic proteases

β-secretases are membrane bound aspartic proteases and involved in the production of the amyloid plaques formed by the accumulation of the 4-kDa amyloid (Aβ) peptide, which is a characteristic feature of Alzheimer's Disease (Glenner and Wong, 1984; Masters et al., 1985). The β-secretase, also referred as Asp1 BACE (Beta site APP Cleaving Enzyme) or memapsin2, is reported to contain the two active site motifs, DTGS at residues 93–96 and DSGT at residues 289–292, which are characteristic of aspartic proteases (Howlett et al., 2000). A second closely related aspartic protease, referred as Asp2, BACE 2 or Down's region aspartic protease or memapsin1, was reported and shown to have 55% homology to Asp2 (Hussain et al., 2000; Howlett et al., 2000). Asp1 and Asp2 show 25 to 30% homology at the amino acid level to other human aspartic proteases (Hussain et al., 1999; Vassar et al., 1999; Lin et al., 2000). A unique feature of Asp1 and Asp2, which distinguishes them from the other human aspartic proteases, is the presence of a C-terminal extension that includes a transmembrane domain and a signal peptide. Asp2 has been reported to have four predicted glycosylation sites in the protein sequence. A distinguishing feature of the protein is the pro-domain (amino acids 22–45), which is shorter than that of other human aspartic proteases.

vi) Putative aspartic proteases

Families of proteases (U22, U33, U34, U23, U24, U25, U11, and U4) are strictly categorized as of unknown catalytic type, but they exhibit certain indications of aspartic type of proteases.

The putative endoproteases of family U22 are encoded by open reading frames that correspond to the *pol* gene of retroviruses (Inouye et al., 1986), whereas that of the *copia* transposon (U23) is encoded by the open reading frame corresponding to the Rous sarcoma virus *gag* gene (Yoshika et al., 1990). The *gypsy* transposon from *Drosophila* is homologous to *Drosophila* transposons in family U22 and has been suggested to contain proteases (Garfinkel et al., 1991). For family U23, deletion of part of the 5' end of yeast *TyB* (including the Asp-Ser-Gly tripeptide) prevents processing, and similar results were obtained by another group subsequently (Garfinkel et al., 1991). For the product of *copia* transposon in *Drosophila*, autocatalytic processing has been shown to be necessary for the release of the protein VPL from the polyprotein precursor, and mutation of the putative catalytic Asp prevents processing (Yoshika et al., 1990). The autocatalytic processing of the *copia* transposon of *Drosophila*, thought to be mediated by the transposon endoproteases, was not significantly inhibited by pepstatin. Family U24 comprises only the putative endoproteases of maize transposon *bs1* (Johns et al., 1989).

Pepstatin-insensitive proteases active at low pH values are known from a variety of fungi (*Aspergillus, Scytalidum*) and bacteria (*Xanthomonas, Pseudomonas, Bacillus*). The bacterial enzymes are inhibited by the carboxyl-specific carbodiimides and by peptide aldehyde tyrostatin. Unlike enzymes from the pepsin family, these endoproteases are thermostable. Scytalidopepsin B from *Scytalidium* and aspergillopepsin II (*Aspergillus* proteases A) have been sequenced and are found to be homologous. Aspergillopepsin II is a secreted enzyme, synthesized as a precursor. Activation involves not only removal of the 59-residue prepropeptide, but also excision of an internal 11-residue peptide to produce a two-chain molecule. The gene for the proteases does not include introns (Inoue et al., 1991).

Among the few proteases that are known from archaebacteria, there is a subtilisin (family S8) and a multicatalytic endoproteases complex (S25). However, thermopsin from the thermophilic *Sulfolobus acidocaldarius* shows no relationship to any other protein. The enzyme has a pH optimum of 2, maximally active at 70°C, and it is covalently attached to the cell membrane. Thermopsin is apparently synthesized as a precursor with a 41-residue prepropeptide. Sensitivity to inhibition by pepstatin suggests

a possible distant relationship to the pepsin clan; however, the typical Asp-Xaa-Gly motif is not present, and there is no evidence of an internal duplication.

Bacterial cell walls contain large quantities of murein lipoprotein. This is a small protein that has Nterminal cysteine substituted on sulfur with the CH2 (OOCR1)CH(OOCR2)CH2- group, and the C-terminal lysine is bound to the membrane peptidoglycan (murein) through the ε-amino group. Secretion of the lipoprotein from the cytoplasm is mediated by a leader peptide, which is cleaved by specialized proteases of the inner membrane known as leader proteases II. Leader proteases II is strongly inhibited by the antibiotic globomycin, but it is also inhibited by pepstatin, which suggests that the enzyme may be an aspartic endoproteases.

Pseudomonapepsin, an acid endoproteases from *Pseudomonas* species, is not inhibited by the standard inhibitors for the pepsin family, pepstatin, DANLME, or EPNP, but it is inhibited by tyrostatin (*N*-isovaleryltyrosyl-leucyl-tyrosinal). Pseudomonapepsin is a secreted enzyme, synthesized as a precursor with a signal peptide and a large propeptide, which is autocatalytically activated by cleavage at a Leu-Ala bond (Oda et al., 1994).

Bacilli produce spores under the direction of a protein known as σ (sigma) E, which switches on the genes necessary for sporulation. The σ factor is produced as a precursor, and the proteases believed to be responsible for processing it is the product of the *spoIIGA* gene. Because of the presence of an Asp-Ser-Gly motif in the processing proteases, the enzyme has been assumed to be aspartic proteases. The proteases is located in the inner membrane and possesses five membrane-spanning domains and large cytoplasmic domain that contain the putative catalytic Asp.

II. Proteases inhibitors

The research interest in proteases inhibitors has evoked tremendous attention in many disciplines. Multicellular organisms possess endogenous protein proteases inhibitors to control proteolytic activity. Most of these inhibitory proteins are directed against serine proteases, although some are known to target cysteine, aspartyl, or metalloproteases. Indeed, inhibitors of serine, cysteine, and metalloproteases are distributed ubiquitously throughout the biological world. In sharp contrast, however, naturally occurring inhibitors of aspartic proteases are relatively uncommon and are

found in only certain specialized locations. Traditionally, proteases inhibitors have been developed by natural product screening for lead compounds with subsequent optimization or by empirical substrate-based methods (West and Fairlie, 1995). This substrate-based drug design has been substantially improved in recent years with the availability of three dimensional structure information for proteases, permitting receptor-based design. The structural information about the active site of the receptor (or proteases) and selection of designed molecules with the aid of computers has helped to design receptor based inhibitors. Combinatorial chemistry also presents opportunities both to discover new molecular entities for assaying and to optimize lead structures for development of proteases inhibitors.

i) Inhibitors of aspartic proteases

Aspartic proteases have received enormous attention because of their significant roles in human diseases. The best-known examples are the involvement of renin in hypertension, cathepsin D in metastasis of breast cancer and the proteases of human immunodeficiency virus (HIV) in acquired immune deficiency syndrome (AIDS). Therefore, the new understanding of the structure and function relationships of these enzymes has a direct impact on the design of inhibitor drugs. Moreover, as structure and function are closely related among the aspartic proteases, model enzymes have been particularly informative. Aspartic proteases are uniquely susceptible to inhibition by pepstatin and by the active site-directed affinity labels, diazoacetyl norleucine methyl ester and EPNP [epoxy-(*p*-nitrophenoxy) propane]. Aspartic proteases-inhibitor crystal structures are currently available on the PDB database for viral proteases (HIV-1, HIV-2, SIV, FIV), Cathepsin D, renin, renin/chymosin, penicillopepsin, secreted aspartic proteases, pepsin, mucoropepsin, retropepsin, saccharopepsin, rhizopuspepsin and plasmapepsin II. Aspartic proteases generally bind 6 to 10 amino acid regions of their polypeptide substrates, which are typically processed with the aid of two catalytic aspartic acid residues in the active site (James and Sielecki, 1997). Thus, there is usually considerable scope for building inhibitor specificity for particular aspartic proteases by taking advantage of the collective interactions between a putative inhibitor, on both sides of its scissile amide bond, and a substantial portion of the substrate-binding groove of the enzyme. Some aspartic proteases also have one or more flaps that close down on top of

the inhibitor, further adding to inhibitor proteases interactions and increasing the basis for selectivity. The scissile amide bond undergoes nucleophilic attack by a water molecule, which is itself partially activated by de-protonated catalytic aspartic acid residue. The protonated aspartic acid donates a proton to the amide bond nitrogen, generating a zwitterionic intermediate, which collapses to the cleaved products. The water molecule that binds between the enzyme and inhibitor is thought to position a peptide substrate, stretching the peptide bond out of planarity toward a tetrahedral transition state that is stabilized by a second water molecule (Chatfield and Brooks, 1995). Aspartic proteases inhibitors can be grouped under two categories by their molecular nature, (1) proteinaceous inhibitors, and (2) low-molecular-weight inhibitors.

a) Proteinaecous inhibitors

Proteinaceous inhibitors of aspartic proteases are relatively uncommon and are found in only a few specialized locations (Bennet et al., 2000). Few of the examples include renin-binding protein in mammalian kidney, which, intriguingly, has now been identified to be the enzyme, *N*-acetyl-D-glucosamine-2-epimerase (Kay et al., 1983; Phylip et al., 2001), a 17-kDa inhibitor of pepsin and cathepsin E from the parasite *Ascaris lumbicoides* (Kageyama, 1998; Ng et al., 2000), proteins from plants such as potato, tomato, and squash (Kreft et al., 1997; Christeller et al., 1998), and a pluoripotent inhibitor from sea anemone of cysteine proteases as well as cathepsin D (Lenarcic and Turk, 1999). There is a report of an 8-kDa polypeptide inhibitor from yeast, which inhibits the vacuolar aspartic proteases (proteases A or saccharopepsin).

b) Low-Molecular-Weight Inhibitors

As compared to the proteases inhibitors from plants and animals, the inhibitors produced by microorganisms are of smaller molecular nature. The presence of proteases inhibitors in microorganisms came into existence from the studies on antibiotics because they act as inhibitors of enzymes that are involved in growth and multiplication. The production of inhibitors of the proteolytic enzymes by microorganisms has probably evolved as a mechanism to provide cell protection. Specific inhibitors of microbial origin have been used as useful tools in biochemical analysis of biological functions and diseases. Polysaccharide sulfates have been reported to be pepsin inhibitors; however, their antipepsin activity is weak, and the effect of such poly anionic compounds is not

specific. Pepstatin, a low-molecular-weight aspartic proteases inhibitor, isolated from various species of *Streptomyces,* is a specific inhibitor of pepsin (Umezawa et al., 1970). *Streptomyces testacus* was reported to produce various pepstatins that differed from one another in the fatty acid moiety (C2-C10). A pepstatin containing an isovaleryl group has been most widely used for biological and biochemical studies. Moreover, as minor components, pepstanone containing (S)-3- amino-5-methylhexane-2-one instead of the C-terminal (3S, 4S)-4-amino-3-hydroxy-6-methylheptanoic acid (AHMHA), and hydroxypepstatin containing L-serine instead of L-alanine, have also been isolated. Pepstatin containing an acetyl group and propanoyl or isobutyryl groups were isolated from *Streptomyces naniwaensis* and *Streptomyces* no. 2907. Pepstatins, pepstanones, and hydroxypepstatins have almost identical activity against pepsin and cathepsin D. However, pepstatin is more effective against renin than are pepstanone or hydroxypepstatin, and its potency against renin increases with the increasing numbers of carbon atoms in the fatty acid moiety. Esters of pepstatin, pepstatinal and pepstatinol possess anti-pepsin activity similar to pepstatins. Several pepstatin analogs have also been synthesized to date. AHMHA and its *N*-acyl derivative exhibit no potency toward pepsin; however, *N*-acetyl-valyl-AHMHA is active, and the addition of another valine between the acetyl and valyl groups does not increase their activity. The addition of L-alanine to the C-terminal group increases the activity about 100 times. This suggests that the acetyl-valyl-AHMHA-L-alanine is the smallest molecular structure that exhibits inhibition against pepsin and cathepsin D similar to pepstatin. Acetyl- L-valyl-L-valyl-[(3S, 4R)-4-amino-3-hydroxy-6-methyl] heptanoic acid prepared by chemical synthesis shows absence of activity. This suggests that the 4S-configuration of AHMHA is essential for activity. The bacterial enzyme that hydrolyzes the isovaleryl bond in pepstatin has been identified, and from the residual peptide benzoyl-L-valyl-AHMHAL-alanyl-AHMHA and L-lactyl-L-valyl-AHMHA-Lalanyl-AHMHA have been synthesized. These analogs are more water soluble than pepstatin and have almost identical activity against pepsin and cathepsin D. However, these water soluble analogs have much weaker activity against renin when compared with pepstatin. The addition of aspartic acid or arginine to the C-terminus of pepstatin increases its water solubility. Such water soluble analogs have same activity against renin as does pepstatin and also have a hypotensive

action (Rich, 1985). Pepstatin also inhibits carageenin-induced edema and suppresses the generation of Shay rat ulcer. Therapeutic effects on stomach ulcers in man have also been observed. Pepstatin has been reported to be effective against experimental muscle dystrophy and enhances the effect of leupeptin. Pepstatin also inhibits leukokinin formation and ascites accumulation in ascites carcinoma of mice. Pepstatin inhibits the growth of *Plasmodium beghei* and inhibits focus formation in murine sarcoma virus (Yuasa et al., 1975). Recently, a new class of peptidomimetics, the unsymmetrical peptidyl ureas, has emerged as powerful inhibitors of aspartic proteases (Dales et al., 2001). These were developed using mechanism-based and substrate-based design techniques and using the computational method GrowMol (Ripka et al., 2001). These newly synthesized inhibitors possess a distinct advantage over the natural inhibitors. The natural inhibitors such as antipain, elastinal, etc. contain urea bonds in place of the amide bonds between the P3 and P4 residues and not between the P1 and P2 residues. Ureas have the ability to form stronger hydrogen bonds than the amide groups. The synthesis of ureas as inhibitors was therefore a natural choice. These synthetic inhibitors of porcine pepsin were generated through computational programs that analyze the target enzyme structure, predict inhibitor structures, and analyze the enzyme-inhibitor complex formed. These structures would help to chemically build up molecules of medicinal value and would give rise to newer classes of drugs.

ii) HIV-1 proteases inhibitors

The proteases of the human immunodeficiency virus (HIV-1 PR) have proven to be an attractive drug target due to its essential role in the replicative cycle of HIV. Several low-molecular-weight inhibitors of HIV-1 PR are now used in humans, including saquinavir, ritonavir, indinavir, nelfinavir, and amprenavir. These are the first successful examples of receptors/structure-based designer drugs and were developed using structures of compounds bound in the active site of HIV-1 PR and with the knowledge of inhibitors of other aspartic proteases (e.g., renin) (Kempf and Sham, 1996). All HIV-1 PR inhibitors developed so far target the active site substrate-binding groove of the homodimeric enzyme, a long cylindrical cavity that binds 6 to 7 amino acids via ionic, van der Waals, or hydrogen bonding interactions (Kempf and Sham, 1996). Two catalytic aspartates in the center of this cavity promote amide bond hydrolysis. Saquinavir became

the first proteases inhibitor designed from a three-dimensional structure of a proteases (structure-based design) to be approved for human use in 1996 (Roberts et al., 1990; Pakyz et al., 1997; Patick et al., 1998), despite its low oral bioavailability due to poor absorption and extensive first-pass degradation by cytochrome P450 (Wacher et al., 1998). It is active in cell culture against both HIV-1 and HIV-2 viruses and in combinations with ritonavir, an inhibitor of cytochrome P450 (Kempf et al., 1997), lead to greatly increased plasma concentrations. Ritonavir itself is a potent inhibitor of HIV- 1 PR with high oral bioavailability (Lea and Faulds, 1996). Indinavir or Crixivan is another potent inhibitor of HIV-1 and HIV-2 proteases that halts the spread of HIV infection in MT4 lymphoid cells and is orally bioavailable. In humans, Indinavir is rapidly absorbed in fasting state, there is significant binding to plasma proteins, and the main degradation pathway is via cytochrome P450 (Lacy et al., 1996). The mesylate salt of nelfinavir, approved for human use in 1997, is a lipophilic proteases inhibitor with good oral bioavailability in rats and monkeys (Shetty et al., 1996; Kaldor et al., 1997). Amprenavir, is water soluble, orally bioavailable inhibitor with long half life, allows less frequent administration of drug, thereby having the potential for less side effects with respect to other marketed HIV proteases inhibitors described above (Kim et al., 1995; Adkins and Faulds, 1998; Fung et al., 2000; Noble et al., 2000). Viral resistance to "monotherapy" with any of these drugs is a significant problem (Erickson, 1995). Serial passages of HIV-1 *in vitro* in the presence of increasing concentrations of a proteases inhibitor cause a rapid emergence of drug-resistant viral strains of HIV-1. Thus, new HIV proteases inhibitors with different resistance profiles are still being actively pursued. A number of second-generation inhibitors have been developed. Lopinavir or ABT-378 was designed to inhibit mutant proteases produced in response to ritonavir (Carrillo et al., 1998; Sham et al., 1998; Hurst et al., 2000). It is 10-fold more potent against ritonavir-resistant strains and displays lower binding to serum proteins. Although the oral bioavailability of lopinavir is very poor, when administered with ritonavir the bioavailability was enhanced (Sham et al., 1998). Kaletra, the HIV proteases inhibitor was developed as a mixture of lopinavir and ritonavir by Abbott. It was the first second-generation inhibitor of HIV proteases to be used successfully as a recommended drug, when the primary therapy with other proteases inhibitors failed (Wlodawer, 2002). CGP-73547 inhibits indinavir and

saquinavir-resistant strains of HIV-1, is orally bioavailable (Bold et al., 1998). One of the most promising preclinical candidates for HIV proteases inhibition is palinavir. This compound is a very potent, orally active inhibitor of HIV-1 and HIV-2 proteases with high antiviral activity (Lamerre et al., 1997). An orally bioavailable inhibitor called as Mozenavir was developed by DuPont Merck and the University of Uppsala. Mozenavir has a seven-membered cyclic urea ring as the starting molecule (Lam et al., 1994). Mozenavir has a *Ki* of 0.3 n*M* and is highly potent in cell cultures. A very different inhibitor, tiprinavir, was developed by Pharmacia and Boehringer-Ingelheim. It is a nonpeptidic molecule with a *Ki* of 5 pM (Turner et al., 1998). Tiprinavir is soluble and highly bioavailable with significant activity against multidrug resistant HIV- 1 strains (Thaisrivongs et al., 1999; Rusconi et al., 2000). L-735, 524, a hydroxyaminopentane amide class peptidomimetic is a highly potent and orally bioavailable HIV proteases inhibitor (Dorsey et al., 1994; Vacca et al., 1994). The Ki values of L-735, 524 for HIV-1 and HIV-2 are 0.38 n*M* and 2.45 n*M*, respectively. This seven-fold difference combined with its enhanced oral bioavailibility offer chances of using this molecule or close structural analogues as effective agents. A report of the inhibitors of HIV-1 proteases dimerization has been published recently. These compounds indicate the first studies of nonpeptidic inhibitors of HIV-1 proteases dimerization (Song M et al., 2001). Compound 1 contained 4-(2-aminoethyl) - 6-dibenzofuranpropionic acid as a conformationally restricted linker. Compound 2 was a nonpeptidic beta strand mimetic, 2-[3-([2-[9-fluorenylmethoxy) carbonyl] hydrazine] carbonyl)-4-methoxyanilino]-2- oxoacetic acid. The *Ki* values of these compounds were 5.4 and 9.1 μ*M*, respectively. A peptide inhibitor has been isolated from an extremophilic *Bacillus* species. It is reported to be a tight binding, noncompetitive inhibitor with a *Ki* value of 17.8 n*M* against HIV proteases (Dash and Rao, 2001). New reports of the HIV proteases inhibitors have suggested that resistance evading inhibitors can be designed (Dash and Rao, 2001). Even though a multitude of proteases inhibitors have been reported, only six, viz., saquinavir, nelfinavir, ritonavir, indinavir, lopinavir, and amprenavir, have been approved as drugs by USFDA (United States Food and Drug Administration) in the treatment of AIDS. Newly emerging resistant strains of HIV enhance the need for newer and more potent drugs. Hence, the research in this field needs to be intense.

iii) Renin inhibitors

The aspartic proteases renin is involved in the rate-limiting step of the renin-angiotensin (RAS) system, by hydrolyzing the α2-globulin angiotensinogen to release the 10-residue peptide angiotensin I. Because of its specificity, renin inhibitors are antihypertensive agents similar in action to ACE inhibitors, and AII antagonists, but are free of some side effects associated with ACE inhibitor administration. For example, Zankiren (A-72517), a potent inhibitor of human plasma renin, is the peptidic inhibitor with significant oral absorption (Kleinert et al., 1992). Renin inhibitors have been developed mainly by modifying substrate fragments from the angiotensinogen cleavage site (Rosenberg, 1995), but their clinical progress has been hampered by their peptidic character, which confers low stability and poor oral bioavailability in humans. Another hurdle in the development of rennin inhibitors has been the high cost of production, compared with current antihypertensives such as ACE inhibitors and AII receptor antagonists. Generally, renin inhibitors need to interact with five subsites (S4-S1') of the enzyme to bind tightly and selectively compared with only three for ACE inhibitors. Several renin inhibitors with low molecular weight, less peptidic character, and improved oral bioavailabilty have emerged recently. CP-108 671 was designed from the cleavage site of angiotensinogen and the structure of the general aspartic proteases inhibitor pepstatin (Hoover et al., 1995). It uses a cyclohexylnorstatine transition-state analogue, a(R)-benzylsuccinate, at P3 for chymotrypsin stability and is a potent inhibitor of human plasma renin. It is highly selective over most aspartic eptidases but does weakly inhibit cathepsin D. BILA 2157 BS is another potent renin inhibitor with some selectivity toward cathepsin D and oral activity (Simoneau et al., 1999). A combination of the X-ray crystal structure of CGP38560 bound rennin (Buhlmayer et al., 1988) and previous information (Goschke et al., 1997) that the S3 subsite can be accessed by extending the P1 residue has helped in developing several other nonpeptidic inhibitors with good activity and specificity. Recently, a new class of renin inhibitors, the substituted piperidines, have emerged (Oefner et al., 1999), which proposes a novel paradigm for the inhibition of the monomeric aspartic proteases. The inhibitors have been developed from a simple 3,4-disubstituted piperidine lead compound. Two representative compounds from this class were tested against recombinant human renin. The first compound, trans (3R, 4R)-2-

naphthyl-methoxy-4-(4-bromophenyl)-piperidine, inhibited renin with a IC_{50} of 5 μ*M*. The bromophenyl substituent allowed the nitrogen of piperidine to close in on the two catalytic carboxylates. Structural variation gave rise to the 3,4,5-trisubstituted- piperidine derivative. This derivative had an IC_{50} of 2 n*M* and formed a better complex with renin.

iv) Plasmepsins inhibitors

Plasmepsins I and II, found in the malarial parasite *Plasmodium falciparum*, are aspartic proteases that are essential for the degradation of its major food source, human hemoglobin (Dame et al., 1994). The inhibition of these enzymes, which have 73% and 35% sequence homology with human cathepsin D, therefore is considered a viable therapeutic strategy for the treatment of malaria (Coombs et al., 2001). Both plasmepepsin I and II are believed to initially cleave the Phe33-Leu34 peptide bond of the α-chain of hemoglobin, followed by cleavage of the polypeptides into smaller fragments that are subsequently processed by the cysteine proteases falcipain (Francis et al., 1997). SC-5003, the first peptidomimetic inhibitor reported to selectively inhibit plasmepsin I and II, was active *in vitro* against the live parasite, preventing hemoglobin degradation (Francis et al., 1994). X-ray crystallographic structure of plasmepepsin II complexed to pepstatin A have been used to develop peptidic inhibitors, which starves the live parasite *in vitro* as well as inhibits human cathepsin D (Silva et al., 1996). Currently, combinatorial synthesis is being used to generate inhibitor libraries for these enzymes. Another class of inhibitors, the allophenyl norstatine based inhibitors, have been shown to be effective and potent inhibitors of plasmempsin II (Nezami et al., 2002). The allophenylnorstatine scaffold contains four different positions where separate functional groups can be introduced. This improves the binding affinity and selectivity toward the selected target. The KNI series of inhibitors that incorporates the allophenylnorstatine moiety with a hydroxymethylcarboxamide isostere is the most effective inhibitor series. The exception is KNI-529, which has the anti diastereoisomer phenylnorstatine replacing the allophenylnorstatine. The best compound of this series, KNI-727, shows a *Ki* of 70 nM. The reaction is favored both enthalpically and entropically. Good oral bioavailability and low toxicity indicates that allophenylnorstatine is a very good scaffold for the development of inhibitors with clinical applications. All compounds developed to date are potent inhibitors of human

cathepsin D, so better selectivity needs to be attained in orally active inhibitors of these enzymes. Interestingly, a combination of cysteine and aspartic proteases inhibitors was found recently to be more effective than either compound alone in inhibiting *Plasmodium* mediated hemoglobin degradation in both culture and a murine malaria model (Semenov et al., 1998). This synergy suggests that combination therapy may be a viable strategy for antimalarial treatment regimes of the future.

v) Cathepsin D inhibitors

Human cathepsin D is an intracellular aspartic proteases found mainly in lysosomes. It has a number of "housekeeping" functions, including the degradation of cellular and phagocytosed proteins. The enzymes may be involved in a variety of disease states, including cancer and Alzheimer's disease. Clinical studies have shown that cathepsin D is overexpressed in breast cancer cells, and this seems to be associated with an increased risk of metastasis due to enhanced cell growth (Rochefort and Liaudet-Coopman, 1999). Cathepsin D or similar aspartic protease is also thought to be involved in formation of the β-amyloid peptide in Alzheimer's disease (Papassotiropoulos et al., 1999; Wolfe et al., 1999). The availability of selective and potent inhibitors will help to further define the role of cathepsin D in disease and possibly lead to therapeutic agents. Relatively few inhibitors of cathepsin D have been reported, partly because of its uncertain role as a viable target for therapeutic intervention. Human cathepsin D was co-crystallized with pepstatin A, and its structure (Baldwin et al., 1993) has promoted some inhibitor studies. One study suggests that the entropy and solvation effects are key determinants of high affinity for pepstatin-cathepsin D binding (Majer et al., 1997). Although a general inhibitor of aspartic proteases, pepstatin A remains the most potent inhibitor known. There have been reports of cyclic inhibitors designed from the X-ray structures using the fact that the enzyme-bound conformation of the P2 and P3' residues of pepstatin are in close proximity to each other (Silva et al., 1996). This allows cyclization of the inhibitor, thereby increasing the proteolytic stability of the three-amide bonds in the cycle. Combinatorial approaches have been carried out for the development of inhibitors to prove the methodology for the optimized specificity against other aspartic proteases.

vi) Secreted aspartic proteases inhibitors

The *Candida* yeast strains *C. albicans, C. tropicalis*, and *C. parapsilosis* exist in small quantities in a healthy intestinal tract, but they become a health problem when the immune system is compromised. Such opportunistic infections arise in AIDS patients where *C. albicans* is a serious pathogen of the mucous membranes (Gruber et al., 1999). It is also the major cause of vaginitis (De Bernardis et al., 1999) and has been implicated in liver toxicity and in the development of multiple chemical allergies. *C. tropicalis* is the predominant cause of fungal infections in neutropenic cancer patients. These organisms have the ability to secrete into the host (Naglik et al., 1999) several aspartic proteases (SAP, secreted aspartic proteases) of broad specificity. These proteases are thought to be linked to the virulent effects of *Candida* strains in humans as proteases deficient mutants reduce the virulence (Hube et al., 1997; Sanglard et al., 1997). Therefore, these enzymes are becoming attractive targets for therapeutic attack. Nine SAPs have been identified in the genome of *C. albicans* to date (SAP1-9) (Monod et al., 1998). From mutation experiments, SAP2 seems to be the dominant isoenzyme for the normal progression of systemic infection, while SAP1 and 3 are also important for overall virulence of *C. albicans* (Naglik et al., 1999). SAP4-6 appears to play a role in the process of induction of SAP2 (Sanglard, D. et al., 1997). X-ray crystal structures have been determined for SAP2 complexed to pepstatin (Cutfield et al., 1995), a close homologue SAP2X bound to the same inhibitor (Abad- Zapetero et al., 1998), and a SAP enzyme of *C. tropicalis* (Symerski et al., 1997). Very little inhibitor design has been reported for SAP2. A-70450 was originally designed to inhibit renin and later found to be nonselective inhibitor of the SAP of *C. albicans*. This inhibitor incorporates the (*S*)-hydroxylethylene isostere with the hydroxyl group positioned in the crystal structure between two catalytic aspartate residues. Interestingly, the terminal methylpiperazine ring of A-70450 is found in a boat conformation that occupies the S3 subsite of the enzyme together with the benzyl group of the ketopiperazine ring. The large S3 subsite is not found in other aspartic proteases, and this difference could be exploited to develop selective inhibitors for SAP2 (Abad-Zapetero et al., 1996). SAPs have been reported to be inhibited by indinavir and ritonavir in the range of 1 to 10 μM (Cassone et al., 1999; Gruber et al., 1999). Reduced amide monohydroxyethylene and diamonidiol-based transition state peptidomimetics were also

reported to inhibit SAPs effectively (Skrbec and Romeo, 2002). A few natural products were iso lated from *Lycopodium cernuum* out of which lycernuic acid C and apigenin-4'-*O*- (2", 6"-di-*O*-*p*coumaryl)- beta-D-glucoside showed inhibition of SAP with IC50 values of 20 and 8.5 μg/ml (Zhang et al., 2002). Further research efforts are needed to screen natural sources for the identification of new inhibitors.

vii) β-Secretase Inhibitors

The feasibility of an inhibitor drug against β-secretase for the treatment of Alzheimer's Disease was substantiated by the success in the design of inhibitor drugs against HIV proteases and the apparent tolerance of the β-secretase gene deletion in mice (Cai et al., 2001; Luo et al., 2001). A first generation inhibitor OM99-2, an 8-residue transition analog with Ki near 1 n*M* was designed based on the substrate specificity (Lin et al., 2000; Ghosh et al., 2000). The crystal structure of the β-secretase-OM99-2 complex resolved at 1.9 Å indicated that S3' and S4' subsites were not well formed in β-secretase (Hong et al., 2002). A further detailed subsite preference of β-secretase (Turner et al., 2001) and preferred binding residues led to the designing of a second generation inhibitor, OM00-3 with a Ki of 0.3 n*M* from a combinatorial inhibitor library (Hong et al., 2002). The crystal structure of β-secretase and OM00-3 at 2.1 Å resolution was determined using the molecular replacement method. The interactions of the P1/P1' region of OM00-3 with the substrate binding cleft of β-secretase and the conformation of the inhibitor from P3 to P2' are the same as those for the OM99-2-β- secretase complex (Hong et al., 2002). The S4 pocket deduced from the crystallographic studies of β-secretase involves Glu11, Gln73, Thr232, and Arg307. The latter was shown to form several ionic bonds with the carboxylate oxygen atoms of inhibitor P4 Glu. These multiple interactions with the proteases contribute to the inhibitor binding. In OM00-3, the leucines at P3 and P1 show contacts with the S3 site of the enzyme as well as with each other and stabilize the conformation of the inhibitor. The locations and the nature of the S3' and S4' binding sites have been defined for the first time. It has been demonstrated that valine at P2' provides better binding with the enzyme. Other binding modes provided for the P2 and P4 side-chains could help in the future designing of inhibitors. The current findings suggest that designed inhibitors should have a strong binding side chain such as Val at P2. The new binding mechanisms proposed at P2 and P4 suggest scope for further

inhibitor design. The recent reports of β-secretase inhibitors have raised the possibilities of inhibitors as therapeutic agents in Alzheimer's disease.

III. Sequence homology

Protein sequence homology has become routine in computational biology and implicated in the prediction of the secondary structure and phylogenetic analysis of proteins. The comparison of the amino acid sequences assists in the study of their evolution. However, no reports of sequence homology studies of aspartic proteases inhibitors are available. Aspartic proteases inhibitors from diverse origins such as plants, animals, and microbes have been selected from the Swiss-Prot entries. Sequence data from eight inhibitors from potato, five from nematodes, and five synthetic peptides were available and have been aligned using the CLUSTAL W online software for multiple alignments (Thompson et al., 1994). The dendrogram drawn suggested that the inhibitors could be classified into three distinct groups. The inhibitors from potato, which are reported to be cathepsin D and pepsin inhibitors, were classified as Group 1. The inhibitors classified under group 2 showed inhibition against pepsin, whereas the group 3 inhibitors were reported to be renin inhibitors. The further analysis of the results indicated that the eight aspartic proteases inhibitors in group 1 showed variations that might have arisen out of mutations or genetic shuffling in a single gene locus giving rise to single amino acid variations interspersed among highly conserved regions. The analyses of group 2 indicated that a stretch of 21 amino acids was conserved with variations at amino acid positions 2, 5, 7, 15, and 16. The most predominant amino acids at these positions were aspartic acid, methionine, glutamine, glutamine, and lysine, respectively. The aspartic acid at position 2 was substituted by valine in two of the sequences. Methionine at position 5 was replaced by serine occassionally. The two glutamines at positions 7 and 15 were substituted by leucine, glycine, or arginine, while lysine at position 16 was replaced by alanine, serine, or glutamine. The analysis of the synthetic peptides constituting group 3 showed that two histidines and phenylalanine were conserved. The variations in the amino acids, however, did not affect the inhibitory activity of the inhibitors. From the survey of the genome databank of NCBI, it was noted that the DNA sequences for the aspartic proteases inhibitors were not available. This could be attributed to the fact that very few natural protein inhibitors have been

investigated for their gene sequence. The peptide sequences were derived as cleavage products, and as a result the nature of their DNA sequence may not have been deduced. Girdwood et al. (1998) have determined the functional relationship between the protein sequences of aspartic proteases inhibitors derived from nematodes belonging to the family Filaridae. Their studies are aimed at correlating similar gene sequences from *Ascaris, Onchocerca,* and other related nematodes to assess their function as aspartic proteases inhibitors.

IV. Inhibitor design and future prospects

Most aspartic proteases inhibitors developed bind to their target enzyme through non covalent interactions (i.e., hydrogen bonds, ionic, or van der Waal's contacts) making them reversible inhibitors of proteases. An effective inhibition relies on the enzyme having greater affinity for the inhibitor than its natural substrate and trying to maximize the number of non-covalent interactions that the inhibitor makes with the enzyme. Incorporation of a transition state isostere into designed inhibitors is one approach that has proven very successful. A transition state isostere is a functional group that can mimic the tetrahedral transition state of amide bond hydrolysis but is itself be hydrolyzed by the enzyme. It has been hypothesized that stable structures, which can resemble the transition state of an enzyme reaction, will be bound more tightly than the substrate for the enzyme-catalyzed reaction. Studies on pepstatin (which incorporates the statine transition state isostere) suggest that this increased affinity can be as great as 104-fold. Renin, pepsin, cathepsin D, and human immunodeficiency virus-proteases, are generally typecast on the basis of their susceptibility to inhibition by acetylated pentapeptides, isovaleryl-, and acetylpepstatin. An analogous yet different strategy where a chemical modification of the scissile peptide bond is used to introduce a non hydrolyzable analogue of the tetrahedral transition state formed during hydrolysis was also reported (Szelke et al., 1982). Instead of using the naturally occurring statine residues as the centerpiece around which the inhibitor is constructed, the complete amino acid sequence of the substrate is retained in the inhibitor except that the scissile peptide bond between P1- P1' of the substrate is replaced by the non hydrolyzable analogue of the transition state. Using this approach, a tight-binding inhibitor of human renin has been developed that is a synthetic analogue based on the sequence of residues known to occur

on either side of the scissile peptide bond of the angiotensinogen but with a reduced -CH_2-NH- isostere in place of the -CONH- of the substrate. It is also possible, of course, to device such inhibitors not on the sequence of residues found in naturally occurring protein substrates but based on synthetic peptides that are known to be good substrates for certain enzymes. Thus, it would appear that although naturally occurring inhibitors of aspartic proteases may have little physiological significance in regulating their target enzymes *in vivo*, nevertheless such compounds and their synthetic counterparts have proved of inestimable value in facilitating distinction among the different types of aspartic proteases. Such inhibitors can be utilized for diagnostic purposes to establish the nature of "newly isolated" proteases. As an illustration of this, consider the inhibition of human pepsin and gastricin by isovaleryl and lactyl-pepstatin (Reid, 1984). Although considerable progress has been made with the structure, activity, and importance (biological and commercial) of the aspartic proteases, much remains to be learned about the distinctions of various architectures and how these are reflected in the functions of the enzymes. Inhibitors (naturally occurring and synthetic) have permitted detailed biochemical and crystallographic investigations to be made, but an understanding of the selectivity of such inhibitors may be of just as much importance for the design and synthesis of specific inhibitors for use therapeutically in controlling individual aspartic proteases.

CHAPTER 2

BIOCHEMICAL CHARACTERIZATION OF AN ASPARTIC PROTEASE INHIBITOR FROM THERMO TOLERANT *BACILLUS LICHENIFORMIS*: INTERACTION WITH PEPSIN

PART 1

ISOLATION AND IDENTIFICATION OF THERMO TOLERANT *BACILLUS LICHENIFORMIS*

SUMMARY

The microorganism was isolated in the laboratory from the fruit tomato. The culture was purified by the single colony plating technique. The strain was an aerobic, motile, gram positive, spore forming rod-shaped bacterium. On nutrient agar at 50°C, the colonies were large, irregular, sticky and pale cream colored. The organism was thermo-tolerant with a broad growth range of 28°C-50°C with optimum growth at 50°C and pH 7. The isolated organism was identified to be *Bacillus licheniformis* based on the biochemical characteristics as described in the Bergey's Manual of Determinative Bacteriology and 16S rDNA sequencing.

INTRODUCTION

Bacillus licheniformis is a Gram-positive, motile, spore-forming, facultatively anaerobic rod belonging to the *B. subtilis* group of Bacilli. It is an apathogenic soil organism, mainly associated with plant and plant materials in nature but can be isolated from nearly everywhere due to its highly resistant endospores. *Bacillus licheniformis* is toxinogenic and food poisoning in humans has been associated with cooked meat, poultry and vegetable dishes (particularly stews and curries which have been served with rice). Food poisoning by *Bacillus licheniformis* is characterised by diarrhoea, although vomiting occurs in half of reported cases.

Bacillus licheniformis is used by industry to produce proteases and amylases. Proteases were first used to improve the effectiveness of a laundry detergent in 1913 by a German named Otto Rohm, the founder chemical company Rohm and Hass. He derived a quite crude proteolytic enzyme from milled animal pancreases. Commercially feasible quantities of proteolytic enzymes are now produced through fermentation of *Bacillus subtilis* or *Bacillus licheniformis.* The proteases and amylases secreted by these strains have the advantage that they work best at the warm alkaline conditions prevailing in washing liquids. They also do not lose their activity in the presence of surface active agents, magnesium or calcium ions, builders (sodium tripolyphosphate), perfumes, and other additives routinely formulated into laundry detergents such as. In the U.S., about 50% of liquid detergents, 25% of powder detergents, and almost all powdered bleach additives now contain enzymes to help break down stains. *B. licheniformis* is also used to make the polypeptide antibiotic Bacitracin.

There are no indications that *B. licheniformis* is pathogenic to plants. The initial results of inoculation of *Bacillus licheniformis* strain on pepper and tomato plants shows the greater effect on pepper than on tomato and treated plants had less disease than non-treated plants. This strain had considerable colonization and competitive ability, and it could be used as a bio-fertilizer or biocontrol agent without altering normal management in greenhouses. This part of the present chapter deals with the isolation and identification of thermo tolerant *Bacillus licheniformis* strain that produces an aspartic protease inhibitor, API.

MATERIALS AND METHODS

Materials

Lysozyme, SDS, EDTA, phenol, chloroform, isoamyl alcohol, isopropanol, RNAase, deoxyribonucleoside triphosphate (dNTP), *Taq* DNA polymerse, agarose, tris base, boric acid, ethidium bromide, polyethylene glycol were from Sigma Chem. Co. USA. 16S rDNA primers commercially obtained from Life technologies, India, NaCl, activated charcoal, luria broth, agar, beef extract, yeast extract, peptone, glucose, magnesium sulfate, dipotassium hydrogen phosphate, soya meal were purchased from Himedia and Qualigens India. All other chemicals were of analytical grade.

Isolation and identification of the microorganism

The organism was isolated in the laboratory from the fruit tomato. The culture was purified by the single colony plating technique on LB agar plates. The organism was identified by carrying out biochemical tests as described in the Bergey's Manual of Determinative Bacteriology (Buchanan and Gibbons, 1974) and by 16S rDNA sequencing using ABI 3700 DNA sequencer. The 16S rDNA sequence was blasted at NCBI.

Isolation of genomic DNA

The bacterial culture was grown in 100 ml of Luria Broth (pH 7.0) at 37°C for 48h with continuous shaking at 200rpm. DNA was isolated according to the method described by Hopwood et al. (1985) with slight modifications. Bacterial cells (1g) washed in 5ml TE buffer (pH 8.0) was centrifuged at 10,000rpm for 10min. at 4^{o}C. The pellet was freezed in liquid nitrogen and powdered for better access by lysozyme. The powdered pellet was re-suspended in 5ml TE containing 2mg/ml lysozyme. It was incubated at 30°C, triturating every 15min. until a drop of suspension on a microscopic slide was completely cleared with a drop of 10% SDS (1 hour). Further, 1.2ml of 0.5 M EDTA was added to the mixture followed by 0.7 ml 10% SDS. The solution was swirled and incubated at 37°C for 2h. Proteins were extracted from the aqueous phase by adding 6ml of a mixture of phenol:chloroform: IAA (isoamyl alcohol) (25:24:1). The mixture was shaken for 5min. and then centrifuged at 10,000 rpm, 4°C for 10min. This step was repeated again for the aqueous phase in a new tube. Finally, 40µg/g of RNAase from a

stock of 10mg/ml was added to pre-weighed aqueous phase and incubated at 37°C for 1h. The genomic DNA was precipitated by adding equal volume of isopropanol and was stored at room temperature for 1h. DNA was spooled with a glass rod and transferred to a fresh tube and dissolved in 5ml of TE buffer, pH 8.0.

PCR Amplification of 16S rDNA

The primers used for the identification of *Bacillus* sp. were universal eubacterial 16S rDNA primers (16F27N- 5'CCA GAG TTT GAT CMT GGC TCA G, 16F536 (5'GTG CCA GCA GCC GCG GTR ATA), 16R1525XP (5'TTC TGC AGT CTA GAA GGA GGT GWT CCA GCC) commercially obtained from Life technologies, India. The 25µl Polymerase chain reaction (PCR) was set by using the genomic DNA and the reaction mixture typically contained Genomic DNA 0.50µl, 10X Buffer 2.50µl, 0.2mM deoxyribonucleoside triphosphate (dNTP) 2.5µl, Forward and Reverse Primers 10-20pmoles, (1.25µl each), distilled water 16.87µl, and 1unit of *Taq DNA polymerse* 0.25µl (Bangalore Genei). All the additions were done on ice and the PCR reaction was performed on Gene Amplifier PCR System 9700 (Perkin Elmer, USA). The PCR conditions for 16SrDNA gene amplification were: Initial denaturation 95°C for 3min.; followed by 35cycles of 94°C for 1min., 55°C for 1min., 72°C for 1min. and final extension at 72°C for 10min. 5µl of the above PCR amplified product was used for electrophoresis using 1.0% agarose gel in 1X TBE buffer (Working solution: 0.5X; Stock: 5X, 54g Tris base, 27.5g boric acid, 20ml 0.5M EDTA [pH 8]). The gel was run at 80V for 90min. using 1X TBE as running buffer. The gel was stained in 1% ethidium bromide for 45min. and was observed under UV illumination.

Purification of PCR amplified product

To 20µl PCR amplified product, 0.6 volumes of 20% PEG-NaCl (Polyethylene glycol - NaCl) solution was added and incubated at 37°C for 30min. It was then centrifuged at 12000rpm for 20min. The supernatant was discarded and the pellet was washed twice with 70% ethanol and separated by centrifuging at 12000rpm for 20min. The pellet was dried and dissolved in 10 µl of double distilled water and stored at -20°C.

Sequencing of the purified PCR product

The sequencing reactions were carried out using *Taq* DNA polymerase dye terminator cycle sequencing using the 'ABI PRISM BigDye Terminator Cycle

Sequencing Ready Reaction Kit' (Perkin Elmer Applied Biosystems Division, Foster City, CA) according to the manufacturer's protocol. This Kit contains the four ddNTPs with different fluorescence labels termed as BigDye Terminators. 2µl PCR product and 3 pmol of the sequencing primer were used in a 20µl sequencing reaction. The sequencing reaction mixes were subjected to 25cycles in a Perkin Elmer thermal cycler 9700. Each cycle consisted of 95°C for 10min., 50°C for 5min. and 60°C for 4min. DNA sequencing was carried out on ABI 3700 DNA sequencer. The analysis of nucleotide sequence was done at NCBI server using BLAST-n (www.ncbi.ncm.gov/blast).

Growth Conditions of the microorganism

The *Bacillus licheniformis* was routinely maintained on LB- agar slants and preserved at 4°C. The pH of the slants was adjusted to pH 7. For long-term storage, 25% glycerol suspension of the 16 h grown culture was kept frozen at -70°C. The bacterial culture was grown at 50°C for 16 h.

The media composition for the growth of the organism was:

Glucose - 1%

Beef extract - 0.75%

Sodium chloride - 0.3%

Magnesium sulfate - 0.1%

Dipotassium hydrogen phosphate - 0.1%

Soyameal - 2%

The cultivation of the organism was carried out by inoculating a loop full of freshly grown culture on LB-agar slant into the inoculums flask containing the liquid media with the above composition at 50°C. The inoculums were developed in for 24 h in the inoculums flasks at 50°C. 10 ml of the inoculums was transferred into 500 ml Erlenmeyer flasks containing 100 ml of the above medium and was incubated under shaking conditions (250 rpm) at 50°C for 48 h.

RESULTS

Identification of the microorganism

The isolated organism was identified to be *Bacillus licheniformis* based on the biochemical characteristics as described in the Bergey's Manual of Determinative Bacteriology. On nutrient agar at 50°C, the colonies were large, irregular, sticky and pale cream colored (Figure 1). The strain was an aerobic, motile, gram positive, spore forming rod-shaped bacterium (Figure 2). The organism was thermo-tolerant showing growth at broad range of temperature (28°C-50°C). The strain showed negative reaction for production of indole, hydrogen sulfide, ammonia and urease, but positive reaction for production of starch, Voges-Proskaeur, catalase and reduction of nitrate. The organism produced oxidase and the ammonia was utilized as a nitrogen source.

Identification of the microorganism by16SrDNA sequencing

The genomic DNA was isolated, loaded on agarose gel and was found to be high molecular weight and intact DNA. The spectrophotometeric analysis of the DNA showed that the DNA had an A_{260}:A_{280} ratio of 2.0, which indicates the purity of the DNA preparation. Fig. 3 shows the 16srDNA sequence from Bacillus sp. On NCBI BLAST, this sequence showed closest homology (99.5%) to *Bacillus licheniformis*. The blast hits have been shown in Figure 4. It revealed that the isolate of *Bacillus sp.* had maximum similarity to *Bacillus licheniformis.*

Optimum growth conditions for the organism

The optimum fermentation condition for *Bacillus licheniformis* conditions was found at temperature 37-50°*C* and pH 7.0 in 48-96 hours. Therefore the organism can be called as thermo-tolerant. The growth of the organism in fermentation media was measured by taking O.D. at 600nm.

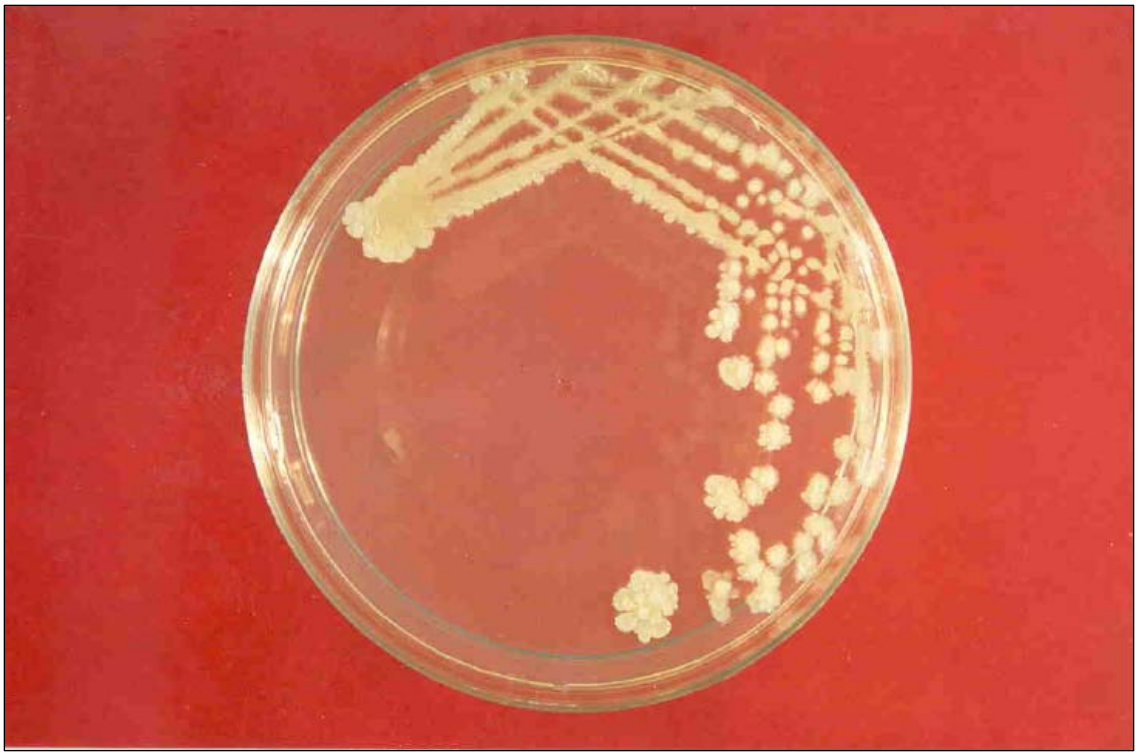

Fig. 1. Large, irregular, sticky and pale cream colored colonies of isolated *Bacillus licheniformis*

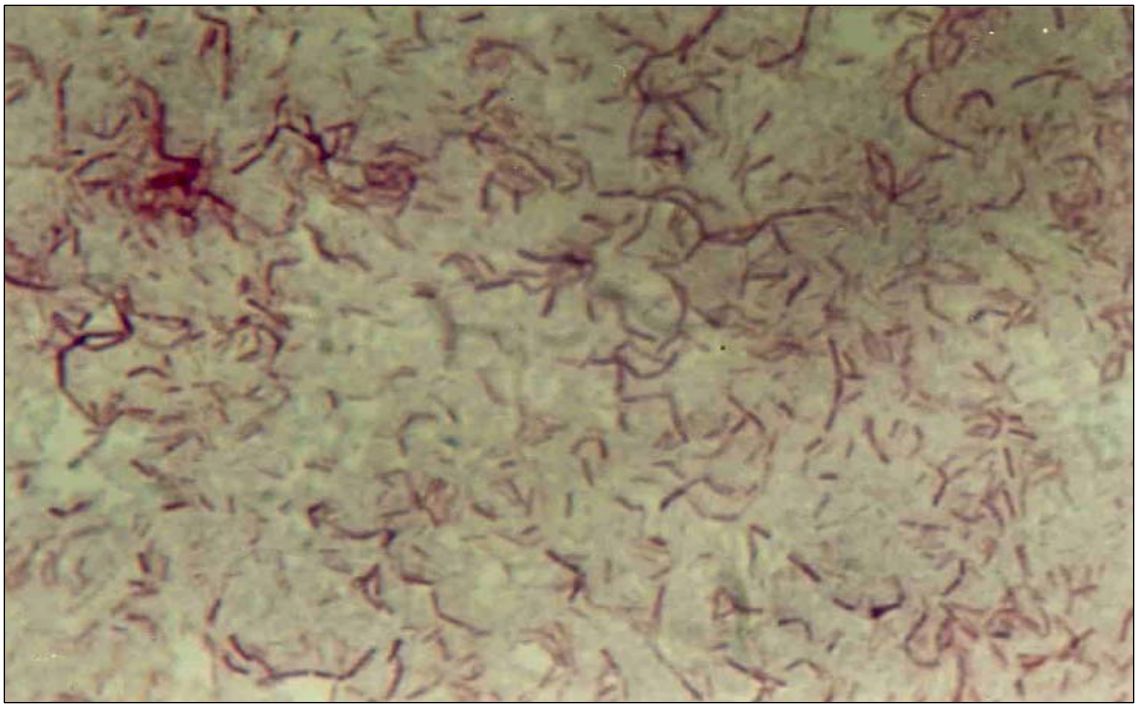

Fig. 2. Aerobic, motile, gram positive, spore forming rod-shaped *Bacillus licheniformis*

ACCAAGGGTTTAGATAAGCTCTCACATTCATGAACCGAAGGGGACCGCCCTATT
CGAACGGTACTTGTTCTTCCCTAACAACAGAGCTTTACGATCCGAAAACCTTCA
TCACTCACGCGGCGTTGCTCCGTCAGACTTTCGTCCATTGCGGAAGATTCCCTA
CTGCTGCCTCCCGTAGGAGTCTGGGCCGTGTCTCAGTCCCAGTGTGGCCGATCA
CCCTCTCAGGTCGGCTACGCATCGTTGCCTTGGTGAGCCGTTACCTCACCAACT
AGCTAATGCGCCGCGGGTCCATCTGTAAGTGGTAGCTAAATGCCACCTTTTATA
ATTGAACCATGCGGTTCAATCAAGCATCCGGTATTAGCCCCGGTTTCCCGGAGT
TATCCCAGTCTTACAGGCAGGTTACCCACGTGTTACTCACCCGTCCGCCGCTAA
CATCAGGGAGCAAGCTCCCATCTGTCCGCTCGACTTGCATGTATTAGGCACGCC
GCCAGCGTTCGTCCTGAGCCAGGATCAAACTCTCCAA

Fig. 3.16SrDNA sequence of *Bacillus* sp.

S000008756 - 0.871 1428 Bacillus sp.; TGS437; AB020195
S000246790 - 0.871 1438 Bacillus mojavensis; JF-2; AY436360
S000358759 - 0.898 1461 Bacillus licheniformis; C16; AY479984
S000362547 - 0.878 1421 bacterium Te21R; AY587808
S000365537 - 0.871 1446 Bacillus sp. TUT1206; AB188212
S000365541 - 0.902 1456 Bacillus sp. TUT1217; AB188216
S000392549 - 0.890 1427 Bacillus licheniformis; Mo1; AF372616
S000425010 - 0.875 1463 Bacillus subtilis; JM4; AY728013
S000434651 - 0.878 1416 Bacillus licheniformis; KL-176; AY030335
S000448045 - 0.888 1458 Bacillus licheniformis; S2; AY052767

```
Query  44   ACCGCCCTATTCGAACGGTACTTGTTCTTCCCTAACAACAGAGCTTTACGATCCGAAAAC  103
            |||||||||||||||||||||||||||||||||||||||||||| ||||||||||||||||
Sbjct  477  ACCGCCCTATTCGAACGGTACTTGTTCTTCCCTAACAACAGAGTTTTACGATCCGAAAAC  418

Query  104  CTTCATCACTCACGCGGCGTTGCTCCGTCAGACTTTCGTCCATTGCGGAAGATTCCCTAC  163
            ||||||||||||||||||||||||||||||||||||||||||||||||||||||||||||
Sbjct  417  CTTCATCACTCACGCGGCGTTGCTCCGTCAGACTTTCGTCCATTGCGGAAGATTCCCTAC  358

Query  164  TGCTGCCTCCCGTAGGAGTCTGGGCCGTGTCTCAGTCCCAGTGTGGCCGATCACCCTCTC  223
            ||||||||||||||||||||||||||||||||||||||||||||||||||||||||||||
Sbjct  357  TGCTGCCTCCCGTAGGAGTCTGGGCCGTGTCTCAGTCCCAGTGTGGCCGATCACCCTCTC  298

Query  224  AGGTCGGCTACGCATCGTTGCCTTGGTGAGCCGTTACCTCACCAACTAGCTAATGCGCCG  283
            ||||||||||||||||||||||||||||||||||||||||||||||||||||||||||||
Sbjct  297  AGGTCGGCTACGCATCGTTGCCTTGGTGAGCCGTTACCTCACCAACTAGCTAATGCGCCG  238

Query  284  CGGGTCCATCTGTAAGTGGTAGCTAAATGCCACCTTTTATAATTGAACCATGCGGTTCAA  343
            |||||||||||||||||||||||||| ||||||||||||||||||||||||||||||||
Sbjct  237  CGGGTCCATCTGTAAGTGGTAGCTAAAAGCCACCTTTTATAATTGAACCATGCGGTTCAA  178

Query  344  TCAAGCATCCGGTATTAGCCCCGGTTTCCCGGAGTTATCCCAGTCTTACAGGCAGGTTAC  403
            ||||||||||||||||||||||||||||||||||||||||||||||||||||||||||||
Sbjct  177  TCAAGCATCCGGTATTAGCCCCGGTTTCCCGGAGTTATCCCAGTCTTACAGGCAGGTTAC  118

Query  404  CCACGTGTTACTCACCCGTCCGCCGCTAACATCAGGGAGCAAGCTCCCATCTGTCCGCTC  463
            ||||||||||||||||||||||||||||||||||||||||||||||||||||||||||||
Sbjct  117  CCACGTGTTACTCACCCGTCCGCCGCTAACATCAGGGAGCAAGCTCCCATCTGTCCGCTC  58

Query  464  GACTTGCATGTATTAGGCACGCCGCCAGCGTTCGTCCTGAGCCAGGATCAAACTCT  519
            |||||||||||||||||||||||||||||||||||||||||||||||||||||||||
Sbjct  57   GACTTGCATGTATTAGGCACGCCGCCAGCGTTCGTCCTGAGCCAGGATCAAACTCT  2
```

Fig. 4. BLAST result hits obtained from NCBI for *Bacillus* sp. 16SrDNA sequence.

PART 2

PURIFICATION AND CHARACTERIZATION OF API FROM THERMO TOLERANT *BACILLUS LICHENIFORMIS*

SUMMARY

The indispensable nature of the aspartic proteases in numerous physiological functions has evoked tremendous response towards isolating new inhibitors from various resources. After extensive screening, a thermo tolerant *Bacillus licheniformis* was isolated, which produces an aspartic protease inhibitor (API). The organism produced API in the peptone beef extract complex media at 50°C and pH 7. The extracellular culture filtrate of *Bacillus licheniformis* was subjected to activated charcoal treatment, ultra filtration and gel filtration to remove the high molecular weight impurities and salts. The gel filtration fractions showing anti pepsin activity were concentrated and loaded in C-8 pre- packed column for rp-HPLC. The anti pepsin activity was associated with the peak A, having a retention time of 5.966 min and other eluted peak B with retention times 7.649, showed no inhibitory activity. Homogeneity of the active fractions was indicated by the single peak as analyzed on rp-HPLC and mass spectrometry (MALDI-TOF) showed Mr 1363 Da. Reverse zymographic SDS-gel electrophoresis showed Mr 1358 Da. The amino acid analysis experiments indicate the presence of 12 amino acid residues having a Mr of 1425 Da, which suggest peptidic nature of API. The amino acid sequence of the purified peptide was found to be Asp-Leu-Tyr-Asp-Gly-Trp-Lys-His-Glu-Ala-Glu-Cys-Ile with a pI value of 4.3. The estimated secondary structure contents from the CD analysis were 7% α-helix, 49% β-sheet, and 44% aperiodic structure. API was stable in a broad range of pH (2-11) and temperature (37-80°C). API was stable for 2 ½ hours and 30 minutes at 90°C and 100°C respectively. A very low inhibitory activity of API was recorded against other aspartic proteases like HIV1 protease, plasmapsin II and cathapsin D. The inhibitor didn't show any inhibitory activity against other classes of the proteases like trypsin, chymotrypsin, papain and subtilisin.

INTRODUCTION

The aspartic proteases of pharmaceutical importance such as pepsin (Friedman and Peterson, 1998) plasma renin (Thaisrivongs, 1989), HIV-1 protease (Debouck and Metcalf, 1990), plasmepsin (Rosenthal, 1998) and lysosomal cathepsin D (Scarborough et al., 1993; Ward & Kodama, 1991) have evoked considerable interest for investigating the kinetic role of their inhibitors and are also of interest as therapeutic targets. These enzymes participate in a variety of physiological processes and the onset of pathological conditions (Phylip et al., 2001). Only in the case of the HIV-1 protease have inhibitors of this class of enzymes attained clinical importance (Kakuda et al., 1998; Thaisrivongs, 1994; Lin, 1997; Vacca et al., 1997). The inhibitors of cysteine, serine and metalloproteases are distributed all over throughout the biological world, however, naturally occurring inhibitors of aspartic proteases are relatively uncommon and are found in only certain specialized locations, e.g., the inhibitor peptide released on activation of pepsinogen(s), acetylated pentapeptides (pepstatins) from various species of *Actinomycetes*, proteins from *Ascaris lumbricoides*, inhibitor of protease A from yeast and the renin-binding proteins. This is due mostly to the lack of bioavailability of the potent inhibitors that have been developed. Also, despite the successes of using protease inhibitors for treatment of HIV, there remain a number of problems with current therapies such as overlapping resistance patterns and long-term side (De Clercq, 2002). Traditional approaches for development of inhibitors have involved natural product screening or replacing the scissile bond of a peptide substrate with a non-cleavable isostere. More recently, peptidomimetic research, which has the ultimate goal of developing inhibitors with improved pharmacokinetic properties, has gained importance (Hirschmann, 1991; Ripka and Rich, 1998; Hruby, 2001).

The enzyme Inhibitors serve as probes for kinetic and chemical processes during catalysis that led to a detailed understanding of enzyme catalytic mechanisms and has provided effective therapeutic agents for the treatment of diseases. They help in elucidating the mode of ligand binding, where the ligand may be an inhibitor, substrate, or substrate analogue. Inhibitors are also used for *in vivo* studies to localize and quantify enzymes in organs or to mimic certain genetic diseases that involve the absence of an

enzyme in given biosynthetic pathway. The other applications for inhibitors are the detection of short-lived enzyme-bound reaction intermediates, or the identification of amino acid residues at the active site that are necessary for the catalytic activity of the enzyme. Although in the past decade, the rational drug discovery has taken the movement away from the development of enzyme inhibitors by screening of natural products, the biodiversity widespread in soil, water, insects, and tropical plants still acquire tremendous potential for the isolation of novel and effective enzyme inhibitors. There have been plethora of reports of synthetic aspartic protease inhibitors; however, there is a paucity of reports of such inhibitors from microorganisms. Furthermore, to our knowledge, there are no reports of peptidic inhibitors of aspartic proteases from thermo tolerant microorganisms. We have exploited the vast diversity of natural sample and isolated a thermo tolerant *Bacillus licheniformis*, which produces an aspartic protease inhibitor, API. This part of the present chapter deals with the purification and biochemical characterization of the inhibitor.

MATERIALS AND METHODS

Materials

Acetonitrile and casein were from E-Merck, Germany. Trifluoroacetate (TFA), Pepsin and other chromogenic substrates were from Sigma Chem. Co. USA. AccQ Fluor Reagent and 3.9×150mm column AccQ.Tag from Waters USA. The other materials used were according to materials section of part 1 of this chapter.

Production of the Aspartic Protease Inhibitor

The media composition for the production of aspartic protease inhibitor (API) was as given below:

Glucose - 0.25%

Pepton - 0.187%

Beef extract - 0.75%

Sodium chloride - 0.3%

Magnesium sulfate - 0.1%

Dipotassium hydrogen phosphate - 0.1%

Soyameal - 5%

The pH of the autoclaved medium was adjusted to 7. Production of the inhibitor was carried out by inoculating a loop full of freshly grown culture from Luria Broth agar slants into the inoculums flask containing the liquid media with the above composition. The inoculum was developed in for 24 h in the inoculum's flasks at 50°C. 10 ml of the inoculums was transferred into 500 ml Erlenmeyer flasks containing 100 ml of the above medium and was incubated under shaking conditions (200 rpm) at 50°C for 72 h.

Production optimization and Time Profile for the Production of API

The production of the inhibitor at various time intervals was checked by removing samples at different time intervals and assaying as described below for its anti-pepsin activity. The time course of production of API was estimated in terms of the inhibitor units against pepsin activity taking equal volume of the charcoal treated culture broth for the assay.

Purification of API

The extracellular culture filtrate of *Bacillus licheniformis* was obtained by centrifugation of growth medium constituents at 10000 rpm, at 4°C for 20 minutes. Further the API was purified by ultrafiltration (UM-10 and UM-3), gel filtration (sephadex G-25) and rp-HPLC by using prepacked UltroPac column (fluka RP-C 8) pre-equilibrated with 90% acetonitrile (CH_3CN) and 0.05% trifluoroacetate (TFA). The fractions were eluted on a linear gradient of 0-90% acetonitrile with H_2O containing 0.05% TFA at a flow rate of 0.5 ml/min and monitored at a wavelength of 210 nm. The eluted sample was lyophilized and dissolved in de-ionized water to check the anti-pepsin activity.

Biochemical characterization of API

The molecular weight of the inhibitor was determined by the mass spectroscopy (MALDI-TOF by using *Applied Biosystems Voyager System 6031*) and SDS-PAGE. The Solutions for SDS-PAGE and reverse zymography SDS-PAGE were prepared according to Q.T. Le and Katunuma, 2004.

The amino acid analysis was done by hydrolyzing the 100 pM with 6N HCl for 24 hours. The hydrolyzed amino acids were derivatized with AccQ Fluor Reagent (6-amino quinolyl-*N*-hydroxysuccinimide carbamate) and run on a prepacked rp-hplc 3.9×150mm column AccQ.Tag.

The amino acid sequence of the purified peptide was analyzed with a protein sequencer (ABI Procise Clc Protein Sequencer) and the sequence homology was done manually after retrieving the peptide sequences from the data bank.

Isoelectric point of API was determined by the modified straight tube method using ampholines in the range of pH 3.0-11.0 (Sathivel et al., 1995). Initially a broad range of ampholines were used to locate the approximate value of the pI, further the pH range was narrowed down to determine the exact pI of API using appropriate ampholines.

CD spectra were recorded in a Jasco-J715 spectropolarimeter at ambient temperature using a cell of 1-mm path length. Replicate scans were obtained at 0.1-nm resolution, 0.1-nm band width and at a scan speed of 50 nm/min. Spectra were averages of six scans with the base line subtracted spanning from 280 to 200 nm in 0.1-nm

increments. The CD spectrum of API (10 μM) was recorded in 50 mM HCl. Secondary structure content of API was calculated using the algorithm of the K2d program.

Assay for inhibitory activity of API towards pepsin

10 μl of pepsin (100 μg/ml) and 100 μl inhibitor solution from each step of purification were incubated at 37°C for 10 min in KCl-HCl buffer, pH 2.0. Then 0.5 ml of hemoglobin (1%) dissolved in the same buffer was added and incubated at 37°C for 30 minutes. The reaction was stopped by the addition of 5% trichloric acid (TCA) acidified with 2.25% HCl. One unit of pepsin was defined as the amount of enzyme that produced an increase in absorbance of 0.001 at 280 nm per minute under the conditions of the assay. One protease inhibitor unit was defined as the amount of inhibitor that inhibited one unit of pepsin activity (Anson, 1940).

Assay for inhibitory activity of API towards other aspartic proteases

The inhibitory activity of API in appropriate concentration against other aspartic proteases was determined by assaying the enzymatic catalytic activity using the specific chromogenic substrates at specific pH and temperature in appropriate pH buffers. The HIV-1 PR activity was assayed using the synthetic substrate Lys-Ala-Arg-Val-Nle-p-nitro-Phe-Glu- Ala-Nle-amide (Dash & Rao, 2001). Synthetic substrate Lys-Pro-Ile-Leu-Phe*Nph-Ala-Leu-Lys was used for plasmampsin II (Westlinget et al., 1999) and hemoglobin was used for cathapsin D (Lenney, 1975). The inhibitory activity of API against other class of protease also determined. Synthetic substrates Bz-L-Arg-*p*NA·HCl for trypsin and papain, Bz-Tyr-*p*NA for chymotrypsin and Z-Ala-Ala-Leu-*p*NA for subtilisin were used (Walsh, 1970; Arnon, 1970; Grant and Bradshaw, 1981).

Temperature and pH stability of API

For the temperature stability experiments, API (25 μl) was incubated at temperatures 25-100°C for 6 h and by estimating its inhibitory activity against pepsin at different intervals of time. The pH stability of API was determined by pre-incubating API (25μl) in a range of pH values in appropriate buffers for 1 h and estimating the anti-pepsin activity.

RESULTS

Production of API

The maximum production (250 inhibitor units) of aspartic protease inhibitor, API (activity evaluated against pepsin) was observed at 72 h of growth using a fermentation media containing glucose (0.25%), peptone (0.187%), beef extract (0.75%), NaCl (0.3%), $MgSO_4$ (0.1%), K_2HPO_4 (0.1%) and soyameal (5%). Figure 1 shows the time profile for the production of API by the organism.

Purification of API

The extra-cellular culture filtrate of *Bacillus licheniformis* was subjected to activated charcoal treatment, ultra filtration and gel filtration to remove the high molecular weight impurities and salts. The gel filtration fractions 16-26 showing the anti pepsin activity (Figure 2) were concentrated and loaded in C-8 pre- packed column for rp-HPLC. The anti pepsin activity was associated with the peak A, having a retention time of 5.966 min (Figure 3A) and other eluted peak, B with retention times 7.649, showed no inhibitory activity. The fractions showing the inhibitory activity were pooled and lyophilized. Homogeneity of the active fractions containing peak A was indicated by the single peak as analyzed on RP-HPLC with the retention time of 5.966 (Figure 3B). The inhibitor was purified with 466 fold purification. Table 1 summarizes the results for the purification of inhibitor.

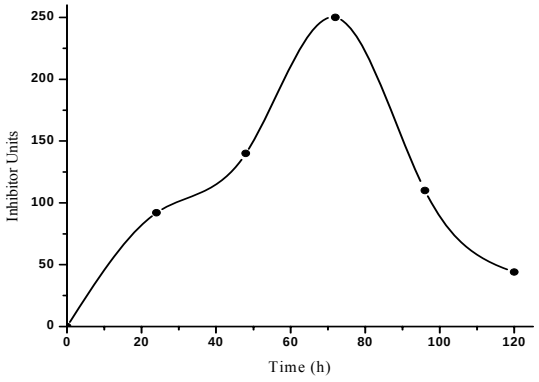

Figure 1. Time profile for the production of API.

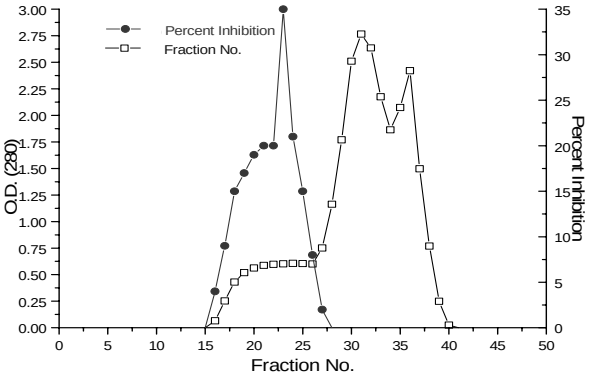

Figure 2. Chromatographic profile of inhibitor on a Sephadex G-25 matrix column. The column was equilibrated with milli Q water, pH 4.0. Protein concentration was determined by absorbance at 280 nm.

Table 1. Purification of API.

Purification Step	Volume (ml)	Total protein (mg)	Total activity (Units)	Specific Activity (Units/mg)	Purification (Fold)	Yield (%)	pH
Centrifugation	750	700	4500	6.428	1	100	8.42
Activated charcoal	600	175	4024	23.00	3.57	89.4	9.30
Ultra filtration 10KDa cut off	575	115	3741	32.53	5.06	83.1	9.19
Ultrafiltration 3 KDa cut off	550	80	3676	46.75	7.27	81.6	9.1
SephadexG-25	10	1.46	2142	1467	228.22	47.6	6.85
Rp-HPLC	3	0.5	1500	3000	466.7	33.3	2.4

Biochemical Characterization of API

Homogeneity of the active fractions containing peak A was indicated by the single peak as analyzed on rp-HPLC, mass spectrometry (MALDI-TOF) showing Mr 1363 Da (Figure 4) and by reverse zymographic SDS-gel electrophoresis showing Mr 1358 Da (figure 5).

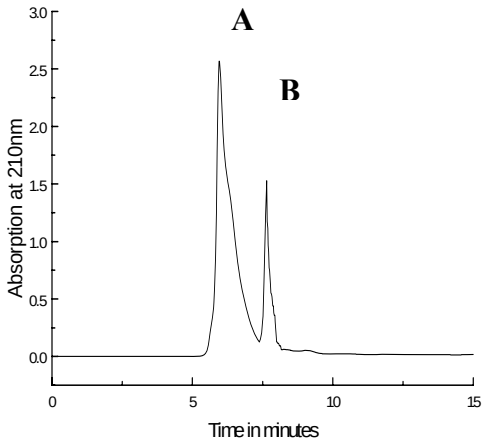

Figure 3A

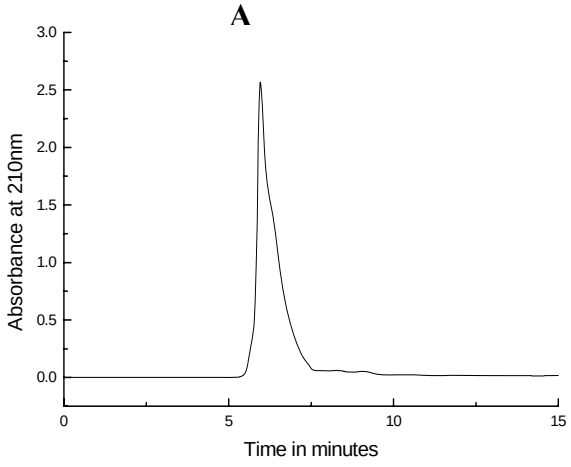

Figure 3B

Figure 2. Reverse phase-HPLC purification of API. (A) 5µl of the lyophilized API sample was loaded on prepacked UltroPac column (fluka RP-C 8) pre-equilibrated with acetonitrile (CH_3CN) and trifluoroacetate (TFA). The fractions containing the peaks A, and B were collected manually and assayed for the anti-pepsin activity. (**B)** 10µl of the pooled fractions containing the peak A (associated with the anti-pepsin activity) was reloaded onto the reverse-phase HPLC system under similar experimental conditions. The peak detected showed a retention time of 5.966 min.

The amino acid analysis experiments indicate the presence of 12 amino acid residues having a Mr of 1425 Da (Figure 6), which suggest peptidic nature of API. API has an amino acid sequence of Asp-Leu-Tyr-Asp-Gly-Trp-Lys-His-Glu-Ala-Glu-Cys-Ile with a pI value of 4.3. The amino acid sequence of the inhibitor was distinctly different from the sequence of the other reported peptidic inhibitors of aspartic proteases. The predominance of the charged amino acid residues in the inhibitor sequence indicates its hydrophilic nature. To evaluate the secondary structure of API, the CD spectra of API analyzed. The estimated secondary structure contents from the CD analysis were 7% α-helix, 49% β-sheet, and 44% aperiodic structure (Figure 7). API was stable in a broad range of pH (2-11) and temperature (37-80°C). API was stable for 2½ hours and 30 minutes at 90°C and 100°C respectively (Figure 8A and 8B).

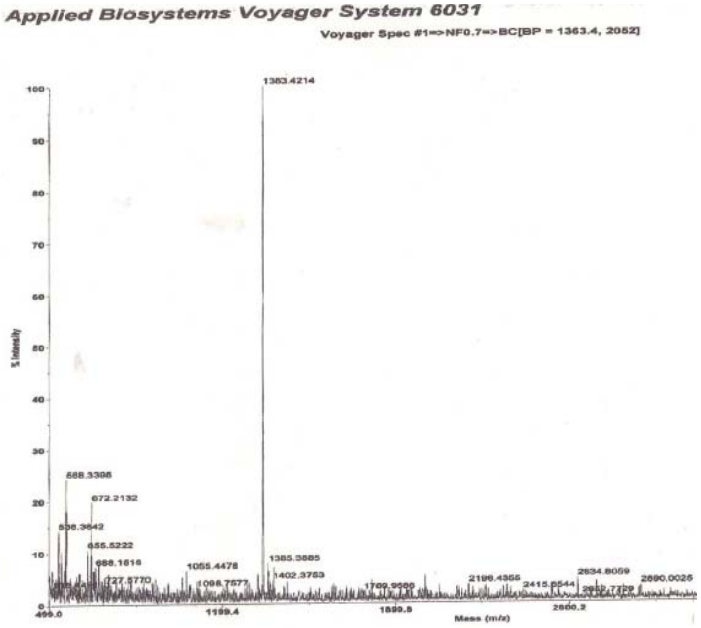

Figure 4. **Molecular mass of API.** The purified API was analyzed for the determination of the Mr by MALDI spectra (1363.46 Da).

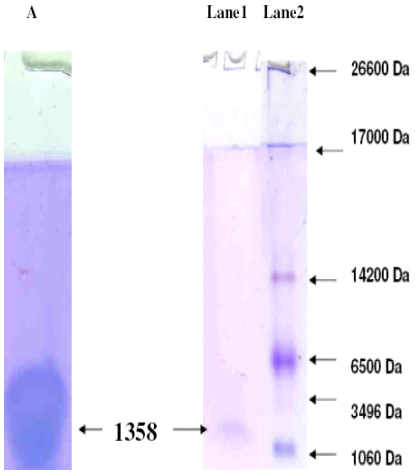

Figure 5. **Reverse zymographic pattern of the inhibitor loaded on the 15% tris-tricine gel.** Lane A shows the reverse zymograph of inhibitor. Lane 1 shows the HPLC purified inhibitor loaded on the 15% tris-tricine gel, lane 2 shows the standard molecular weight marker.

Inhibitory activity of API towards other aspartic proteases

A very low inhibitory activity of API was recorded against other aspartic proteases like HIV1 protease, plasmapsin II and cathapsin D. The inhibitor didn't show any inhibitory activity against other classes of the proteases like trypsin, chymotrypsin, papain, and subtilisin.

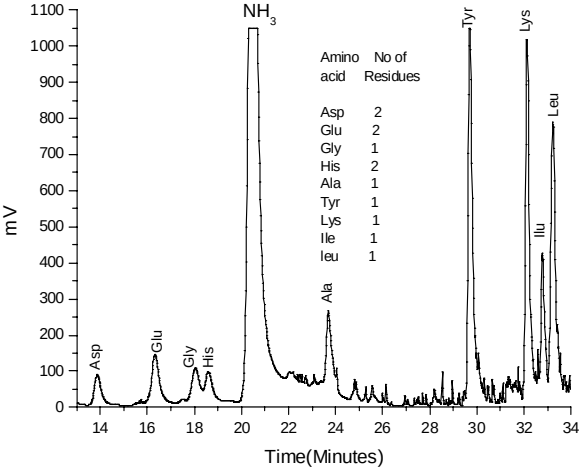

Figure 6. Amino acid analysis of API done by hydrolyzing 100nM peptide with 6N HCl for 24 hours and run on a prepacked rp-hplc column after derivatizing with AccQ Fluor Reagent.

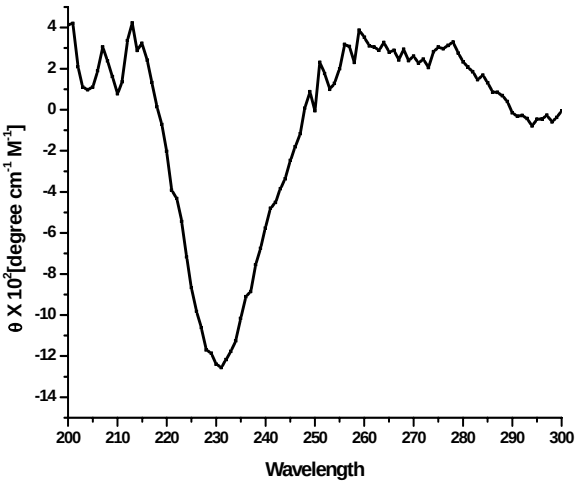

Figure 7. Far-UV CD spectra analysis of API to analyze the secondary structure. API dissolved in 0.05N HCl and the CD spectra were recorded from 300 to 190 nm at 25 °C.

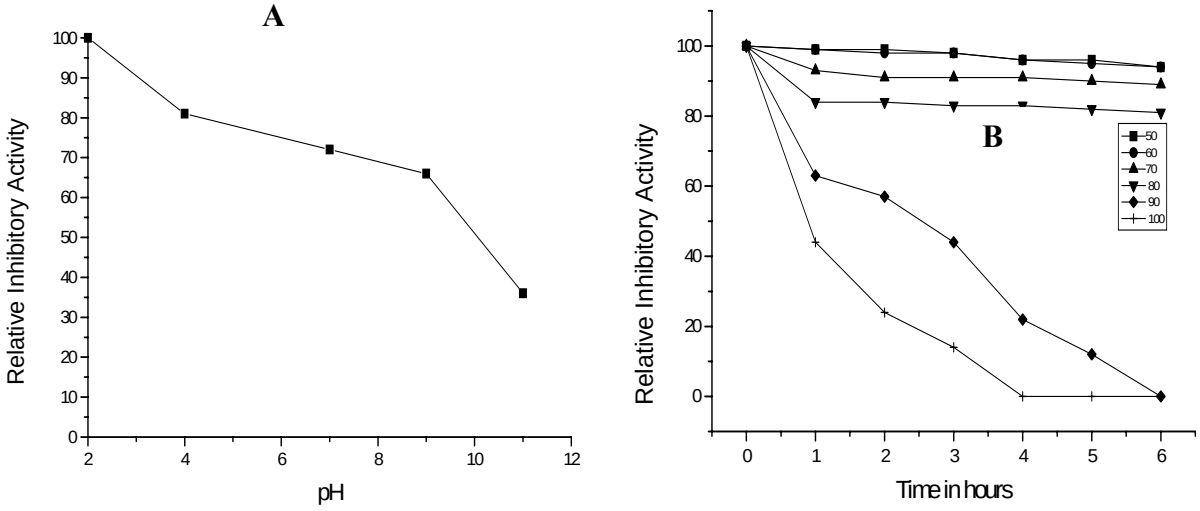

Figure 8. pH and temperature stability of API. **(A)** API was treated with various buffers of different pH and its anti-pepsin activity was determined. (**B)** API was incubated at 50 (■), 60 (●), 70 (▲), 80(▼), 90 (♦), and 100 °C (+) for the time specified and the anti-pepsin activity was determined at 37°C.

PART 3

INTERACTION OF API WITH PEPSIN: IMPLICATIONS IN THE MECHANISM OF INACTIVATION

SUMMARY

The Kinetic studies of Pepsin-API interactions reveal that API is a slow-tight binding competitive inhibitor of pepsin with the IC_{50} and K_i values 4.0 nM and (3.83 nM-5.31nM) respectively. The overall inhibition constant K_i* value is 0.107 ± 0.015 nM. The progress curves are time-dependent and consistent with slow-tight binding inhibition: E + I ⇄ (k_4, k_5) EI ⇄ (k_6, k_7) EI*. Rate constant k_6 =2.73 ± 0.32 s^{-1} reveals a fast isomerization of enzyme-inhibitor complex and very slow dissociation as proved by k_7=0.068±0.009s^{-1}. The Rate constants from the intrinsic tryptophanyl fluorescence data is in agreement with those obtained from the kinetic analysis; therefore, the induced conformational changes were correlated to the isomerization of EI to EI*. On the basis of our foregoing results, it is concluded that, concomitant with the kinetic characterization; fluorescence studies will be useful for the evaluation of inhibitor kinetic constants in the absence of enzyme turnover number and the deciphering the inhibition mechanism of aspartic proteases by slow tight binding inhibitors.

INTRODUCTION

Pepsin is a well studied enzyme whose activity has been extensively studied since Northrop crystallised it in 1929 (Northrop, 1930). It belongs to the family of the aspartic proteases, together with catepsin D, quinosine, renine and the HIV-protease. The recognition of the HIV-protease as a member of this family (Pearl and Taylor, 1987) has renewed the interest in this type of enzymes and in their inhibition (Velazquez-Campoy et al., 2000). There is a wide range of specific inhibitors that can bind to the active site and electively remove the activity of pepsin. One of the best known ones is pepstatin (Umezawa, 1970) that, at acidic pH, tightly binds to the catalytic site of both pepsin and its precursor: pepsinogen (Marciniszyn et al., 1976; Glick et al., 1986). The pepstatin-pepsinogen complex, however, cannot be formed above pH 3 because the active site is blocked by a propeptide sequence (Marciniszyn et al., 1976; Cooper et al., 1990; James and Sielecki, 1986). Below pH 5, pepsinogen is self-cleaved to produce active pepsin (McPhie, 1972). Pepsin is a monomeric, two domain, mainly L-protein, with a high percentage of acidic residues (43 out of 327) leading to a very low pI. The catalytic site is formed by two aspartate residues, Asp32and Asp215, one of which has to be protonated, and the other deprotonated, for the protein to be active (Antonov et al., 1978). This occurs in the 1-5 pH intervals (Cornish-Bowden et al., 1969; Lin et al., 1992). Above pH 7, pepsin is in a denatured conformation that retains some secondary structure (McPhie, 1989; Konno et al., 2000). This denaturation is not fully reversible (Favilla et al., 1997), the lack of reversibility being attributed to the N-terminal domain (Lin et al., 1993). In the 5-7 pH interval the conformation of pepsin is poorly characterized. Although some conformational changes experienced by pepsin in the acidic region have been reported (Favilla et al., 1997; Wang and Edelman, 1971), the intermediate conformations associated to them have not been studied in detail.

Enzyme inhibitors with specificity for a target enzyme are of interest for two general reasons. On one hand, their action provides background information for the development of specific bioactive compounds whose action may be beneficial to patients as chemotherapeutic agents. On the other hand, they are useful probes of the kinetic and chemical mechanisms of enzyme-catalyzed reactions. Of particular importance in these

connections are compounds that act as inhibitor analogs of substrates and have high affinities for enzymes with *K*i values in nM range and less. The classification of inhibitors depends on the reversibility, strength and rates of their interaction with enzyme. The four categories of reversible inhibitors are classical, tight-binding, slow binding, and slow-tight-binding inhibitors (Morrison, 1982). The categories are generally differentiable based on the ratio of total inhibitor (It) to total enzyme (Et) under experimental conditions and the qualitative time required for attainment of the equilibrium between the enzyme, inhibitor, and enzyme-inhibitor complex. The classification is essentially for inhibitors whose actions cannot be described by Michaelis-Menten kinetics. For classical reversible inhibitors, the affinity for the inhibitor is sufficiently low that It >> Et and the rates at which the inhibitor associate and dissociate from the enzyme are relatively high. When the affinity of an enzyme for the inhibitor is very high, tight-binding situations arise, then the experiment would be performed in concentration regimes where It ≅ Et. Under such conditions steady-state treatments are inadequate and incorrect, even though the net binding and release of inhibitors may be described by fast steps (Morrison, 1969; Henderson, 1972; Cha, 1975; Cha, 1976).

There have been some development of the kinetic theory for tight-binding inhibitors (Goldstein, 1944; Strauss and Goldstein, 1943; Ackermann and Potter, 1949; Reiner, 1959; Eason and Stedman, 1936), but few studies have been undertaken in sufficient detail to test the theoretical predictions. The future development of tight-biding inhibitors for chemotherapeutic purpose will undoubtedly depend on application of kinetic techniques that yield quantitative information about the behavior of the inhibitors. When the structure of tight-binding inhibitor can be correlated with the dissociation constants for the enzyme-inhibitor complexes, a systematic approach can be made towards the synthesis of more effective inhibitors for a particular enzyme. Delineating the inhibition mechanism and understanding of the binding efficiency will thus provide further insight into their *in vivo* efficacy. While classical and tight-binding inhibitors have been recognized for a very long time, awareness of compounds that cause inhibition of enzymes in a time-dependent manner is much more recent (Morrison, 1982; Cha, 1975; Cha, 1976; Williams and Morrison, 1979). A number of enzymatic reactions do not

respond to the presence of competitive inhibitors instantly, but rather display a slow-onset of the inhibition. In some cases the inhibitor interacts slowly with the enzyme, in others the formation of the enzyme-inhibitor complex takes place in a very short time. Such inhibition is called slow-binding inhibition and the inhibitor is refereed to as slow-binding inhibitor (Williams and Morrison, 1979; Szedlacsek and Duggleby, 1995; Sculley et al., 1996). From the kinetic point of view, the possible mechanisms for the slow-binding inhibition phenomena are described in Scheme I. Scheme 1 a assumes that the formation of an EI complex is a single slow step and the magnitude of k_4I is quite small relative to the rate constants for the conversion of substrate to product. However, scheme I b demonstrates the two-step slow-binding inhibition, where the first step involves the rapid formation of a reversible EI complex, which undergoes slow isomerization to a stable, tightly bound enzyme-inhibitor complex, EI* in the second step. The two-step mechanism of inhibition can be considered as the prototype of slow-binding inhibition on a steady state time scale. The ratio between the kinetic constants of k_6/k_7 can be taken as an index of the accumulation of E.I* and the energetic of its formation. The higher the values of k_6/k_7 ratio, the longer-lived is the E.I* and the more likely the inhibitor is to have a useful *in vivo* lifetime. The weakness in the use of classical enzyme inhibitors as drugs of clinical condition is that enzyme inhibition results in the upstream accumulation of the substrate for the enzyme, which has an impact on the isomerization of E.I* to E.I and hence reversal of the inhibition which will be of immense value in clinical applications. Inhibitors, which inhibit the enzyme-catalyzed reactions at concentrations comparable to that of the enzyme and under conditions where the equilibria are set up rapidly, are referred as tight binding inhibitors. The establishment of the equilibria between enzyme, inhibitor, and enzyme inhibitor complexes, in slow binding inhibition occurs slowly on the steady-state time scale (Morrison, 1982), which has been thoroughly reviewed (Morisson and Walsh, 1988; Yiallouros et al., 1998; Ploux et al., 1999; Merker et al., 1990; Pegg and Itzstein, 1994; Kati et al., 1998). As yet, no general paradigm has emerged for relating inhibitor and/or enzyme structure which allows the predictions to be made about the design of compounds that would give rise to slow-binding inhibition. However, understanding the basis of the isomerization of EI

complex to EI* complex could lead to design inhibitors that allow titration of the lifetime of the EI* complex.

Early investigations of pepsin gave rise to a variety of mechanistic proposals, which were resolved in favor of the mechanisms shown in Scheme I (Suguna et al., 1987). E stands for free enzyme, I is free inhibitor, EI is a rapidly forming pre-equilibrium complex and EI* is the final enzyme inhibitor complex. Binding between enzyme and inhibitor may either involve a single step, having a slow association and dissociation rates (Scheme I a) or have an initial fast binding step, followed by a slow reversible transformation of EI to another entity EI* (Scheme 1 b), or have an initial slow inter conversion of the enzyme E into another form E* which binds to the inhibitor by a fast step (Scheme 1 c).

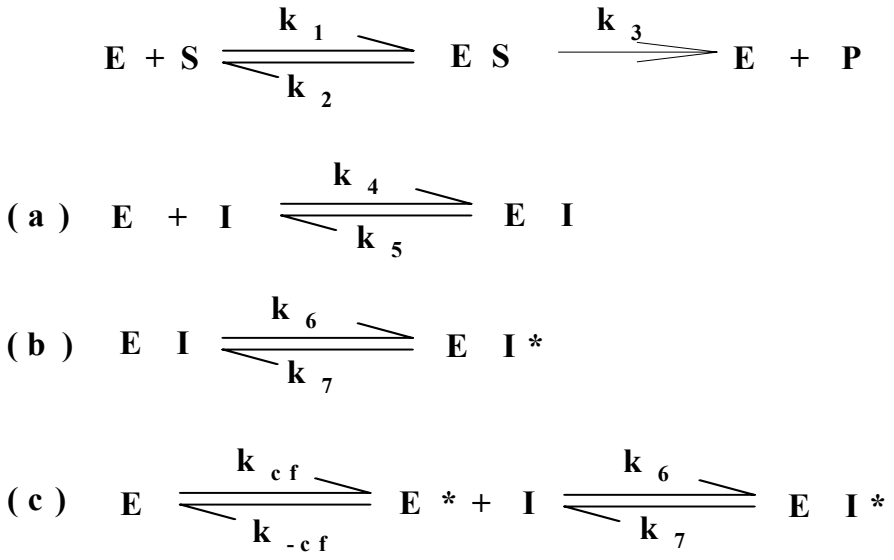

The future development of slow-tight binding inhibitors will undoubtedly depend on application of kinetic techniques that yield quantitative information about the properties of the inhibitors. An efficient inhibitor *in vivo* is characterized not only by its tight-binding but also by the rapid binding to prevent undesirable degradation of biological substrates during the formation of inhibitor complex. Considering the physiological importance of the aspartic proteases and their role in various diseases, there is a lacuna in the studies of slow binding inhibitors, which could provide greater insight into the inhibition mechanism and their *in vivo* efficacies. Investigations of the inhibition

mechanism have generated enormous attention to unravel the interaction between potent inhibitors and the target enzymes. The best-known slow-biding inhibitor of pepsin is pepstatin (Umezawa et al., 1978), with the $t_{1/2}$ for the dissociation 2.5 h. This lifetime is long enough for medicinal chemists to proceed to incorporate the statyl group into design of inhibitors for other proteases such as renin. Several analogs of pepstatin have been prepared to analyze the structural features required to express slow, time-dependent onset of enzyme inhibition (Rich and Sun, 1980). There have been also reports where two approaches have been combined in protease inhibitor design, by the use of a statyl-type residue along with a group that could accumulate as a stabilized tetrahedral (Gelb et al., 1985). However, the hydrophobic nature of pepstatin holds a disadvantage for its poor oral bioavailability.

This part of the chapter deals with the evaluation of the kinetic parameters of the slow-tight binding inhibition of the aspartic proteases pepsin from porcine gastric mucosa by API. API exhibited time-dependent inhibition against pepsin with a two-step binding mechanism. The fluorescence studies revealed that the binding of API induced localized conformational changes in the enzyme, as reflected during the isomerization of the EI complex to EI* complex.

MATERIALS AND METHODS

Assay for inhibitory activity of API towards pepsin for inhibition kinetics

Pepsin was assayed in the presence of the synthetic substrate *N*-acetyl-L-phenylalanyl-L-3, 5-diiodotyrosine (APD) purchased from Sigma-Aldritch, USA. 0.25 ml of the enzyme solution (50 nM) was incubated with 0.125ml of 0.05N HCl at 37°C. After 10 minutes, 0.125 ml of APD solution was added to the test reaction and 0.5 ml of ninhydrin reagent was added to the blanks (final enzyme conc. 12.5 nM). After 30 minutes more, 0.5 ml ninhydrin reagent was added to the test reactions and at any time 0.125 ml of APD solution was added to the blanks. All the tubes were placed in a boiling water bath for exactly 15 minutes and cooled. The contents of tubes were diluted with 2.5 ml of 60% (v/v) ethanol and then shaken to mix the solutions. The absorbance of the solutions at 570 nm was read against water. The activity can be expressed in APD units. One APD unit is the quantity of enzyme which librates 1 micromole of diiodotyrosine per minute under the above conditions (Ryle, 1970). For the kinetic analysis and rate constant determinations, the assays were carried out in triplicate, and the average value was considered throughout this work.

Initial kinetic analysis

The kinetic parameters for the substrate hydrolysis were determined by measuring the initial rate of enzymatic activity. The inhibition constant K_i was determined by Dixon (Dixon, 1953) method and also by the Lineweaver-Burk equation. The K_M value was calculated from the double-reciprocal equation by fitting the data in to the computer software Origin 6.1. For the Lineweaver-Burk analysis, pepsin (12.5 nM) was incubated with API at 1nM and 5nM and assayed at increased concentration of APD (10–100 uM) at 37°C for 30 min. The reciprocals of substrate hydrolysis (1/*v*) for each API concentration were plotted against the reciprocals of the substrate concentrations, and the K_i was determined by fitting the resulting data. In Dixon's method, hydrolytic activity of pepsin (12.5 nM) was measured in the presence of 50 μM and 100 μM APD, at concentrations of API ranging from 1-10 nM at 37 °C for 30 min. The reciprocals of substrate hydrolysis (1/*v*) were plotted against the API concentration and the K_i was determined by fitting the data using ORIGIN 6.1.

Demonstration of the time dependence of inhibition

The API (1-10 nM) from 1 mM stock solution in milli Q water was added to 50nM pepsin in appropriate volume of 50 mM HCl (final conc. 12.5 nM). After 0-30 min of preincubation, 0.25 ml of the pepsin-API mixture was added into 250 μM of APD solution at 37°C. After 30 min, the release of diiodotyrosine was quantified as described above.

Determination of Initial apparent inhibition constants

Inhibition studies were performed by adding 0.25 ml of pepsin (12.5 nM) to 0.25 ml of 1 mM APD solution in standard buffer containing varying concentrations of API (1-10 nM) at 37°C. After 30 min. the release of diiodotyrosine was quantified as described above. Relative enzymatic activity, R, was computed from the ratio of product amounts obtained in the presence and absence of API as $R = 1 - [P]/ (P]_0$. The relative inhibition was fit by nonlinear least-squares regression to eq 1, where $[I]_0$ is the total concentration of API and K_{app}, the fitting parameter, is the apparent inhibition constant.

$$R= [I]_0/(k_{app}+[I]_0) \quad (1)$$

Time dependence of apparent inhibition constants

Experiments were conducted as described above, except that the pepsin was added to API at varying concentrations, and then assayed after preincubation for 0, 15 and 30 min.

Measurement of the reaction progress

1-10 nM API was mixed with 100 μM APD in 0.25 ml of 0.05 N HCL 0.25 ml of pepsin, 12.5 nM, was added to initiate the reaction. Aliquots were removed from 0 minutes to 30 min and product formation was monitored as described above.

Substrate progress curve analysis

The percentage of product formed, p, vs reaction time, t, was fitted to the recursive integral rate equ.2, a variant of a known method for the estimation of K_M and V_{max} from the reaction progress (Duggleby, 1986). The instrumental offset parameter p_0 accounts for the possible systematic error of the detection method. Other optimized parameters in the least-squares regression were the specific molar instrumental response of the reaction product r_P, the Michaelis constant K_M and the maximum velocity V_{max}.

The fixed parameter were the mixing delay time (tD = 0) and the initial substrate concentration $[S]_0$. Auxiliary variables α and [P] are defined in equations (2a) and (2b).

$$p^{(m+1)} = p^{(m)} + r_p(1 - [P]/[S]_0 - \exp \alpha)/(1/[S]_0 - \exp \alpha /K_M) \quad (2)$$

$$\alpha = ([P] - t\, V_{max})/K_M \quad (2a)$$

$$[P] = (p^{(m)} - p_0)/r_p \quad (2b)$$

Inhibitor progress curve analysis

The progress curves for the interaction between API and Pepsin were analyzed using equation 3.

$$p = p_0 + V_s t + (V_o - V_s)[1 - \exp(-k_{app} t)]/k_{app} \quad (3)$$

Each individual progress curve was fitted separately. The local fitting parameters were the initial velocity V_0, the steady-state velocity V_s, the apparent first order rate constant k_{app}, and the instrumental offset p_0. These fitting parameters were analyzed to extract approximate inhibition constants. Several reaction progress curves, obtained in the presence and absence of inhibitor at various concentrations, were combined and fitted as a whole in the eq 4,

$$p = p_0 + r_p[P]t \quad (4)$$

in which the concentration of product $[P]t$ at time t is obtained by numerical integration of the system of differential eqs. 5a-g.

$$d[E]/dt = -k_1[E][S] + (k_2 + k_3)[ES] - k_4[E][I] + k_5[EI] \quad (5a)$$

$$d[S]/dt = -k_1[E][S] + k_2[ES] \quad (5b)$$

$$d[ES]/dt = k_1[E][S] - (k_2 + k_3)[ES] \quad (5c)$$

$$d[P]/dt = k_3[ES] \quad (5d)$$

$$d[I]/dt = -k_4[E][I] + k_5[EI] \quad (5e)$$

$$d[EI]/dt = k_4[E][I] - (k_5 + k_6)[EI] + k_7[EJ] \quad (5f)$$

$$d[EJ]/dt = k_6[EI] - k_7[EJ] \quad (5g)$$

Numerical integration of the differential system (eqs 5a-g) was performed by using the Livermore Solver of Ordinary Differential Equations (Hindmarsh, 1983). A modification of the Marquardt-Levenberg least-squares fitting algorithm (Reich, 1992) as used to perform the regression of experimental data as described by Moss et al., 1996. The optimized fitting parameters were all rate constants except the bimolecular association rate constant k_1, the total enzyme concentration $[E]_0$ for each progress curve

(within 10% titration error), the molar response coefficient *rp*, and the offset *p*0 for each progress curve. The regression analysis was performed by using the computer programs DYNAFIT (BioKin, Ltd., Madison, WI), ORIGIN 6.1, and GRAPH PAD PRISM.

Fluorescence analysis

Fluorescence measurements were performed on a Perkin-Elmer LS50 luminescence spectrometer connected to a Julabo F20 water bath. Protein fluorescence was excited at 295 nm and the emission was recorded from 300 to 500 nm at 25°C. The slit widths on both the excitation and emission were set at 5 nm and the spectra were obtained at 1 nm/min. Fluorescence data were corrected by running control samples of buffer and smoothed. For inhibitor binding studies, pepsin (8.2 nM) dissolved in 0.05N HCL. Titration of pepsin with API was performed by the addition of different concentrations of API each time to a new pepsin solution. The magnitude of the rapid fluorescence decrease (F_0 - F) occurring at each inhibitor concentration was computer fitted to the equation $(F_0 - F) = \Delta F_{max} / \{1 + (K_i/ [I])\}$ to determine the calculated value of K_i and ΔF_{max}. The first-order rate constants for the slow loss of fluorescence, k_{obs}, at each API concentration [I] were calculated by computer fitting of the remaining data, starting 1 sec after inhibition addition, to a first order equation y = a + b*exp ($-k_{obs}$*t) using ORIGIN 6.1 software (origin lab). These values of k_{obs} were then computer fitted to the equation $k_{obs} = k_6 [I] / (K_i + [I])$ for the determination of k_6 under the assumption that, for a tight-binding inhibitor, k_7 can be considered negligible at the onset of the slow loss of fluorescence (Houtzager et al., 1996). Time courses of the protein fluorescence following the addition of inhibitor were measured for up to 5 min with excitation and emission wavelengths fixed at 295 and 342 nm, respectively. Data points were collected at 1.0 s intervals during time courses. Corrections for the inner filter effect were performed as described by the formula $F_c = F \text{ antilog } [(A_{ex} + A_{em})/2]$, where Fc and F are the corrected and measured fluorescence intensities, respectively, and A_{ex} and A_{em} are the solution absorbance at the excitation and emission wavelengths, respectively (Lakowicz, 1983). Background buffer spectra were subtracted to remove the contribution from Raman scattering.

RESULTS

Determination of K_M and K_i

API was found to inhibit pepsin with an IC_{50} value (50% inhibitory concentration) of 4.2 nM (Figure 1). The inhibition of pepsin followed a hyperbolic pattern with increasing concentrations of the inhibitor. However, the secondary plot (the slope of inhibition graph versus API concentration) was not linear, suggesting that the application of Michaelis-Menten inhibition kinetics was not appropriate in this study. The inhibition constant K_i, determined by the classical double reciprocal Dixon plot was 4.0 nM (Figure 2), which is almost equal to the IC_{50} value of the inhibitor. The Lineweaver-Burk reciprocal plot (Figure 3) showed that API was a competitive inhibitor of pepsin and the K_M value for the pepsin of APD was 77µM and K_i value was 4.5 nM.

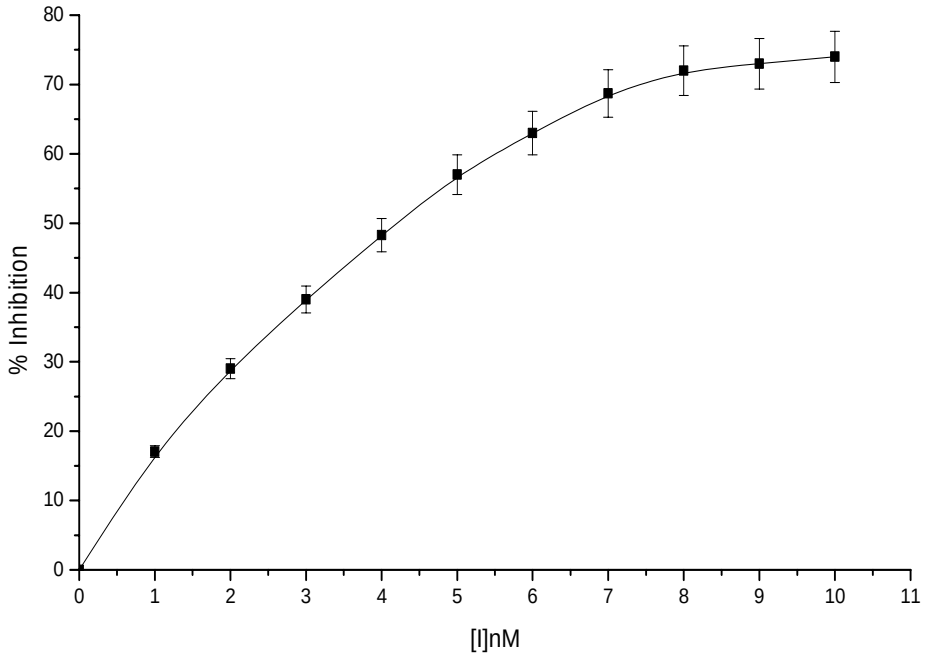

Figure 1. The hyperbolic curve indicates the best fit for the percentage inhibition data obtained, and the IC_{50} value was calculated from the graph.

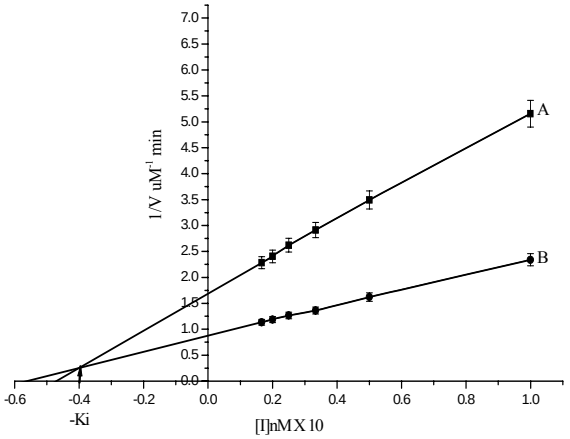

Figure 2. Enzymatic activity of the pepsin (12.5 nM) was estimated using the substrate APD=100 μM (B) and 200 μM (A) at different concentrations of API for determining *Ki* value from Dixon plot.

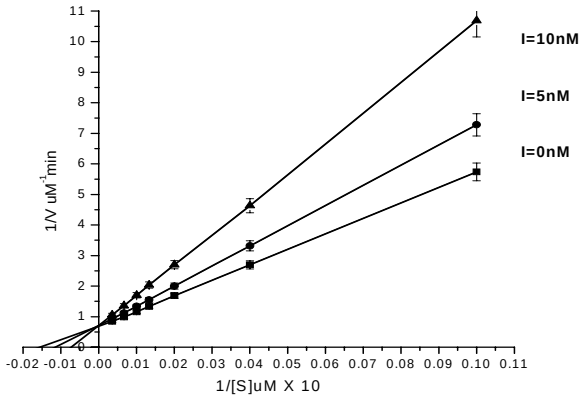

Figure 3. Pepsin (12.5 nM) was incubated, without (■) or with API at 5 nM (●) and 10 nM (▲) concentrations and assayed at increasing concentrations of the substrate for determining K_i value from Lineweaver-Burk plot.

Substrate Kinetics

A preliminary substrate kinetic analysis was performed by using the standard initial velocity method, which gave K_M of 77 μM of APD for pepsin. A more accurate estimate of K_M and V_{max} came from the analysis of the substrate progress curve. Figure 4 shows the results of nonlinear least-squares fit to equ. 2. The initial substrate concentration, $[S]_0$, was fixed at 200 μM, while the best-fit values of the adjustable fitting parameters were V_{max} = 0.207 ± 0.02 nM s^{-1}, K_M = 66 ± 0.5 μM , *r*p =0.478 ± 0.007 au nM^{-1}, and *p*0= -0.21 ± .05 au. The arbitrary unit (au) of molar response is defined as percent of product formed in the reaction. From the results of fit, the maximum velocity expressed in the arbitrary units is 0.478 × 0.207 = 0.099% of product per second, and for control, the maximum conversion is 0.478 ×200 + 0.21 =95.8% of product.

The progress curves collected at different substrate concentrations (10, 20, 50, 100, 150, and 200 μM) showed the possibility of product inhibition (Figure 5). The data were fitted simultaneously to the mathematical model for the simple Michaelis-Menten reaction mechanism, represented by the system of differential equations (equ. 6a-d) and the response function (equ. 4). While the bimolecular association rate constant k_1 was kept constant at 10^8 $M^{-1}s^{-1}$, as was the assumed enzyme concentration (50nM), the best-fit values of the remaining rate constants were k_2 = 66.2 ± 1.7 s^{-1} and k_3 =0.9±0 .024 s^{-1}.

$$d[E]/dt = -k_1[E][S] + (k_2 + k_3)[ES] \quad (6a)$$

$$d[S]/dt = -k_1[E][S] + k_2[ES] \quad (6b)$$

$$d[ES]/dt = k_1[E][S] - (k_2 + k_3)[ES] \quad (6c)$$

$$d[P]/dt = k_3[ES] \quad (6d)$$

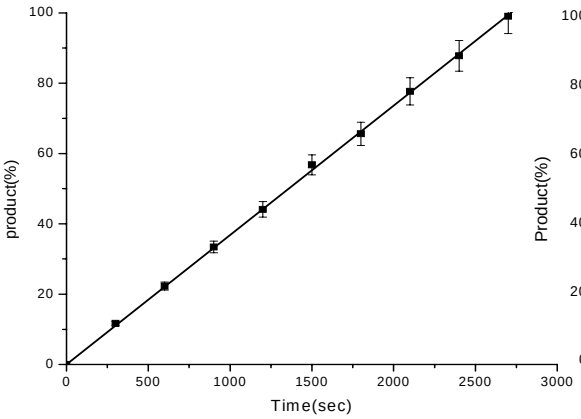

Figure 4. The substrate curve kinetics. Least-squares fit of substrate progress curve (12.5 nM Pepsin, 200 μM APD) to the modified integral Michaelis-Menten eq 2. The best-fit values and standard errors of adjustable parameters were V_{max} =0.207 ± 0.02 nM s^{-1}, K_M = 6.6×10^4 ± 0.5 nM, rp =0.478 ± 0.007 au nM^{-1}, and p0= -0.21 ± .05 au, where the arbitrary unit (au) is the percentage of the product formed.

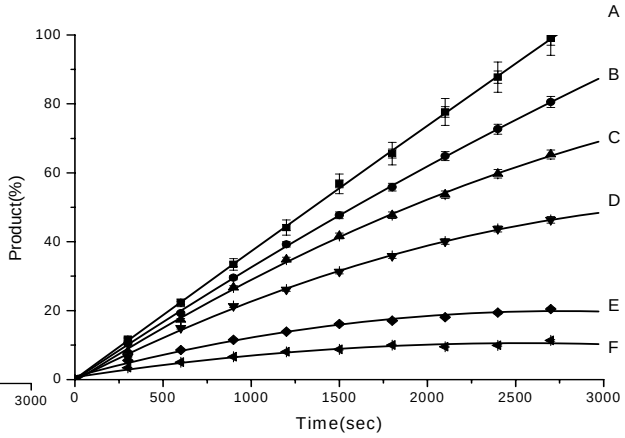

Figure 5. Simultaneous least-squares fit of substrate progress curves to equ. 4 and the system of differential eqs. 6a-d. The constant parameters were $[E]_0$ = 12.5 nM, and p0= 0. Substrate concentrations were 10, 20, 50, 100, 150 and 200 μM, respectively, for curves A-F. The best-fit values and standard errors of adjustable parameters were k_2 = 6.62±0.17 s^{-1}, k_3 = 0.9±0.024 s^{-1}, and r_P =.91 ± 0.1 cpm nM^{-1}.

Pre-incubation experiments with API

Pre-incubation experiments show that, whether the API, was time-dependent inhibitor of the pepsin. The concentration of APD was set to a value below the Michaelis constant (K_M) 50 μM, so that the reactions were approximately first-order in APD. API showed time dependent inhibition (Figure 6). The results from the pre-incubation experiments with the API are shown in Table 1. The apparent inhibition constants decreased 5 fold over a 30 min period (Figure 7).

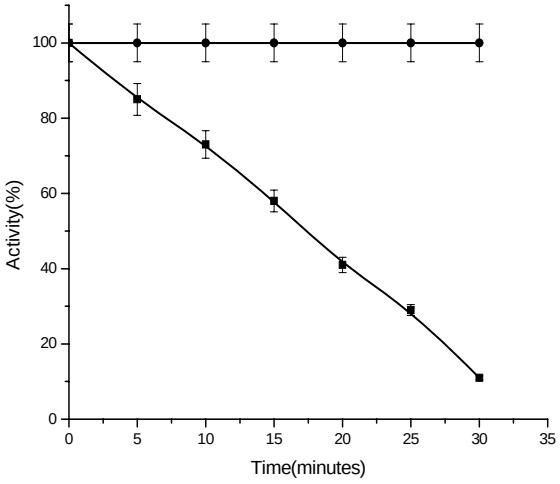

Figure 6. Loss of residual enzyme activity upon pre-incubation of pepsin (12.5 nM) with API (10 nM, squares) and Control (no inhibitor) is represented by circle. See Experimental Procedures for details.

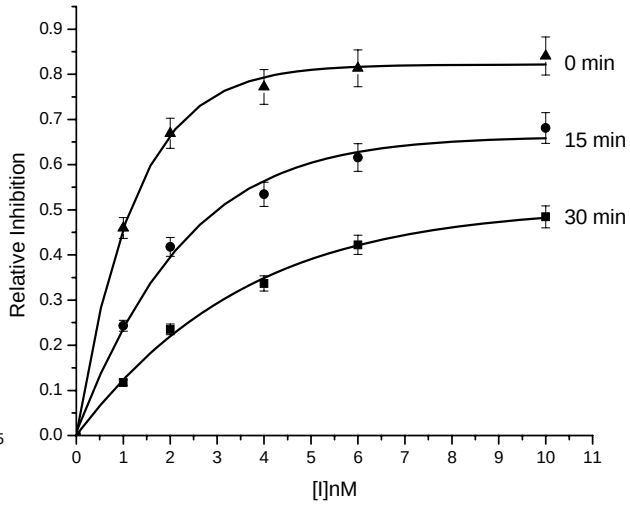

Figre 7. The pre-incubation kinetic studies. Apparent Inhibition Constants with or without pre-incubation of API (0-10 nM) with pepsin (12.5nM). Results are described in table-2.

Table 2. Apparent inhibition constants with or without pre-incubation of inhibitor (0-10 nM) with Pepsin (12.5 nM).

----------k_{app} (nM)[a]----------		
t =0 min	t = 15 min	t = 30 min
5.0 ±0.12	2.1±0.14	0.99±0.18

[a]Pepsin was pre-incubated with varying concentrations of inhibitor for 0, 15, or 30 min before the assay. Remaining residual enzyme activity was measured in a 30 min assay.

Regeneration of pepsin activity after inhibition

The API was tested to determine if it was a reversible inhibitor. Pepsin (12.5 nM) was pre-incubated with and without the equimolar concentration of API for 60 minutes in 0.05N HCl. Further, the enzyme inhibitor mixture was diluted 100 fold into the assay mixture containing the substrate at 10 K_M. After pre-incubation, 1.0 ml of sample was removed and diluted to 10.0 ml in 0.05N HCl. At the specified time, aliquots were removed and assayed for the proteolytic activity. From the rate of product formation, the recovered enzyme concentration could be estimated as approximately 6 nM and the

reduction of APD was observed at a steady-state velocity of approximately 47% relative to the control.

Simplified Progress curve analysis for API

The reaction progress was analyzed by two different methods (Moss et. al., 1996). The results of a preliminary analysis, based on the assumption of rapid equilibrium, are shown in Figure 8. The progress curves obtained at 1, 2, 4, 6 and 10 nM API were fitted individually to eq 3. The best-fit values of adjustable parameters, for each concentration of the API, are listed in Table 2.

For a one-step inhibition mechanism, without an intermediate enzyme-inhibitor complex, the initial velocity V_0 should be constant, and the apparent rate constant k_{app} should increase linearly with the inhibition concentration $[I]_0$. These properties of the one-step mechanism are expressed in eq. 7a-c (Szedlacsek & Duggleby, 1995).

$$V_0 = V_{max}[S]_0/([S]_0 + K_M) \quad (7a)$$

$$V_S = V_{max}[S]_0/([S]_0 + K_M(1 + [I]_0/K_i)) \quad (7b)$$

$$k_{app} = k_7 + k_6[I]_0/(1 + [S]_0/K_M) \quad (7c)$$

On the other hand, for a two-step mechanism (Scheme 1), the initial velocity should decrease with the inhibitor concentration, by following a typical binding curve, and the apparent rate constant should depend on $[I]_0$ as a hyperbola, according to eq. 8a-c.

$$V_0 = V_{max}[S]_0/([S]_0 + K_M(1 + [I]_0/K_i)) \quad (8a)$$

$$V_S = V_{max}[S]_0/([S]_0 + K_M(1 + [I]_0/K_i^*)) \quad (8b)$$

$$k_{app} = k_7 + k_6([I]_0/K_i)/(1 + [S]_0/K_M + [I]_0/K_i) \quad (8c)$$

The parameters listed in Table 2 favor the two-step mechanism, because the initial velocity does decrease with the concentration of the inhibitor, as predicted by eq 8a. Also, the increase of the apparent rate constant with $[I]_0$ is hyperbolic, instead of linear. The nonlinear least squares fit of V_0, V_S, and k_{app} to eq. 8a-c is shown in Figure 9. From fitting of V_0 to eq. 8a, the dissociation constant K_i of the initial complex is 3.83 ± 0.41 nM; the fitted value of V_{max} is 0.097 ± 0.001 au s^{-1}, in good agreement with the substrate kinetic analysis V_{max} was 0.099 au s^{-1} from fitting the substrate progress curve in Fig. 6. From fitting of V_S to eq. 8b, the overall dissociation constant K_i^* is 0.0431 ± 0.005 nM; the fitted value of V_{max} is 0.098 ±0.001 au s^{-1} in this case. From fitting of k_{app} to eq. 8c (fig. 8B *inset*), the initial inhibition constant K_i was 4.42 ± 0.12 nM. The isomerization

rate constants were $k_6 = 5.94 \pm 0.1 \times 10^{-2}$ s^{-1} and $k_7 = 0.217 \pm 0.06 \times 10^{-2} s^{-1}$, from which the total dissociation constant $K_i^* = K_i k_7 / k_6$ is 0.16 nM.

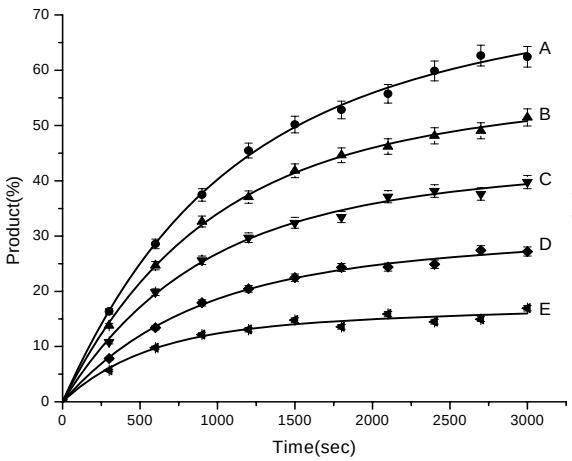

Figure 8. Least-squares fit of progress curves from the inhibition of pepsin (12.5 nM) by API to equ. 3. The initial substrate concentration was 200 μM. The API concentrations were 1, 2, 4, 6 and 10 nM for curves A-E, respectively. For experimental condition and the best-fit values of adjustable parameters see text.

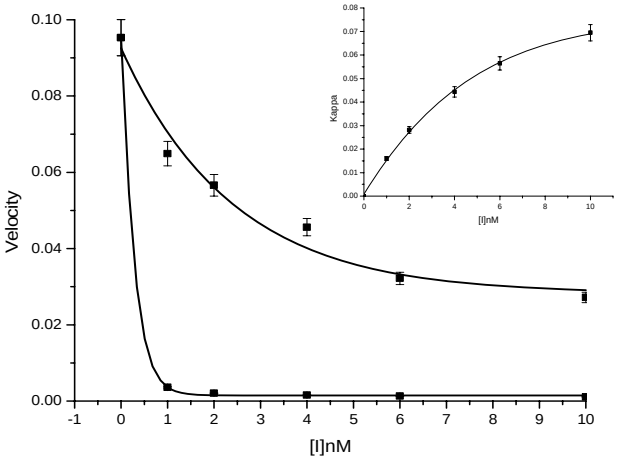

Figure 9. Least-squares fit of the initial velocities V_0 from Table 3 to eq. 8a, the steady-state velocity V_S to eq. 8b, and the apparent first-order rate constant k_{app} to eq. 8c. The best fit values of adjustable parameters k_i, k_i^*, k_6, and k_7 are listed in the text

The inhibition progress curves for inhibitor were analyzed more thoroughly by using a complete differential model where the rapid equilibrium assumption is not made (Moss et. al., 1996). The collection of progress curves in Fig. 8 was fitted as a whole to the system of eqs. 4 and 5. The constant parameters were the initial concentration of the substrate ($[S]_0$ = 200 μM) and the API ($[I]_0$ = 0, 1, 2, 4, 6, and 10 nM), the initial concentration of the pepsin in the assay where inhibitor was absent ($[E]_0$=12.5 nM), and the bimolecular rate constant for the formation of the Michaelis complex (k_1 = 100 μM^{-1} s^{-1}). The best-fit values of globally optimized parameters were $k_2 = 4.92 \pm 0.5$ s^{-1}, $k_3 = 0.98 \pm 0.02$ s^{-1}, $k_4 = 5.1 \pm 0.5$ nM^{-1} s^{-1}, $k_5 = 21.43 \pm 2.5$ s^{-1}, $k_6 = 2.73 \pm 0.32$ s^{-1}, $k_7 = 0.068 \pm 0.006$ and $r_P = 0.45 \pm 0.02$. All enzyme concentrations in assays where the inhibitor was present were considered as locally optimized parameters, within the estimated 10% titration error. The best fit values of locally optimized concentrations were $[E]_0 = 13 \pm 1$ nM, [E]0 = 15 ± 2 nM, $[E]_0 = 13 \pm 1$ nM, $[E]_0 = 11 \pm 0.5$ nM, and $[E]_0 = 12 \pm 1$ nM, for

the assays at 1, 2, 4, 6, and 10 nM API, respectively. From the best-fit values of rate constants k_4 and k_5, the dissociation constant of the initial complex, K_i, was calculated as k_5/k_4 = 4.33 nM. Similarly, the overall dissociation constant of the final complex, K_i*, was calculated as k_5k_7/k_4k_6 = 0.107 nM. This value is bracketed by the results obtained by the simplified method above, as shown in Table 4 (K_i* = 0.043 nM and 0.16 nM by using eq 8b or 8c, respectively). The kinetic constants determined in this study are summarized in Table 3.

Table 2. Best-Fit Values of Adjustable Parameters, Obtained in Fitting the Progress Curves Shown in Figure 8 (12.5 nM pepsin, 200 µM APD, pH 1.5, 37 ˚C) to Equation 3.

$[I]_0$ (nM)	V_S (%P s^{-1})	V_0 (%P s^{-1})	k_{app} (s^{-1})
0[a]	0.0953	0.0953	---------
1	0.00359	0.0649	0.01600
2	0.00205	0.0506	0.02813
4	0.00160	0.0456	0.04433
6	0.00129	0.0322	0.05064
10	0.00107	0.0272	0.06948

[a] Initial velocity from fitting the substrate progress curve shown in Figure 8.

Effect of API binding on the Fluorescence of pepsin

The kinetic analysis revealed a two-step inhibition mechanism, where the *E*I complex isomerizes to a tightly bound, slow dissociating *E*I* complex. This isomerization is a consequence of the conformational changes induced in pepsin due to the binding of API. The tryptophanyl fluorescence of pepsin exhibited an emission maxima (λ_{max}) at 342 nm, as a result of the "radioactive" decay of the π-π* transition from the Trp residues (Figure 10). The binding of inhibitor resulted in a concentration-dependent quenching of the fluorescence with saturation reaching at or above 10nM inhibitor (Fig. 10 *inset*). The absence of blue or red shift in λ_{max} negated any drastic gross conformational changes in the three-dimension structure of the enzyme due to API binding. Binding of API resulted an exponential decay of the fluorescence intensity as indicated by a sharp decrease in the quantum yield of fluorescence followed by a slower

decline to a stable value. Furthermore, titration of inhibitor against pepsin revealed that the magnitude of the initial rapid fluorescence loss (F_0-F) increased in a saturation-type manner (Figure 11), which corroborated the two-step slow-tight binding inhibition of pepsin by inhibitor.

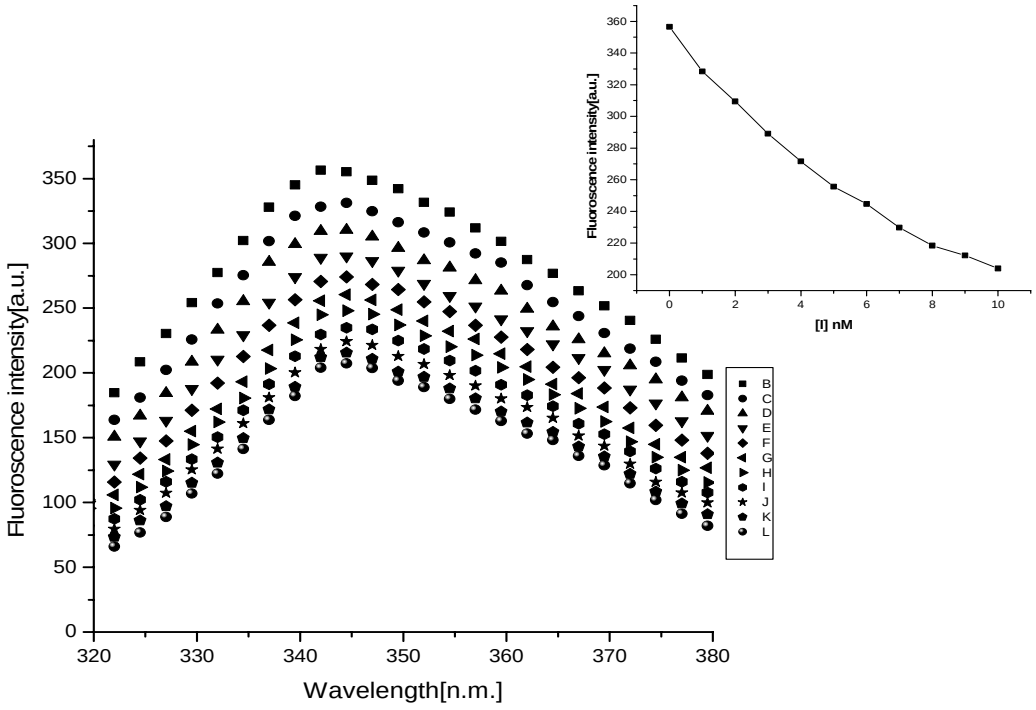

Figure 10. Steady-state fluorescence emission spectra of pepsin as a function of inhibitor. Protein fluorescence was excited at 295 nm, and emission was monitored from 320–380 nm at 25 °C. Titration was performed by the addition of different API concentrations to a fixed concentration of pepsin. Concentrations of API used were 0-10 nM (B-L). The curve in the *inset* represents the best fit of the fluorescence quenching data of pepsin at 342 nm (λ_{max}) as a function of API concentration.

The value of K_i determined by fitting the data for the magnitude of the rapid fluorescence decrease (F_0-F) was 4.74±0.19 nM. The subtle conformational changes induced during the isomerization of EI to EI* was monitored by analyzing the tryptophanyl fluorescence of the complexes as a function of time (Figure 12). The k_6 and K_i values were determined from the data derived from the slow decrease in fluorescence were 2.42±0.2s^{-1} and 5.31±0.5 respectively (fig 13). These rate constants are in good

agreement with that obtained from the kinetic analysis (table 4). Therefore, the initial rapid fluorescence decrease can be correlated to the formation of the reversible complex EI, whereas the slow, time-dependent decrease reflected the accumulation of the tight bound slow dissociating complex *E*I*.

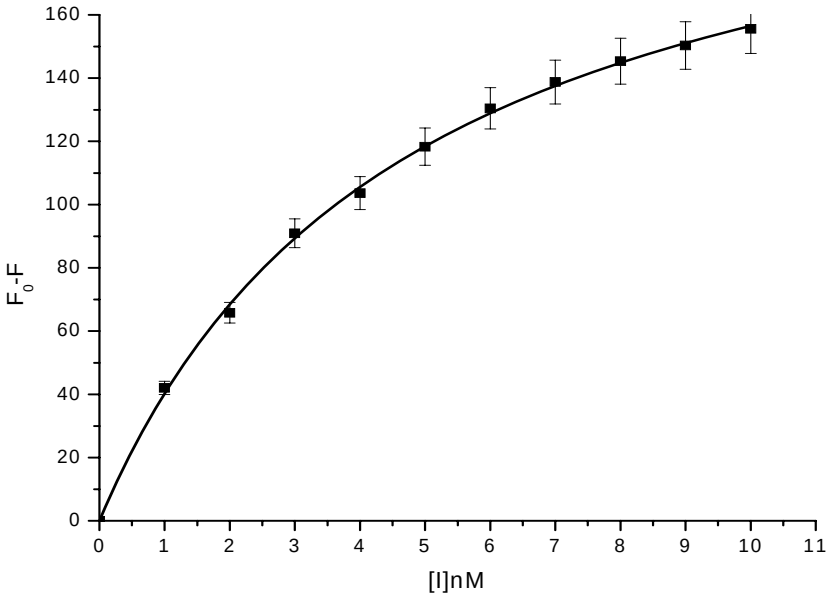

Figure 11. The fluorescence changes (F_0-F) were plotted against the API concentrations. The resulting hyperbola curve was fitted to the equation ((F_0 - F) = Δ F_{max} / (1 + (K_i/ [I])) to give the calculated value of K_i.

Table 3. Summary of Kinetic Constants[a].

Method	K_i (nM)	K_i* (nM)	k_4 (nM^{-1} sec^{-1})	k_5 (sec^{-1})	k_6 (sec^{-1})	k_7 (sec^{-1})
A[b]	3.83±0.41	0.0431±0.005				
B[c]	4.42±0.12	0.16± 0.03			0.0594±0.005	0.00217±.0006
C[d]	4.33±0.15[e,]	0.107±0.015 [e,]	5.1±0.5	21.43±2.5	2.73±0.32	0.068±0.009
D[f]	4.74±0.19					
E[g]	5.31±0.5				2.42±0.2	
F[h]	4.0±0.3					
G[i]	4.5±0.45					

[a]Uncertainties of parameters expressed with the "±" sign are standard errors from nonlinear regression. [b] From fitting initial velocities V_0 and pseudo-steady-state velocities V_S to eqs 8a and 8b, respectively. [c] From fitting apparent first-order rate constants to eq 8c. [d] From fitting progress curves to differential eqs. 5a-c. [e]Computed from rate constants. [f] From fitting progress curves to equation (F_0 - F) = Δ F_{max} /{1 + (K_i/[I])}.[g]From fitting progress curves to equation k_{obs} = k_6 [I] / (K_i + [I]). [h] From initial kinetics with inhibitor (fig 2). [i] From initial kinetics with inhibitor (fig 3).

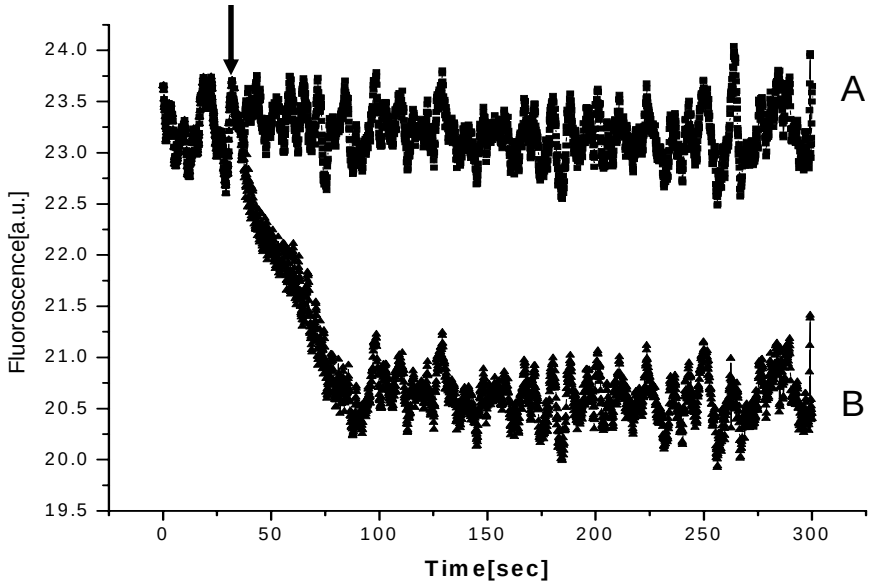

Figure 12. Time-dependent effect of API on the fluorescence quenching of pepsin. **(A)** API was added to pepsin (8.2 nM) at the specified time (indicated by the *arrow*), and the fluorescence emission was monitored for 300 s, at a data acquisition time of 0.1 s. The excitation and emission wavelength were fixed at 295 and 342 nm, respectively. The data are the average of five scans with the correction for buffer and dilutions. The concentrations of inhibitor used were 0 nM (A), 5 nM (B).

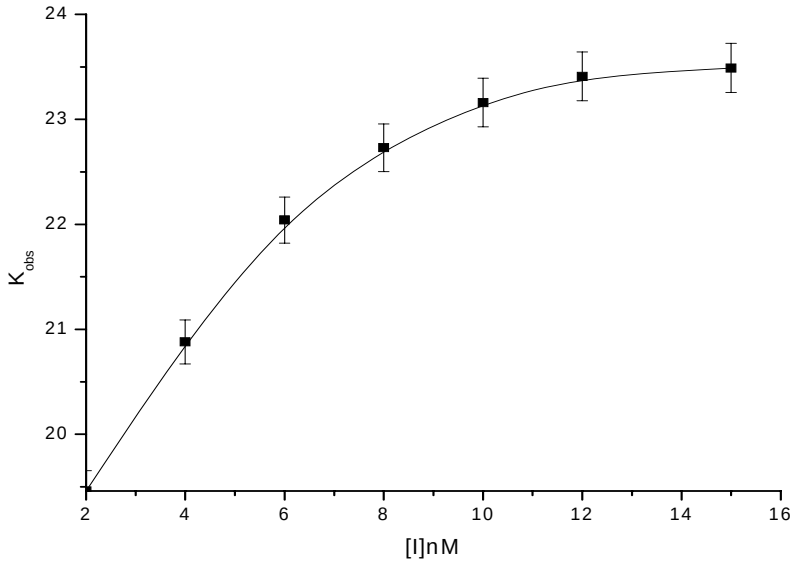

Figure 13. The slow decay of pepsin fluorescence at each concentration was fitted to a first order rate equation to obtain k_{obs} (see material and method). The k_{obs} values were then computer fitted to the equation $k_{obs}=k_6$ [I]/(K_i+[I]) to give calculated values of K_i and k_6.

DISCUSSION

Aspartic proteases play significant roles in determining the pathogenicity of both viruses and fungi (Erikson et al., 1990; Fitzgerald, 1993; Hoegl et al., 1999; Tomasselli and Heinrikson, 2000; Leung et al., 2000; Richman, 2001; Brik and Wong, 2003; Borg-von Zeppelinet, 1999; De Bernardis et al., 1999; Staib et al., 2000; Stewart and Abad-Zapatero, 2001; Atzori et al., 2000). The design and synthesis of high affinity inhibitors of these enzymes can thus provide useful leads for the development of potential anti-infective drugs (Erikson et al., 1990; Fitzgerald, 1993; Hoegl et al., 1999; Tomasselli and Heinrikson, 2000; Leung et al., 2000; Richman, 2001; Brik and Wong, 2003; Stewart and Abad-Zapatero, 2001; Kempf, 1994).

To be exploited as potential drug leads, the protease inhibitors must possess a relatively low molecular weight and a hydrophilicity/hydrophobicity ratio suitable for a sufficient level of bioavailability (Tomasselli and Heinrikson, 2000; Leung et al., 2000; Brik and Wong, 2003). In this context, there is an effort to develop a flexible approach for the design and synthesis of such inhibitors (Tossi et al., 1995; Miertus et al., 1996; Benedetti et al., 1997, Frecer et al., 1998; Tossi et al., 1999; Benedetti et al., 1999; Tossi et al., 2000; Skrbec and Romeo, 2002; Benedetti et al., 2002).

Inhibitors of aspartic proteases have tremendous applications in biomedical research, because they are responsible for the physiological regulation of proteases, which are involved in biochemical regulation of cellular functions. Pepsin is a major aggressive factor in the GERD (Gastro-Easophgeal Reflux Diseases). Alginate containing products are currently used in the treatment of GERD (eg. Gavicon Advance) that interact with pepsin in vitro, in a non-competitive manner. To our knowledge, the known slow-binding inhibitors of pepsin are pepstatin, its analogues and a low molecular weight (1147Da) inhibitor. However, there is a paucity of inhibitors from natural resources. To our knowledge, there have been no reports of aspartic protease inhibitors from thermo-tolerant microorganisms. Here, *Bacillus licheniformis* was isolated from the surface of rotten tomato, which produced an aspartic protease inhibitor, API. API was determined to be an efficient inhibitor of aspartic protease pepsin. The inhibitor was purified to homogeneity and was stable over a pH range of 2-11. API has an amino acid sequence of

Asp-Leu-Tyr-Asp-Gly-Trp-Lys-His-Glu-Ala-Glu-Cys-Ile with a pI value of 4.3. Amino acid composition and the sequence data revealed the abundance of charged amino acid residues in the peptide, and homology search with other peptidic inhibitors of aspartic proteases revealed no similarity. The inhibitor has a molecular mass of 1363 Da, thus belonged to low molecular weight class of inhibitors. API was highly specific towards inhibiting the aspartic protease class of enzyme, as it failed to inhibit the representative enzymes of other classes of proteases. Being a low molecular weight hydrophilic peptide, and produced from a bacteria source, API possesses tremendous potential for the economical and effective production.

The determined kinetic data for the enzyme-inhibitor interactions were linked with the conformational changes induced in the pepsin due to the API binding. During the initial kinetic analysis, the inhibitor showed competitive inhibition against pepsin in vitro. The 1:1 molar ratio of the interaction of inhibitor with pepsin classified it under the "tight-binding inhibitor" group (Williams and Morrison, 1979; Wolfenden1, 1976). Inhibitor was found to inhibit pepsin with an IC_{50} value (50% inhibitory concentration) of 4.2 nM (Figure 1) and inhibition constant K_i, determined by the different methods was found between 3.83 nM to 5.31nM (table 3), which are almost equal to the IC_{50} value of the inhibitor. The Lineweaver-Burk reciprocal plot (Figure 3) shows that inhibitor was a competitive inhibitor of pepsin. For the inhibition kinetic studies, the pepsin activity was monitored in the presence of various concentrations of inhibitor and substrate as a function of time. In the region of K_i, both k_4I, and k_5 values would be low. These low rates of association and dissociation would lead to slow-binding inhibition (Scheme1). Alternatively, binding may also involve two steps where there is a rapid formation of an initial collisional complex, EI that subsequently undergoes slow isomerization to form the final tight complex EI*. The nature of these changes has been discussed (Lenarcic and Thyroglobulin, 1999; Jencks, 1975). The extent of EI* formation depends on the affinity of the EI complex and the relative rates of formation of EI* and its relaxation to EI. Slow-binding inhibitor can also arise due to an initial slow interconversion of the enzyme E into another form E* which binds the inhibitor by a fast step (Scheme 1c). As found in most of the ground-state inhibitors, formation of the first reversible complex pepsin-API, was too rapid to be measured at steady-state kinetics and was likely to be near diffusion

control (Scheme 1a). The rate of formation of the second enzyme inhibitor complex, pepsin-API*, was slow and relatively independent of the stability of the pepsin-API complex or of the ability of the inhibitor to stabilize the pepsin -API* complex (Scheme 1b). Thus the major variable for slow-binding inhibition is k_7, the first-order rate at which pepsin-API* relaxes to pepsin-API. An equivalent statement is that the apparent inhibitor constant, K_i*, depends on the ability of the inhibitor to stabilize the pepsin-API* complex. It is interesting to comment on the kinetic data of inhibitor in the light of the extensive kinetic analysis of pepstatin, a known tight-binding inhibitor of pepsin. The values of K_i and K_i* for inhibitor were observed higher than those of pepstatin. The slow-binding inhibitors combine at the active site and induce conformational changes that cause the enzyme to clamp down in the inhibitor, resulting in the formation of a stable enzyme-inhibitor complex. The time-dependent inhibition kinetics of pepsin by inhibitor followed a two-step mechanism, which was also reflected in the quenching pattern of the fluorescence. On the basis of our fluorescence studies, it is proposed that the rapid fluorescence loss was due to the formation of the reversible pepsin-API complex, whereas the subsequent slower decrease was a result of the accumulation of the tightly bound pepsin-API* complex. The kinetically observable isomerization of pepsin-API to pepsin-API* does not involve a major alteration in the three-dimensional structure of the enzymes as reflected in the absence of any shift in the tryptophanyl fluorescence. Further, agreement of the rate constant values determined from kinetic and fluorescence analysis prompted us to correlate the localized conformational changes to the isomerization of pepsin-API to pepsin-API*. Any changes in the environment of individual tryptophan residues may result in an alternation of fluorescence characteristics such as emission wavelength, quantum yield, and susceptibility to quenching (Pawagi and Deber, 1990). Fluorescence quenching can also result from the energy transfer to an acceptor molecule having an overlapping absorption spectrum (Cheung, 1991). As the API has no absorption in the region of 290-450 nm, it was ruled out the quenching of fluorescence due to the energy transfer between the inhibitor and the tryptophan residues. The results of our investigation demonstrated that the inactivation of pepsin by inhibitor followed the slow tight binding inhibition mechanism and can be conveniently monitored by fluorescence spectroscopy.

CHAPTER 3

PURIFICATION AND CHARACTERIZATION OF AN ASPARTIC PROTEASE FROM MID GUT OF *PLUTELLA XYLOSTELLA*: INACTIVATION BY API

SUMMARY

An aspartic protease from *Plutella xylostella* (PxAP) was purified to homogeneity by ammonium sulphate precipitation; gel filtration and affinity chromatography with 110 fold purification. The enzyme exhibited a Mr. of 46.1 kDa on SDS-PAGE with an optimum pH and temperature of 3.4 and 37°C respectively. The enzyme hydrolyzed hemoglobin with a K_M value of 538 µM. The enzyme properties are consistent with those of aspartic proteases as it was inhibited by a universal inhibitor of aspartic proteases, pepstatin. The enzyme was also inhibited by an aspartic protease inhibitor, API, recently reported from our laboratory. The kinetic analysis of PxAP-API interaction suggested the competitive mode of inhibition with IC_{50} and K_i values of 44.0µM and 55.0 µM respectively.

INTRODUCTION

The aspartic proteases such as pepsin (Friedman and Peterson, 1998), plasma renin (Thaisrivongs, 1989), HIV-1 protease (Debouck and Metcalf, 1990), plasmepsin (Rosenthal, 1998) and lysosomal cathepsin D (Scarborough et al., 1993) participate in the control of several biological processes. In insects, acidic proteases are suggested to be involved in the hydrolysis of storage and intracellular proteins. There are few reports of aspartic proteases from insect mid-gut and fat bodies such as *Ceratitis capitata* (Rabossi et al., 2004), *Callosobrochus maculatus* and *Zabrotes subfasciatus* (Silva and Xevier-filho, 1991). However many insects like flesh fly *Sarcophaga peregrine* (Whitten, 1964), *Lygus Hesperus* (Wrighta et al., 2006), *Drosophila melanogaster* (Kotani et al., 2005), mosquito (Cho et al., 1991), *Aedes aegypti* (Dittmer and Raikhel, 1997), Cockroaches (Gustchina et al., 2005) and Colorado potato beetle (*Leptinotarsa decemlineata)* (Brunelle et al., 2005) also reported to produce aspartic proteases by different organs where they play very important roles according to the requirement of the insect. The efficacies of plant defensive proteins are dependent upon the fates of those proteins in the digestive systems of insects, where insects can compensate for the inhibition of major proteolytic activities by applying different modes of action. A thorough characterization of the types and activities of digestive proteases is crucial in understanding the degradation of nutritional proteins and in determining the effects of inhibitors on an insect's digestive system.

An aspartic protease was isolated and characterized from the mid-gut of *Plutella xylostella,* Diamondback moth (Lepidoptera: Plutellidae), which is a serious pest of cruciferous vegetables (Talekar, 1992). This is the only insect pest that has developed resistance to *B. thuringiensis* formulations under field conditions (Mohan and Gujar, 2002). However, little is known concerning the enzymes responsible for the proteolytic processing of the protoxin to the active toxin, some serine proteases were found to play a major role in proteolytic processes in Lepidopteran larval guts (Christeller et al., 1992; Mohan and Gujar, 2003). Inhibitors of aspartic proteases from insects are relatively uncommon. Few examples include proteins from the plants such as potato, squash, inhibitor from sea anemone and yeast (Christeller et al., 1998). Pepstatin, a low molecular

weight inhibitor isolated from *Streptomyces* is universal inhibitor of aspartic proteases (Lenarcic and Turk, 1999) and has been widely exploited as a research tool for unraveling the mechanism of aspartic proteases from insects (Devaux et al., 1976). Digestive proteolytic apparatus of insects is remarkably plastic to study protease inhibitor interactions in highly complex plant pest systems which allow target pests to hydrolyze the inhibitors with non target proteases. The system compensate for the loss of proteolytic functions by producing either more inhibitor-sensitive or inhibitor-insensitive proteases.

The choice and development of more appropriate, suitable inhibitors is a primary determinant in the success or failure of any pest control strategy. New, broad spectrum inhibitors of natural origin are currently considered for the improvement of protease inhibitor based pest control strategies. In the present chapter, the potency of an aspartic protease inhibitor, API from *Bacillus licheniformis,* was assessed to inhibit aspartic protease purification and characterized from mid-gut of *Plutella xylostella*. API also inhibits pepsin as recently reported in our laboratory (Kumar and Rao, 2006).

MATERIALS AND METHODS

Materials

Hemoglobin, Na-*p*-tosyl-L-lysine chloromethyl ketone (TLCK), N-tosyl-L-phenyl alanine chloromethyl ketone (TPCK), elastatinal, bovine serum albumin (BSA) (electrophoresis-marker grade), pepstatinA-agarose and bovine trypsin were purchased from Sigma Chemical (St. Louis, MO, USA). The chemicals and reagents for SDS–PAGE, Ethylenediaminetetraacetic acid (EDTA), and other chemicals were purchased from reputed firms (Genei, Bangalore and Qualigens Fine Chemicals, Mumbai) in India and of analytical grade.

Rearing of Plutella xylostella

The diamondback moth, *P. xylostella* larvae were reared on cabbage leaves at 25±1^{o}C with a light:dark cycle of 16:8 and 60–70% relative humidity. Before larvae emerged as adults, pupae were separated. *P. xylostella* were collected and placed into plastic honey jars until moth emergence. The moths were maintained on a diet of honey and water.

Preparation of P. xylostella mid-gut homogenate

Fifth instar larval (those reared in laboratory conditions) gut homogenate of *P. xylostella* was prepared by extracting midgets (dissecting in 0.5M NaCl) with 50 mM acetate buffer, pH 3.5. Freshly dissected midgets were homogenized manually using a close fitting glass pestle maintained in ice. The homogenate was centrifuged at 15,000 g for 20 min at 4°C and the resulting supernatant was used for enzymes assays and purification of aspartic protease.

Isolation and purification of Plutella xylostella aspartic protease (PxAP)

The *P. xylostella* mid-gut homogenate extracted from 500 mid-guts was precipitated with 40-60% ammonium sulphate at 4^{o}C for 2 hours, centrifuged at 15000g for 20 minutes and dissolved in an appropriate volume of same buffer. 1 ml (1mg/ml) homogenate was then applied to a Sephadex G-75 column (2.0 X 50.0 cm) equilibrated and eluted with the same buffer. Fractions (2.0 ml) were collected and those containing hemoglobin hydrolyzing activity sensitive to pepstatin were pooled and applied to a pepstatinA-agarose affinity coloumn (1.0 X 5.0 cm) equilibrated with 50mM acetate

buffer, pH 3.5. The enzyme was eluted with 50 mM Tris/HCl buffer pH 7.0. Active fractions of aspartic protease were pooled, concentrated and the pH was adjusted at 3.5. 12% SDS-Polyacrylamide Gel Electrophoresis was applied to determine the molecular weight of the active fractions (Laemmli, 1970). All protein determination was made by the dye binding assay of Bradford (Bradford, 1976), using bovine serum albumin as standard.

Enzymes assays

The proteolytic activity of gut homogenate and purified enzyme was measured by incubating with hemoglobin (1mM) in 0.2 M acetate buffer, pH 3.5 for 30 minutes (Lemos et al., 1990). The following inhibitors, pepstatin, EDTA (ethylene diamine tetraacetic acid), E-64 (L-*trans*-epoxysuccinyl-leucyl-amido (4-guanidino)-butane), TPCK (tosyl-phenylalanyl-chloromethyl-keton and TLCK (tosyl-lysyl-chloromethyl-keton) were utilized for inhibition studies. One unit of enzyme was defined as the amount of enzyme that produced an increase in absorbance of 0.001 at 280 nm per minute under the conditions of the assay (Anson 1940).

Optimum pH and temperature of the purified enzyme

The effect of pH on the proteolytic activity was determined by assaying the enzyme as described above in the range of 2.0 to 10.0 by adjusting with variety of 100 mM buffers (pH 3.0 to 5.0), phosphate (pH 5.0 to 8.0), and tris-HCL (pH 8.0 to 10.0). The effect of temperature on the proteolytic activity was determined at pH 3.5 in the range of 25 ^{o}C to 80 ^{o}C.

Purification and biochemical characterization of API

The inhibitor was purified and characterized from extra cellular culture filtrate of *Bacillus licheniformis* as described previously in part 2 of chapter 2 (Kumar and Rao, 2006).

Assay for PxAP inhibition by API

100 µl of enzyme (50 µM) and 100 µl API (100 µM) solution were incubated at 37°C for 30 min in 0.2 M acetate buffer, pH 3.5. Then 0.5 ml of hemoglobin (1mM) dissolved in the same buffer was added and incubated at 37°C for 30 minutes. The reaction was stopped by the addition of 5% trichloric acid (TCA) acidified with 2.25% HCl. One unit of enzyme was defined as the amount of enzyme that produced an increase

in absorbance of 0.001 at 280 nm per minute under the conditions of the assay. One API unit was defined as the amount of API that inhibited one unit of enzyme activity (Anson, 1940).

Initial kinetic analysis

The kinetic parameters for the substrate hydrolysis were determined by measuring the initial rate of enzymatic activity according to described in chapter 2 (part 2). For the Lineweaver-Burk analysis of enzyme (100 μM) was incubated with API at 50 μM and 100 μM and assayed at increased concentration of hemoglobin (0.1-1mM) at 37°C for 30 min. In Dixon's method, hydrolytic activity of enzyme 100μM was measured in the presence of 0.5mM and 1mM hemoglobin, at concentrations of API ranging from 10-100 μM at 37 °C for 30 min.

RESULTS

Detection of aspartic protease activity in gut homogenate

The gut homogenate of *P. xylostella* showed hemoglobin hydrolyzing activity at pH 3.5 suggesting the presence of aspartic protease type activity. It was also confirmed by the 35% inhibition of mid-gut homogenate proteolytic activity by a universal inhibitor of aspartic proteases, pepstatin.

Purification of aspartic protease from the gut homogenate

The enzyme was purified from *P. xylostella* mid-gut homogenate extract by 40-60% ammonium sulphate precipitation, Sephadex G-75 column and pepstatinA-agarose affinity coloumn. Gel filtration in sephadex G-75 coupled with protease assay employing the substrate hemoglobin (at pH 3.5) in the presence and absence of inhibitor pepstatin, showed the presence of aspartic protease (Figure 1). The fractions from 30-45 showed proteolytic activity at pH 3.5 suggest the presence of aspartic protease which was confirmed by the inhibition of the proteolytic activity by pepstatin. The active fractions were concentrated and applied to pepstatinA-agarose affinity coloumn. The gut homogenate showed 730 U of acidic protease with a specific activity of 5.88 U/mg. The proteolytic activity remains 132 U with a specific activity of 647 U/mg after affinity column and the enzyme was purified 110 fold (Table 2). SDS-PAGE showed a single band of Mr 46.1 kDa (Figure 2) confirming the homogeneity of the enzyme. The purified enzyme showed an optimum pH and temperature of 3.5 (Figure 3) and 37^{o}C (Figure 4) respectively. Pepstatin shows 82% inhibition of the purified enzyme while other inhibitors had no significant effect (Table 1).

Table 1 Effect of various enzyme inhibitors purified PxAP.

Inhibitor (1mM)	% Inhibition
Non	0
EDTA	0
E-64	0
Pepstatin A	82
TLCK	0
TPCK	0

% Inhibition activities are the average of three determinations.

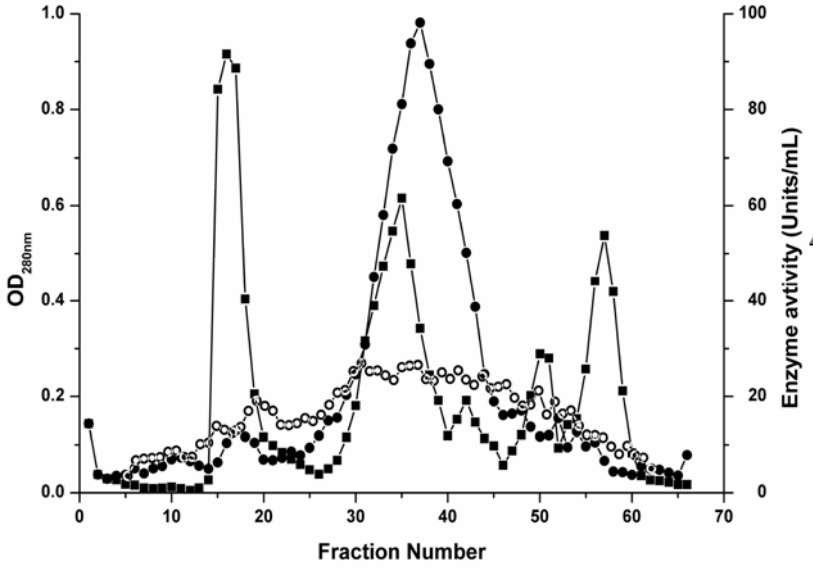

Figure 1. 60% ammonium sulphate precipitated mid-gut homogenate dialyzed and loaded on a Sephadex G-75 gel-filtration chromatography column. Fractions were each of 2.0 ml. Proteolytic activities against hemoglobin was measured in the absence (●) and presence of pepstatin (o). Absorbance at 280 nm (■).

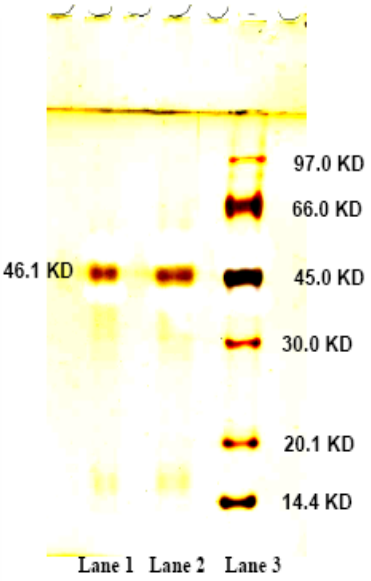

Figure 2. The fractions from affinity chromatography column collected, concentrated and applied to 12% SDS-PAGE. Lane1 shows 2µg enzyme, Lane2 shows 5µg enzyme and lane 3 shows the standard molecular weight markers.

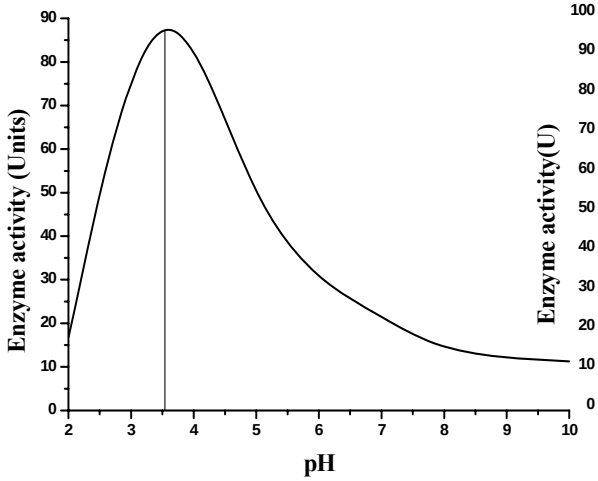

Figure 3. Optimum pH of the enzyme

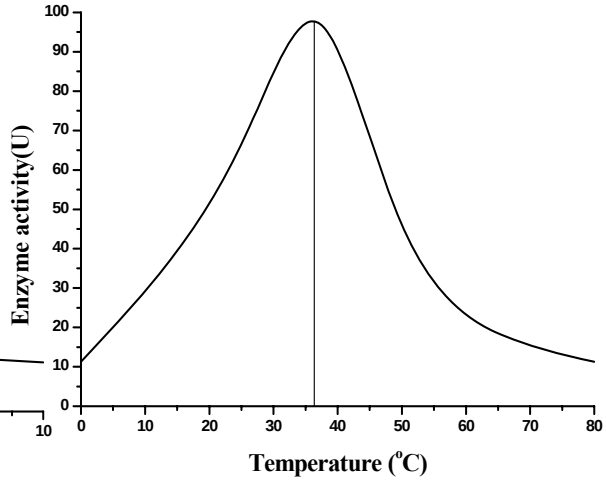

Figure 3. Optimum temperature of the enzyme

Biochemical properties of API and determine K_M and K_i

API, a peptidic inhibitor of aspartic proteases, produced extracellularly by thermo tolerant *Bacillus licheniformis* as has an amino acid sequence of Asp-Leu-Tyr-Asp-Gly-Trp-Lys-His-Glu-Ala-Glu-Cys-Ile and a pI value of 4.3 (Kumar and Rao 2006).

The inhibition of PxAP followed a hyperbolic pattern with increasing concentrations of the inhibitor. PxAP was inhibited by API with an IC_{50} value of 44μM (Figure 3). The kinetic analysis of PxAP-API interaction suggested the competitive mode of inhibition. The Lineweaver-Burk reciprocal plot (Figure 4A) showed that the K_M value of PxAP for hemoglobin was 538 μM. The inhibition constant K_i determined by Lineweaver-Burk and Dixon plot was found to be 59 μM and 55 μM respectively (Figure 4A and 4B).

Table 2- *P. xylostella* larval mid-gut aspartic protease purification.

Step	Proteolytic activity(Units)	protein (mg)	Specific activity (units/mg)	Purification
Homogenate	730	124	5.88	1
Ammonium sulphate	285	2.8	101.78	17.31
SG-75	205	0.6	341	58
PepstatinA-agarose	132	0.204	647	110

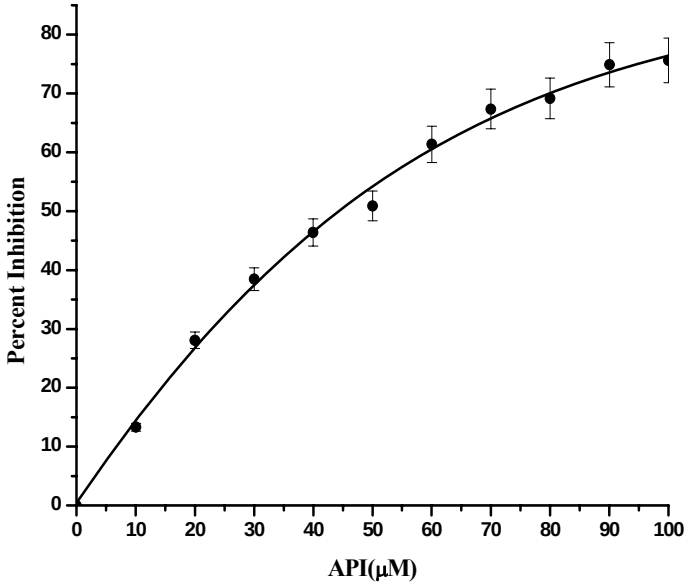

Figure 3. The hyperbola curve indicates the best fit for the percentage inhibition data obtained, and the IC_{50} value was calculated from the graph.

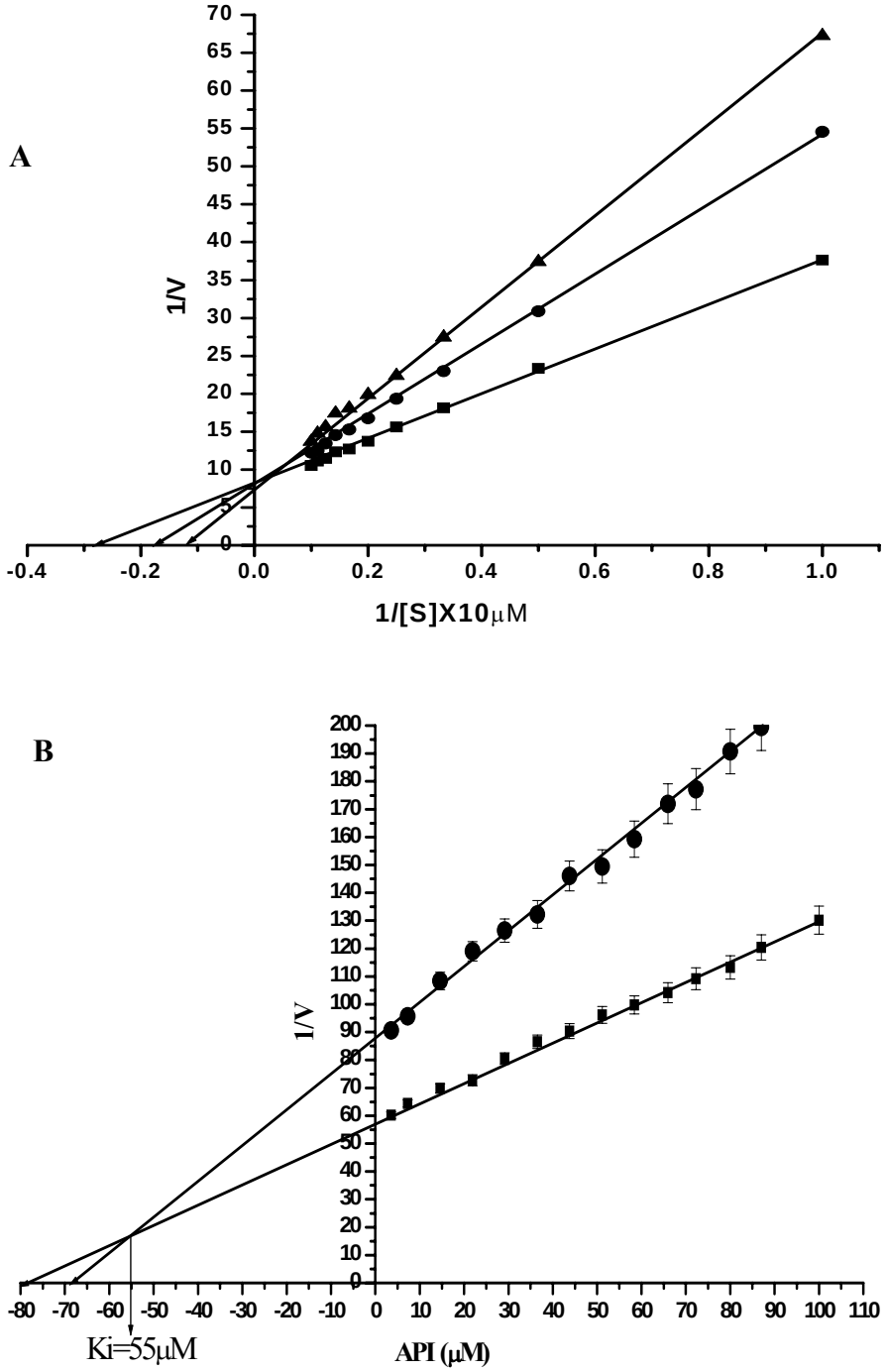

Figure 4. Binding of API to PxAP and inhibition kinetics analysis. (A) Lineweaver-Burl plot, PxAP (100μM) was incubated, without (■) or with API at 50 μM (●) and 100 μM (▲) concentrations and assayed at increasing concentrations of the substrate (se material methods for more details). (B) For, Dixon plot, Enzymatic activity of PxAP (100μM) was estimated using hemoglobin= 0.5mM (●) and 1mM (■) at different concentrations of API.

DISCUSSION

The presence of serine type of activity in *Plutella xylostella* larvae was previously reported by Mohan and Gujar, 2003. The present work demonstrates the hemoglobin hydrolyzing activity of gut homogenate is partly due to the aspartic protease also. The purified enzyme was inhibited by pepstatin (which is a known inhibitor of aspartic proteases) while the inhibitors of serine (TPCK and TLCK), cystein (E-64) and metalloprotease (EDTA) had no effect. The optimum pH for hydrolysis of hemoglobin isolated fraction was 3-4 while the optimum of fraction of mid-gut contents on the same substrate was 6-7. This was also observed by Houseman et al., 1984 when working with a Cathapsin D-like proteinase from *R. prolixus*, and while working with Cathapsin B&D-like proteases in *C. maculates* (Kitch and Murdock, 1986). The utilization of aspartic and cysteine proteases for extracellular digestion was first described in Hemiptera feeding in blood or seeds (Houseman et al., 1984). Later cathapsin B like proteases were described in the bruchids *C. maculates* (Kitch and Murdock, 1986), and *A. obtectus* (Wieman and Nielsen, 1987). After detection and characterization of aspartic protease (this work) and serine protease in the larval mid-gut of *P. xylostella* (Mohan and Gujar, 2003), it seems that both kinds of proteases are much more widespread than was originally suggested (Mohan and Gujar, 2003). To gain further insight into the details of the hydrolytic mechanism of aspartic proteases from insect source, specific inhibitors like pepstatin are necessary, which can act as mechanistic and structural probes.

In this chapter, a novel aspartic protease from *Plutella xylostella* mid-gut and its inhibition by API, is reported. During the initial kinetic analysis, PxAP was found to be inhibited by the Inhibitor with an IC_{50} and K_i values of 45 μM and 55 μM respectively. The Lineweaver-Burk reciprocal plot (Fig. 5) shows that inhibitor was a competitive inhibitor of PxAP.

CHAPTER 4

BIFUNCTIONAL ROLE OF API: STRUCTURAL AND MECHANISTIC INSIGHTS INTO THE INHIBITION OF CHITINASE

SUMMARY

The inhibition of 1, 4-β-poly-*N*-acetylglucosaminidase (Chitinase A) from *Serratia marcescens* by API is reported in this chapter. ChitinaseA-API kinetic interactions reveal noncompetitive, irreversible and tight binding nature of API with an IC_{50} value 710 nM and K_i value 510-920 nM. The inhibition progress curves show a two step slow tight binding inhibition mechanism where first step involves a rapid equilibrium for formation of reversible enzyme inhibitor complex (*E*I) that isomerizes to a stable complex (*E*I*) in the second step because of inhibitor induced conformational changes in ChitinaseA (ChiA) with rate constant k_6 ($8.74\pm0.1\times10^{-3}s^{-1}$). Slower dissociation rate constant k_7 ($7.3\pm0.6\times10^{-5}$ s^{-1}) for *E*I* to *E*I and overall inhibition constant K_i* (6.3-7.5 nM) indicates the tight binding nature of API. CD-spectra analysis and time dependent Tryptophanyl fluorescence quenching of ChiA incubated with incresing API concentrations indicates malicious changes in secondary and tertiary conformation of ChiA, which is correlated to the isomerization of *E*I to *E*I* and to the irreversible conformationally locked *E*I** complex. Abolished isoindole fluorescence of *o*-phthalaldehyde (OPTA)-labeled ChiA proves that Asp1 residue of API binds to the Lysine and Histidine residues present near active site of ChiA which disrupt electronic microenvironment and hydrogen-bonding network near the active site of ChiA. For the first time, it is also shown the importance of near active site residues in ChiA and model can be applied to study other enzymes.

INTRODUCTION

I. Chitinases

Chitinases (EC 3.2.1.14) hydrolyze the β-1, 4-glucosidic bonds of chitin (Flach et al., 1992) and are commonly found in a wide variety of organisms, including virus (Hawtin et al., 1997), fungi (Gooday et al., 1986; Chet and Inbar, 1994; Ohtakara, 1961), plants and animals (Boller, 1985; Powning and Irzykiewez, 1965; De Jong et al., 1993; Overdijk et al., 1994; Stintzi et al., 1993), insects (Hamamura and Kanehara, 1940), crustaceans (Lunt and Kent, 1960) and bacteria (Clarke and Tracey, 1956; Roberts and Cabib, 1982; Watanabe et al., 1990; Morgavi et al., 1994). The roles of these chitinases differ in the various hosts. In fungi, chitinase activity plays a physiological role in apical growth and morphogenesis of fungal hyphae (Gooday et al., 1986; Ohtakara, 1961). The production of chitinases in higher plants is considered part of their defense system against fungal infection (Shinshi et al., 1987). Bacterial chitinases appear to have a nutritional or scavenging function in the decomposition of insoluble chitin and also the utilization of chitin as a carbon and energy source. In recent years, bacterial chitinase genes from *Alteromonas* (Tsujibo et al., 1993), *Bacillus circulans* (Watanabe et al., 1990), *Vibrio harveyi* (Soto-Gil and Zyskind, 1984) and *Vibrio vulnifucus* (Wortman et al., 1986) have been cloned and characterized. Some of these microorganisms produce several chitinase species with different molecular masses (Diekmann et al., 1989; Takayanagi et al., 1991; Tarentino and Maley, 1974; Watanabe et al., 1990). This diversity in the microbial chitinases has been studied. Some chitinase isoforms derive from other chitinases. Recently it has been proposed that several chitinases can derive from a larger primary gene product by post-translational proteolytic cleavage in *Streptomyces olivaceoviridis* (Romaguera et al., 1992). In *Janthinobacterium lividum*, a 56-kDa extracellular chitinase was derived from a 69-kDa chitinase (Gleave et al., 1995). Watanabe et al., 1990 reported that the multiplicity of chitinases in *Bacillus circulans* is due to proteolytic modification of one or two precursor proteins. However, Sang et al., 1997 previously cloned genes encoding small 22-kDa chitinases from *Serratia marcescens* KCTC2172, which indicates that not all small chitinase species are derived from higher molecular mass chitinases by post-translational proteolysis.

i) Classification of chitinases

Based on amino acid sequences of glycosyl hydrolases, (Henrissat, 1991) grouped chitinases in to three families 18 and 19. Both families 18 and 19 are comprised of endochitinases from different sources, such as viruses, bacteria, fungi, insect and plants. Family 19 mainly comprising of plant chitinases. The enzymes *N*-acetylglucosaminidase (EC 3.2.1.30) from *Vibrio harveyi*, *N*-acetylhexosaminidases (EC 3.2.1.52) from human and *Dictyostelium discoideum* are grouped in family 20. In 1993, 1995 and 1996, Henrissat and Bairoch, studied additional sequences and included enzymes like endo-*N*-acetylglucosaminidase (EC 3.2.1.96) from *Flavobacterium* species in to family 18. With the help of known chitinase gene sequences, Perrakis et al., 1993 attempted to group them in to two distinct Classes I and II that correspond to families 19 and 18 of glycosyl hydrolases, respectively from the classification by Henrissat, 1991. Plants produce a large number of chitinase isozymes, as defense response against pathogens, which are tissue-specific and developmentally regulated. They are classified according to their sequences into six classes (Iseli et al., 1996a). The characteristics that determine class of chitinases include: N-terminal sequence, localization of the enzyme, isoelectric pH, signal peptide and the inducers. For instance, the characteristics of chitinases belonging to Class I were: cysteinerich N-terminal, leucine or valine- rich signal peptide and vacuolar localization (Flach et al., 1992). It was further subdivided as sub Class Ia and Ib based on the basic and acidic nature, respectively of chitinases. The Class I chitinases were found to be restricted to the plant sources, whereas Class II enzymes were present in plants, fungi and bacteria too. Class II chitinases that were pathogen induced, lack the cysteinerich N-terminal domain, but had sequence similarity with Class I chitinases. Most of the Class I chitinases were endo-chitinases and Class II chitinases had exo-action. Class III chitinases did not show any sequence similarity to enzymes of Class I or II (Collinge et al., 1993). Although Class IV chitinases had similar characteristics as Class I chitinases including immunological properties, but they were significantly smaller than Class I chitinases (Collinge et al., 1993). Classes V and VI included single examples (Iseli et al., 1996a). The nettle lectin precursor (Class V) showed two chitin binding domains in tandem. Based on the sequence data, it was suggested that chitin-binding (cysteine-rich) domain seemed to have been lost several times in the evolution of higher plants. The

nettle lectin must have evolved faster, due to the reduced selective pressure where the catalytic domain had lost its function. Considering the significance of all the three systems of classification, the criteria used for IUB classification of chitinases are important because finally reaction catalyzed by the enzyme is its key information to understand its roles and biotechnological applications.

ii) Three dimensional structure of chitinases

Enzymes exhibit their function when the proteins fold properly to form appropriate threedimensional structures. Thus, information of the three-dimensional structure is essential for studying catalytic mechanism of the enzymes. X-ray crystallography and NMR spectroscopy are now important strategies for obtaining the three dimensional structure of macromolecules. The crystal structure of 26 kDa chitinase from barley seeds, *Horduem vulgare* L., which is classified into family 19, was first solved by Robertus and his colleagues at the University of Texas (Hart et al., 1993). After that, the structures of a 60 kDa chitinase A from *Serratia marcescence* and a 29 kDa chitinase from rubber tree, *Hevea brasiliensis* (hevamine) were solved and reported in the same journal (Perrakis et al., 1994; Terwisha van Scheltinga et al., 1994). Both are family 18 enzymes. Figures (1) and (2) show the crystal structures of barley chitinase (family 19) and *Serratia marcescence* chitinase A (family 18). Barley chitinase is composed of two lobes, each of which is rich in α-helical structure. From a docking calculation of the chitinase and $(GlcNAc)_6$, the substrate binding cleft is estimated to lie between the two lobes (Hart et al., 1995). The hypothetical binding cleft is composed of two α-helices and three-stranded β-sheet. The structure of family 18 chitinase from *S. marcescence* (chitinase A) is completely different from that of family 19 chitinase from barley seeds. The family 18 chitinase has a typical $(\alpha/\beta)_8$ barrel structure composed of eight α-helices and an eight stranded β-sheet. In addition to the main barrel domain, it has an N-terminal β-strand-rich domain and a small (α+β) domain. The crystal structures of other family 18 chitinases exhibit similar barrel structure. Apparently, in family 18 chitinases, the sequence homology results in the similarity in three-dimensional structure.

iii) Catalytic mechanism of family 18 and 19 chitinases

The reaction mechanisms of family 18 and 19 chitinases differ significantly and are both well established. Chitin binds to the active site groove of family 18 chitinases

with the GlcNAc units stacking on the solvent exposed tryptophans, with the -1 sugar assuming a boat conformation (step (i), Fig. 3).(Tews et al., 1997; van Aalten et al., 2001; Brameld and Goddard, 1998). Furthermore, chitin binding results in a reorientation of the Asp175 side chain, replacing its hydrogen bond to the carboxyl group of Asp173 with hydrogen bonds to the carboxyl group of the catalytic acid Glu177 and the -1 C2- Aceta-mido group of the substrate. Nucleophilic attack of the carbonyl oxygen of the acetamido group on the anomeric C1 carbon of the same pyranose ring occurs concurrently with protonation of the glycosidic oxygen by the catalytic acid, generating the leaving group from the reducing end of chitin as well as an oxazolinium ion intermediate (step (ii), Fig. 3).(van Scheltinga et al., 1995; Tews et al.,1997; van Aalten et al. 2001; Brameld and Goddard, 1998). This step differs from the classical retaining mechanism of glycosyl hydrolases such as lysozyme, cellulase, xylanase and *endo*-1,3-1,4-β-D-glucan-4-glucanohydrolase that use a carboxylate side chain as the nucleophile (Zechel and Withers 2001). For the family 19 chitinases, HPLC (Iseli et al., 1996b) NMR (Hollis et al., 1997) and modeling studies (Brameld and Goddard 1998) have shown that these enzymes use a carboxylate as a base to activate a water molecule that attacks the C1 position resulting in an inversion of configuration at the C1 anomeric carbon as part of a single step mechanism. Formation of the oxazolinium ion intermediate in family 18 chitinases has been questioned on the basis of a combined structural and mutational study on chitinase A from the bacterium *Serratia marcescens* (*Sm*ChiA) Papanikolau et al., 2001. However, substrate-assisted catalysis is strongly supported by kinetic data on *Sm*ChiA that show that the polarity of the carbonyl group is essential for enzymatic activity (Honda et al., 2004). Formation of the oxazolinium ion intermediate is supported by molecular mechanics calculations (Brameld et al., 1998), whereas mutation studies have indicated that the formation of the intermediate and its stabilization is assisted by Tyr245 that forms a hydrogen bond to the *N*-acetyl oxygen (Bokma et al., 2002), thereby generating an interaction with the oxazolinium oxygen (Tews et al., 1997; van Aalten et al., 2001).

Fig. 1. Three dimensional structure of barley chitinase (PDB number 1CNS). This figure was created using RasMol 2.6.

Fig. 2. Three dimensional structure of *S. marcescence* chitinase A (PDB number 1CTN). α-helices are shown by red, and β-strands by yellow. This figure was created using RasMol 2.6.

The reorientation of Asp175 to the "up conformation", hydrogen bonding with Glu177 and the oxazolinium nitrogen, is believed to be important for stabilization of the positive charge on the intermediate (van Aalten et al., 2001). In the final step, hydrolysis of the oxazolinium ion, regenerating the *N*acetyl group, results in overall retention of the stereochemistry at the C1 anomeric carbon as well as re-protonation of Glu177, and reorientation of Asp175 to re-generate the hydrogen bond with Asp173 (step (iii), Fig. 3). Retention of configuration at the anomeric carbon is supported by the binary complexes of the pseudotrisaccharide allosamidin with hevamine (van Scheltinga et al., 1995). *Serratia marcescens* chitinase B (*Sm*ChiB) (van Aalten et al., 2001) *Coccidioides immitis* chitinase (*Ci*Chi) (Bortone et al., 2002) and *Sm*ChiA (Papanikolau et al., 2003). These complexes have the allosamizoline aglycone moiety in an equivalent position to the oxazolinium ion reaction intermediate (van Aalten et al., 2001). A specific, structurally well-defined water molecule, located opposite the leaving group (O7 oxygen) relative to the C1 anomeric carbon, is a putative C1 attacking group whose position is consistent with retention of the C1 stereochemistry (van Aalten et al., 2001). NMR studies using family 18 chitinases A1 and D from *Bacillus circulans* WL-12 also support a molecular mechanism retaining the anomeric configuration (Armand et al., 1994).

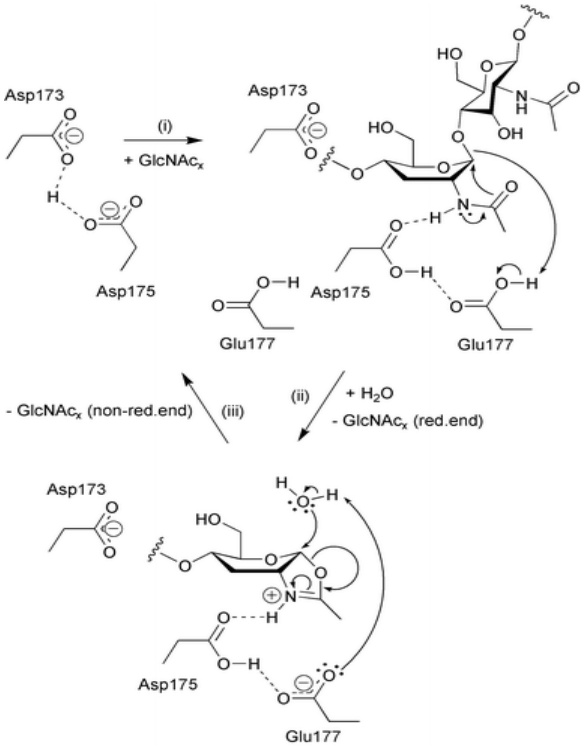

Fig. 3. The catalytic cycle of family 18 chitinases. Arrows indicate electron transfers of the subsequent step, whereas dashed lines represent hydrogen bonds. (i) Binding of GlcNAc; (ii) cleavage of GlcNAc releasing product from the reducing end; (iii) release of product from non-reducing end. The figure is based on reaction schemes from Tews et al., 1997 and van Aalten et al., 2001.(Andersen et al.,2005)

iv) Transglycosylation

Several chitinases belonging to family 18 were found to catalyze the transglycosylation as well. On the other hand, there is no report on the transglycosylation for family 19 chitinases. How does the transglycosylation relate to the retaining mechanism? A site-directed mutagenesis study of T4 phage lysozyme afforded important information on the mechanism of transglycosylation. T4 phage lysozyme is an inverting enzyme, and the enzyme itself does not catalyze the transglycosylation. The crystal structure of the enzyme is very similar to that of barley chitinase or *Streptomyces* sp. N174 chitosanase (Monzingo et al., 1996). Glu11 and Asp20 are essential for catalysis as a proton donor and an activator of water molecule, respectively.

v) Applications of chitinases

Chitinases have many agricultural and industrial applications (Shaikh and Deshpande, 1993; Zikakis, 1989) that require different types of preparations.

a) Chitinases in plant defence mechnisms

In many plant species, the pathogen invasion induces production of pathogenesis - related proteins (PR- proteins) like chitinases, β-1,3- glucanases, proteinases, proteinase inhibitors, etc. (Kombrink and Somssich, 1995). As fungi and insects contain chitin in their protective covers, induction of chitinases in plants is the main defense response. Most of these chitinases are induced in vegetative plant organs by infection but some are also present in seeds. Hadwiger and Beckman, 1980 demonstrated that extracts of the pea endocarp contain chitinase and chitobiase activity. Most of the chitinases preferentially cleave highly acetylated substrates and the activities decrease with decrease in the degree of acetylation. Therefore, increase in the deacetylation level on the surface of hyphae may be useful for the fungus to resist plant chitinases. And the presence of chitin deacetylase activity during the formation of infection structures supported this hypothesis (Deising and Siegrist, 1995). According to Roberts and Selitrennikoff, 1988 chitinases isolated from the grains of wheat, barley, and maize functioned as endochitinases and inhibited hyphal elongation of test fungi. In contrast, bacterial chitinases from *S. marcescens, S. griseus* and *Pseudomonas stutzeri* act as exo-enzymes and had no effect on hyphal extension of test fungi like *T. reesei* and *Phycomyces blackesleeanus.* The data presented by Blaak et al., 1993 and Watanabe et al., 1993 on the presence of fibronectin

type III domain in bacterial chitinases supported this viewpoint. However, Ordentlich et al., 1988 attributed slower disease development by *Sclerotium rolfsii* on bean seeds in presence of *S. marcescens* to its high chitinase activity. Furthermore, Shapira et al., 1989 cloned *S. marcescens* chitinase gene in *E. coli* and the chitinase preparation obtained was found to be effective in reducing disease incidence caused by *S. rolfsii* in beans and *R. solani* in cotton under greenhouse conditions. This contradiction in the observations made by Roberts and Selitrennikoff, 1988 versus Ordentlich et al., 1988 and particularly, Shapira et al., 1989 may be attributed to the difference in the test fungi used and other factors that contribute in the killing of pathogenic fungus. *S. violaceusniger* was reported to be antagonistic to many plant pathogenic fungi (Trejo–Estrada et al., 1998). The antagonistic activity was attributed to the production of enzymes like chitinase and glucanase and antifungal compounds, such as AFA (Anti-*Fusarium* activity), nigericin and geldanamycin. Several species of fungi are very potent biocontrol agents of plant pathogenic fungi and insects. The mycoparasitic and entomopathogenic fungi produce chitinases for invasion and as one of the host killing components (Mathivanan et al., 1998; Kang et al., 1998; Higuchi et al., 1998). A *Fusarium chlamydosporum* strain, a mycoparasite of groundnut rust, *Puccinia arachidis* produces an endo-chitinase that inhibits germination of uredospores of the rust fungus. This indicates the significant contribution of chitinase in the biocontrol of groundnut rust (Mathivanan et al., 1998). Chitinolytic enzymes of *T. harzianum*, a most studied mycoparasitic fungus, were found to be inhibitory to a wider range of deleterious fungi than similar enzymes from other sources (Lorito et al., 1993). *M. verrucaria* crude mycolytic preparation (Vyas and Deshpande,1989; Deshpande, 1998) was found to be effective against *S. rolfsii*, a rootinfecting fungus of groundnut. Govindsamy et al., 1998 and to control a groundnut rust, *P. arachidis*. The insect-pathogenic fungi, *Beauveria bassiana, B. brongniarti* and *Verticillium lecanii* produced cuticle degrading enzymes when grown on chitin containing medium.

b) Mosquito control

The worldwide socio-economical aspects of diseases spread by mosquito make them potential targets for various pest control agents. In the case of mosquitoes, entomopthogenic fungus like *B. bassiana* could not infect eggs of *Aedes aegypti,* a vector

of yellow fever and dengue, and other related species may be due to aquatic environment. The scarabaeid eggs laid in the soil found to be susceptible to *B. bassiana* (Ferron, 1985). *M. verrucaria,* a saprophytic fungus, produces a total complex of an insect cuticle degrading enzymes (Shaikh and Deshpande, 1993; Deshpande, 1998). It has been seen that both first (I) and fourth (IV) instar larvae of a mosquito, *A. aegypti*, can be killed within 48 h with the help of the crude preparation from *M. verrucaria* (Mendonsa et al., 1996).

c) Chitinase as a target for biopesticides

Chitin is present in the exoskeleton and gut linings of insects. The insect molting enzyme, chitinase has been described from *Bombyx mori*, *Manduca sexta* and several other species. Similarly, chitinases have been implicated in different morphogenetic events in fungi (Villagomez–Castro et al., 1993). The pseudotrisaccharide, allosamidin, is a potent inhibitor of chitinases from most of the sources (Sakuda, 1996). The allosaminidin was found to be inhibitory after ingestion to the growth of mite, *Tetranychus urticae* and a larva of a housefly, *M. domestica* (Sakuda, 1996).

d) Production of chitooligosaccharides

Biologically active chito-oligosaccharides act as elicitors of plant defense, involved in the signaling for root nodule formation and are potentially useful in human medicine too as they showed anti-tumor activity. A chitinase from *Vibrio alginolyticus* was used to prepare chitopentaose and chitotriose from colloidal chitin (Murao et al., 1992). *N*,*N* 9-Diacetylchitobiose has been widely used as a starting material for synthesis of biologically active compounds (Terayama et al., 1993, Kobayashi et al., 1997). A chitinase preparation from *S. griseus* was used for the enzymatic hydrolysis of colloidal chitin. The chitobiose produced was subjected to chemical modifications to give novel disaccharide derivatives of 2-acetamido-2-deoxy-D-allopyranose moieties that are potential intermediates for the synthesis of an enzyme inhibitor. Kobayashi et al., 1997 reported use of *Bacillus* chitinase for the synthesis of chitobiose by combining GlcNAc and a sugar oxazoline derivative. The GlcNAc itself also is an anti-inflammatory drug and synthesized from glucose. The GlcNAc administered by iv, intramuscular (im) and even oral routes was reported to be effective as an anti-inflammatory drug useful for the treatment of ulcerative colitis and other gastrointestinal inflammation disorders

(Friedman and Skehan, 1980, Aloise et al., 1996). Nanjo et al., 1989 observed accumulation of hexamer when tetramer or pentamer were incubated with *Nocardia orientalis* chitinase. A chitinase from *T. reesei* also exhibited similar type of efficient transglycosylation reaction (Usui et al., 1990). Stoyachenko et al., 1994 reported four major chitinases from *S. kurssanovii*. One of them (Chi-26) showed accumulation of hexamer in the reaction medium containing tetramer and pentamer.

e) Single cell protein production

Revah–Moiseev and Carrod, 1981 used chitinase from *S. marcescens* and yeast, *Pichia kudriavzevii* to hydrolyze chitinous material to single cell protein (SCP) that was acceptable as aquaculture. Fungi, in general used as the source for SCP are *Hansenula polymorpha, M. verrucaria, Candida tropicalis, P. kudriavzevii, S. cerevisiae* etc. (Vyas, 1991). The criteria used to evaluate SCP production are growth yield, total protein and nucleic acid contents. The best reported organism was *S. cerevisiae* that exhibited 60% protein and 1 to 3% nucleic acid contents. The *P. kudriavzevii* had 45% protein and 8 to 11% nucleic acid contents (Revah–Moiseev and Carroad, 1981). Vyas and Deshpande, 1991 used *M. verrucaria* chitinase preparation for chitin hydrolysis and *S. cerevisiae* for SCP. The high *N*-acetylglucosaminidase activity in the culture filtrate of *M. verrucaria* yielded high levels of GlcNAc. The total protein contents were reported to be 61% with very low contents of nucleic acids (3.1%).

f) Application of chitinases in biological research

As chitinases play a very critical role in the dissolution of cell walls of fungi, they are very useful for the generation of fungal protoplasts. Dissolution of cell wall by chitinase was first observed by Skujins et al., 1965 where they found a *Streptomyces* chitinase to effectively lyse hyphal walls of *Aspergillus oryzae* and *Fusarium solani*. Next, Johnson et al., 1979 used a chitinase containing cul-ture filtrate of *Bacillus circulans* WL12 to generate spheroplasts of *Phaffia rhodozyme*. Similarly, a commercial preparation of chitinase and cellulase was used to release protoplast from *Caprinus pellucidus* (Yanagi and Takabe, 1984) and *Caprinus macrorhizus* (Moringa et al., 1985). Chitinase from *Trichoderma harzianum* has shown most effeciency in the generation of a variety of fungal protoplasts (Kitamoto et al., 1988; Kumari and Panda, 1992). Likewise, the use of chitinase (either separately or as a combination with other enzymes) in

generation of protoplasts has been extensively examined (Moriguchi and Kotegawa, 1985; Ishikawa and Oishi, 1985; Hermova and Selitrennikoff, 1987; Sandhu, et al., 1989; Yu and Chang, 1987; Ramaguero et al., 1993).

g) Use of chitinase in degradation of fish waste

The monomer of chitin, N-acetyl-D-glucoseamine is very useful in the manufacture of chemical and pharmaceutical intermediates and food products such as sweeteners and growth factors (GyoÈrgy and Rose, 1955). N-acetyl- D-glucosamine is conventionally prepared by complete hydrolysis of chitin with strong mineral acids or by chemical synthesis from glu coseamine (Purchase and Braun, 1946; Inouye et al., 1956). These processes involve high cost and corrosion problems due to which the costs of N-acetyl-D-glucoseamine or its oligimers are still prohibitive. In the last two decades there has been a lot of focus on the production of N-acetyl-D-glucosamine through enzymatic hydrolysis of chitin. Revah-Moiseev and Carroad, 1981 as well as Tom and Carroad, 1981 have described a process for the bioconversion of shell fish waste to N-acetyl glucose-amine and other valuable products.

h) Miscellaneous applications

Fungal protoplasts have gained substantial importance in the mycological research as well as in strain improvement program for biotechnological applications (Peberdy, 1989; Lee et al., 1993; Gokhale, 1992). One of the major components of the fungal cell wall lysing enzyme complex is chitinase/chitosanase. It has been seen using various mycolytic enzyme preparations singly or in combination for protoplast isolation that high chitinase levels permit effective fungal mycelia degradation (Vyas and Deshpande, 1989; Kelkar et al., 1990). The lectins due to their specific monosaccharide-binding properties can be used to locate sugar residues in thin sections of plants and fungi. Similarly chitinases can also be employed to locate fungal pathogens that have chitinous cell wall. The chitinase-gold complex can be used for this purpose (Benhamou and Asselin, 1989). A wide spread ability to produce *N*-acetylglucosaminidase has been observed in fungi in presence and absence of added chitin in the growth medium. Although *N*-acetylglucosaminidase activity was found to be expressed in a limited number of bacteria (Miller et al., 1998). Therefore, *N*-acetylglucosaminidase activity measured on fluorogenic substrates of the soil samples was significantly correlated with

the estimate of fungal biomass, based on the levels of 18:2w6 phospholipid fatty acid and ergosterol. Similarly, using chitinase and chitin-binding protein a method has been suggested for the detection of fungal infection in humans (Laine and Lo, 1998).

vi) Cloning and molecular genetics of chtinases

The genetic improvement plays an important role in chitinases biotechnological applications. The mutation, protoplast fusion and molecular cloning are being effectively used to achieve overproduction of chitinases, to change in their localization viz. periplasmic or extracellular and to understand the organism itself. Molecular cloning of chitinase genes has been reviewed earlier (Shaikh and Deshpande, 1993; Flach et al., 1992, Kramer and Muthukrishnan, 1997; Sahai and Manocha, 1993, Tews et al., 1996a,b). The constitutive, extracellular activity the co-transformation of *Trichoderma reesei* protoplasts with *Aphanocladium album* chitinase was reported (Deane et al., 1999). Number of reports on molecular cloning for chitinases either to increase biocontrol efficiency of *B. thuringiensis*, to prepare highly active chitinase preparation or even transgenic plants for the increased resistance has been described (Wiwat et al., 1996; Watanalai et al., 1997, Tantimavanich et al., 1997). The *B. thuringiensis* strains produce β-toxin that kills number of insect pests. Two chitinase genes from *Coccidioides immitis*, a human pathogenic fungus have been cloned and sequenced (Pishko et al., 1995). To obtain large amount of chitinase for chemotherapeutic studies, a *Cht* gene from *B. malayi* microfilariae from infected jirds was cloned and expressed in *E. coli* (Southworth et al., 1996). In plants, chitinases are induced by the pathogen attack, elicitors, growth regulators, heavy metals as well as wounding (Kombrink and Somssich, 1995; Kim et al., 1998, Ancillo et al., 1999). The molecular cloning was used to study their localization, expression pattern and molecular properties. The Class II chitinase encoded by *Rcht 2* gene of rice was produced as a fusion protein in *E. coli* confirming that the gene codes for a functional enzyme (Kim et al., 1998). The induction of Rcht 2 chitinase by fungal elicitor is affected by phosphorylation/ dephosphorylation mechanism (Kim et al., 1998). In potato a distinct basic chitinase, Cht C of Class I gene family was reported to be expressed in the epidermal cells (Ancillo et al., 1999).

II. Chitnases inhibitors

Chitinase inhibitors have chemotherapeutic potential against fungi (Hollis et al., 2000; Sandor et al., 1998), insects (Sakuda et al., 1987) and malaria transmission (Vinetz et al., 1999; Vinetz et al., 2000). Recently, chitinase inhibitors were also suggested to have anti-inflammatory potential against asthma and allergic diseases, including atopic dermatitis and allergic rhinitis (Zhu et al., 2004). Although a few synthetic chitinase inhibitors for family 18 exist, the majority of effective (*i.e.* nM range) inhibitors are natural products. These vary widely in structure and include cyclic peptides (Izumida et al., 1996; Omura et al., 2000; Arai et al., 2000; Shiomi et al., 2000; Arai et al., 2000), amino acidderived materials (Tabudravu et al., 2002), pseudotrisaccharides (Sakuda et al., 1987; Nishimoto et al., 1991; Sakuda et al., 1986), complex alkaloids (Kato et al., 1995) and simple purinederived heterocycles (Rao et al., 2005). The need to understand the mode of binding of such inhibitors has led to detailed crystallographic investigations of chitinase–inhibitor complexes along with complementary kinetic, mutational and computational studies. These studies have also elucidated the reaction mechanism of this family of enzymes, and numerous examples of bound inhibitors mimicking reaction intermediates have been observed (Rao et al., 2005; van Aalten et al., 2001).

i) Kinetics and modes of binding of chitinase inhibitors

Most known chitinase inhibitors are classical reversible inhibitors that compete with the substrate by blocking its binding site, usually mimicking the stacking to one or more of the subsite tryptophans through π-π or other hydrophobic interactions and generating hydrogen bonds with potential partners in the active site. However, over the past two decades a range of natural product chitinase inhibitors have been identified and characterized, and in recent years, numerous crystal structures of chitinase-inhibitor complexes have been published (Tabudravu et al., 2002; Rao et al., 2005; Bortone et al., 2002; Papanikolau et al., 2003; Rao et al., 2003; Vaaje-Kolstad et al., 2004; van Aalten et al., 2001; Houston et al., 2002; Rao et al., 2005a; Houston et al.,2002a; Houston et al., 2004). Most of these inhibitor complexes are of the “bacterial-type” chitinases, whereas only one “plant-type” chitinase complex has been published (van Scheltinga et al., 1995).

i) The pseudotrisaccharide allosamidin and its derivatives

Allosamidin (Fig. 4b), a pseudotrisaccharide first isolated from the mycelium of *Streptomyces* sp. (Sakuda et al.,1987; Sakuda et al., 1986) is the most extensively studied chitinase inhibitor. Various biological properties have been reported associated with its activity as a chitinase inhibitor, including inhibition of cell separation in fungi (Kuranda and Robbins, 1991; Sakuda et al., 1990), toxicity towards insect larvae (Sakuda et al., 1987; Sakuda et al., 1986; Blattner et al., 1994) and blocking of malaria parasite penetration into the mosquito midgut (Shahabuddin et al., 1993). Most recently, allosamidin has been shown to ease lung inflammation in a mouse model of asthma (Zhu et al., 2004). Allosamidin is in general reported to be a competitive chitinase inhibitor (Dickinson et al., 1989), although non-competitive inhibition has also been reported (McNab and Glover, 1991). The structure of allosamidin is composed of two *N*-acetylallosamine residues and an aminocyclitol aglycone, allosamizoline (Fig. 5). Investigation of the biosynthesis of allosamidin in *Streptomyces* sp. has revealed that both *N*-acetylallosamine sugars and the carbocyclic moiety of allosamizoline are derived from Dglucosamine whereas the oxazoline group is derived from L-Arg and L-Met (Fig. 6) (Zhou et al., 1992). Binding of allosamidin to chitinases has been investigated through crystal structures using hevamine (van Scheltinga et al., 1995), *Sm*ChiB (Vaaje-Kolstad et al., 2004; van Aalten et al., 2001), *Ci*Chi (Bortone et al., 2002), human chitotriosidase (HCHT) (Rao et al., 2003), *Sm*ChiA (Papanikolau et al., 2003) and *Af*ChiB1 (Rao et al., 2005). It is likely that bound allosamidin resembles the oxazolinium ion reaction intermediate of the substrate-assisted reaction mechanism, thus generating favourable interactions leading to tight binding. *K*i values of 60nM and 230nM have been reported for *Candida albicans* chitinase (Dickinson et al., 1989) and *Ci*Chi (Bortone et al., 2002) respectively. IC_{50} values have also been reported for allosamidin against numerous chitinases (Table 2) ranging from strong inhibition of HCHT (Rao et al., 2003) and *Bombyx mori* chitinase (Sakuda, 1996) to relatively weak inhibition of *Saccharomyces cerevisiae* chitinase (Nishimoto et al., 1991). Allosamidin binds to the different chitinases in a similar way, with the two *N*-acetylallosamine sugars occupying the -3 and -2 subsites in an identical fashion to the corresponding *N*-acetylglucosamine substrate units. The allosamizoline unit binds in the -1 subsite as an exactmimic of the oxazolinium ion

reaction intermediate, making similar hydrogen bonds from the allosamizoline nitrogen and oxygen to the side chains of Asp175 and Tyr245, respectively (Rao et al., 2003; van Scheltinga et al., 1995; Vaaje-Kolstad et al., 2004; van Aalten et al.; 2001). Moreover, Asp175 is in the "up conformation" forming an additional hydrogen bond with Glu177, similar to that observed for the reaction intermediate (Papanikolau et al., 2003; Rao et al., 2003; van Scheltinga et al., 1995; Vaaje-Kolstad et al., 2004; van Aalten et al., 2001). In addition to conserved stacking interactions with Trp52 (only present in "bacterial-type" family 18 chitinases) and Trp384, hydrogen bonds are formed between the allosamizoline C6-hydroxyl and the side chain of Asp246, between the allosamizoline C4 hydroxyl and the backbone nitrogen of Trp137, between the acetyl of the-2 sugar and the side chain of Trp384, between the C5 hydroxyl of the -2 sugar and the backbone nitrogen of Thr 138, between the acetyl group of the -3 sugar and the side chain of Thr138 and between the C5 hydroxyl of the -3 sugar and the side chains of Arg57 and Glu322. These interactions are almost fully conserved amongst family 18 chitinases. Several naturally occurring analogues of allosamidin have been identified and isolated (Nishimoto et al., 1991) from *Streptomyces* sp., and tested for chitinase inhibition, namely methylallosamidin, (Isogai et al., 1989), *N*-demethylallosamidin, methyl-*N*-demethylallosamidin, glucoallosamidinsA and B (Somers et al., 1987) and didemethylallosamidin (Zhou, et al., 1993). *N*-demethylallosamidin has been shown to be a better protector of lysis of *Saccharomyces cerevisiae* daughter cells (Cabib et al., 1992) and is a stronger inhibitor of HCHT than compound allosamidin (Rao et al., 2003).

Table 2. IC_{50} values of allosamidins against various family 18 chitinases (nM)[(Ole et al., 2005).]

Chitinase	Allosamidin derivative					
	1	3	4	5	6	7
HCHT[(Rao et al., 2003)]	40	2.6	1.9	N.d.	N. d.	8.0
Mouse acidic mammalian chitinase[(Boot et al., 2001)]	400	N. d.	N. d.	N.d.	N. d.	N. d.
Neurospora crassa[(McNab and Glover, 1991)]	1600	N. d.	N. d.	N.d.	N. d.	N. d.
Trichoderma harzianum[(Sakuda, 1996)]	1300	1900	1300	N.d.	N. d.	2600
Bombyx mori[(Sakuda, 1996)]	48	65	81	N.d.	N. d.	65
Candida albicans[(Nishimoto et al.,1991;Dickinson et al., 1989)]	300/10000	14000	1200	960	5300	1300
Saccharomyces cerevisiae [(Nishimoto et al., 1991)]	54 000	58000	490	640	49000	800
Trichoderma sp. [(Nishimoto et al., 1991)]	1300	1900	1300	210	1400	2600

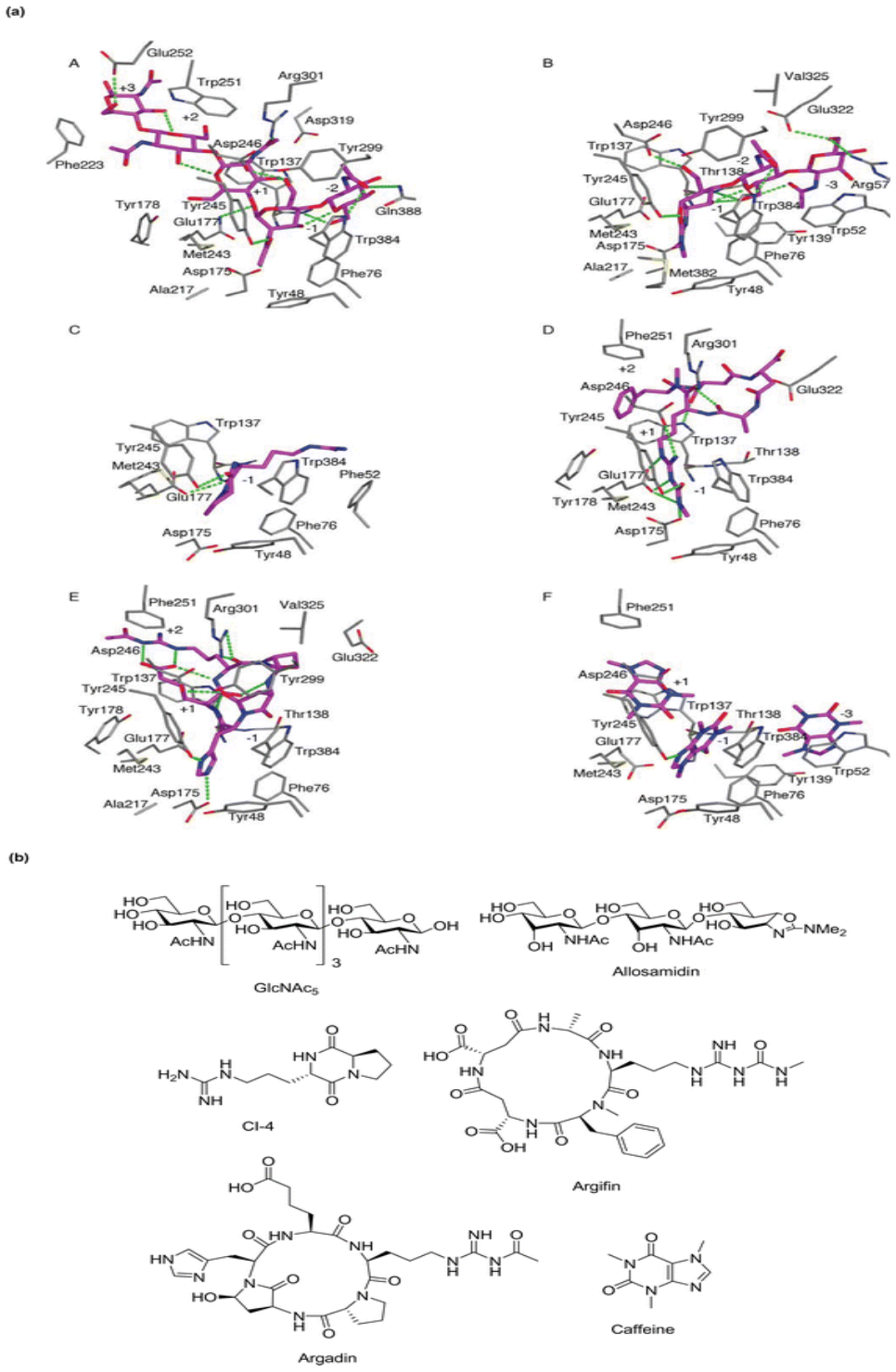

Fig. 4 (a) Ligand binding to chitinase active sites. A *Sm*ChiB–GlcNAc5, B *Af* ChiB1–allosamidin, C *Sm*ChiB–CI-4, D *Af* ChiB1–argifin, E *Af* ChiB1–argadin and F *Af* ChiB1–caffeine. Residues involved in direct ligand interactions are shown (selected residues in A omitted for clarity). Residue numbering is according to *Af* ChiB1 for all complexes; hydrogen bonds defined by WHAT IF120 are shown in green. Ligand carbon, magenta; protein carbon, grey; oxygen, red; nitrogen, blue; sulfur, yellow. Subsites (+2, +1, −1, −2 *etc.*) are also indicated. (b) Chemical structures of ligands depicted in Fig. 4a. (Andersen et al., 2005)

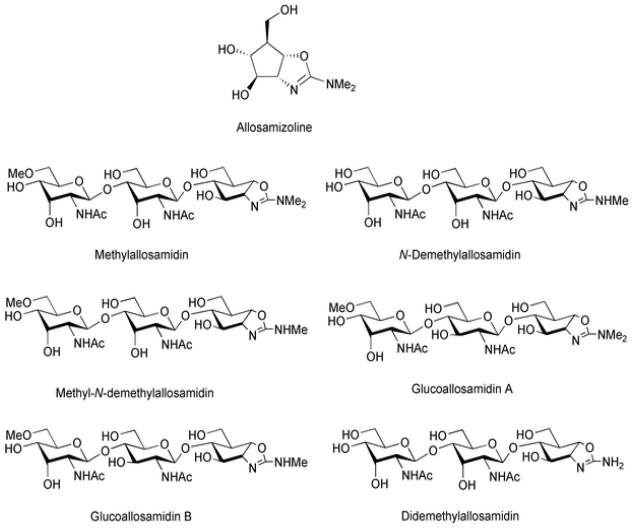

Fig. 5. Allosamizoline and naturally occurring allosamidins.

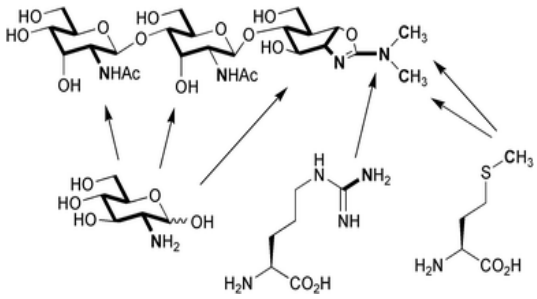

Fig. 6. Biosynthetic origin of allosamidin.

ii) Psammaplins

PsammaplinA (Fig.7) is a member of a family of compounds with antibacterial and antitumour properties that are derived biosynthetically from bromotyrosine and cysteine. PsammaplinA was originally isolated from the sponge *Psammaplysilla purpurea*, collected in the region of Tonga by Quinoa et al., 1987; Jimenez andCrews, 1991 and subsequently identified independently from other sources by the groups of Rodriguez et al., 1987 and Arabshahi and Schmitz, 1987. Tabudravu et al., 2002 showed that psammaplinA is a modest inhibitor of *Bacillus* sp. Chitinase (IC_{50} = 68μM) giving a mixed non-competitive inhibition at lower concentrations and an uncompetitive inhibition at higher concentrations. PsammaplinA was further determined to be a non-competitive inhibitor of *Sm*ChiB with a *K*i of 148 μM and an IC_{50} of 100 μM (Tabudravu et al., 2002). The closely related derivatives psammaplinK and L (Fig.7), and the dimeric analogue, bisaprasin (Fig.7) showed no significant inhibition of *Bacillus* sp. chitinase. Further members of the psammaplin family have since been isolated by Pina et al., 2003 but no chitinase inhibitory activity has so far been reported. The crystal structure of *Sm*ChiB in

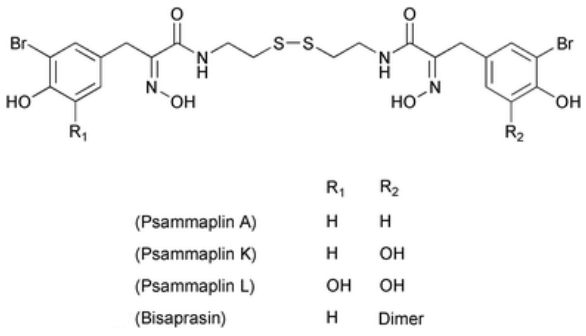

	R_1	R_2
(Psammaplin A)	H	H
(Psammaplin K)	H	OH
(Psammaplin L)	OH	OH
(Bisaprasin)	H	Dimer

Fig. 7. Psammaplins tested for chitinase inhibitory activity.

complex with psammaplinA shows undefined electron density in the active site consistent with conformational flexibility and disordered binding of the inhibitor (Tabudravu et al., 2002). Asp175 is partially in the "up conformation" pointing towards Glu177 indicating partial binding in the -1 subsite. The precise binding mode of this inhibitor to family 18 chitinases has thus so far not been established.

iii) Styloguanidines

The styloguanidines are a small group of natural products that possess a unique hexacyclic bis-guanidine structure. Styloguanidine (Fig. 8) itself and two brominated analogues A and B (Fig. 8) were isolated by Kato et al., 1995 from the sponge *Stylotella aurantium*, collected in the Yap Sea. Also isolated was the isomeric alkaloid palau'amine C (Fig. 8), which had previously been obtained by Kinnel et al., 1993 and Kinnel et al., 1998 from *Stylotella agminata*, collected in the Western Caroline Islands. Kato reported that styloguanidine and analoques (A &B) showed inhibitory activity towards a bacterial chitinase from *Schwanella* sp. and also inhibited the moulting of cyprid larvae of barnacles. Although a range of interesting biological properties has been reported for C (cytotoxic, antibiotic, antifungal, immunomodulatory), no inhibition of chitinases has yet been noted.

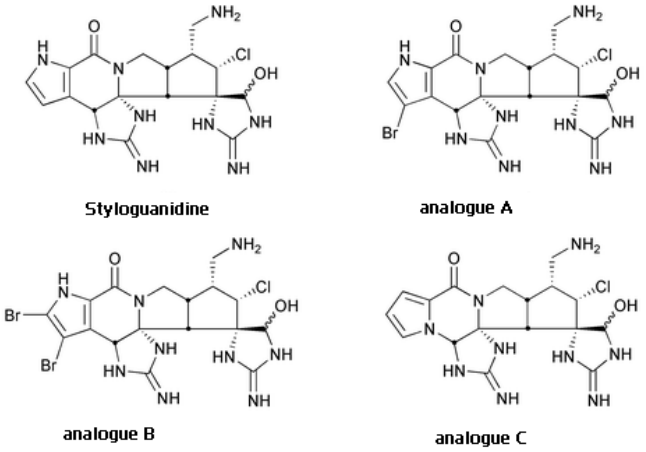

Fig. 8. Styloguanidines, palau'amine and synthetic intermediates.

iv) Cyclic proline-containing dipeptides

The cyclic dipeptide, cyclo (L-Arg–D-Pro) (CI-4, Fig. 4b), produced by the marine bacterium *Pseudomonas* sp. IZ208, was isolated and identified as a chitinase inhibitor by Izumida et al., 1996a. They prepared CI-4 and the stereoisomers A and B (Fig. 9) and evaluated them against chitinase from *Bacillus* sp. CI-4 gave 17.2% inhibition of this enzyme at a concentration of 1 mM, the L–L diastereoisomer A was slightly more potent giving 18.4% inhibition at the same concentration, while B only showed 4.9% inhibition (Izumida et al.,1996a). Using the agar plate method, Izumida et al.,1996a also

detected chitinase inhibitory activity for CI-4 and A at a concentration of 50 µgper disk, whereas weaker inhibition was observed for B, consistent with the enzyme kinetics data. CI-4 has since been shown to competitively inhibit *Sm*ChiB with a *K*i of 0.65 mM (Houston et al., 2002a) and an IC_{50} of 1.2 mM (Houston et al., 2004) whereas an IC50 value of 6.3 mM has been reported for A (Houston et al., 2004). CI-4 was also shown to inhibit cell separation in *Saccharomyces cerevisiae* and blocked morphological changes in *Candidaalbicans*, presumably through inhibition of chitinases in these organisms (Izumida et al., 1996a). Crystallographic and kinetic studies of other cyclic dipeptides related to CI-4 have also been reported (Houston et al., 2004). The structure of *Sm*ChiB in complex with CI-4 shows that the latter mimics the reaction intermediate (panel C, Fig. 4a) with the proline unit and the cyclic dipeptide backbone of the similarly sized two-ring structure coinciding with the oxazoline and pyranose rings of the reaction intermediate, respectively (Houston et al., 2002a). The hydrogen bond between the D-Pro carbonyl oxygen and the Tyr245 hydroxyl group also imitates the corresponding hydrogen bond involving the oxazoline nitrogen of the reaction intermediate. Likewise, the hydrogen bond between the L-Arg carbonyl oxygen and the main chain nitrogen of Trp137 reproduces the corresponding interaction that involves the hydroxyl group of the pyranose moiety. Additionally, a water-mediated hydrogen bond is observed between the L-Arg backbone nitrogen to the carboxyl group of Asp246, mimicking the direct hydrogen bond from the hydroxymethyl group of the intermediate to the Asp residue. An additional hydrogen bond involves the L-Pro backbone nitrogen and the side chain of Glu175.

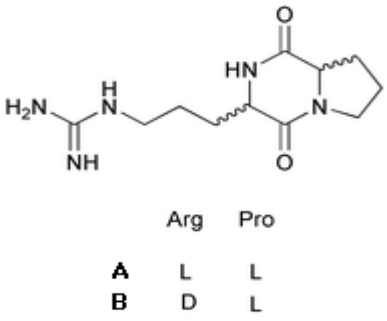

Fig. 9. Stereoisomers of 100 (CI-4) tested for chitinase inhibitory activity.

v) The cyclopentapeptides argifin

The cyclopeptide argifin (Fig. 4b), isolated from the fungal strain *Gliocladium* sp. FTD-0668 (Omura et al., 2000; Arai et al., 2000; Shiomi et al., 2000) was the first non-sugar molecule to show chitinase inhibition in the submicromolar range (Shiomi et al., 2000). Cyclopeptide argifin consists of an *N*-methyl carbamoyl-derivatised L-Arg, an *N*-methyl L-Phe, two β-L-Asp and a D-Ala residue. The unusual acylated Arg residue plays

a key role in the binding of cyclopeptide argifin to family 18 chitinases. IC_{50} values of 3.7, 1.1 and 4.5 μM were obtained against *Lucilia cuprina* (blowfly) chitinase (Shiomi et al., 2000), *Af* ChiB1 and HCHT (Rao et al., 2005a) respectively. A *K*i of 33 μM was obtained against *Sm*ChiB (Houston et al., 2002) whereas a K_d of 0.46 μM has been reported for *Af* ChiB1 (Rao et al., 2005a). Crystallographic structures of binary enzyme-cyclopeptide argifin complexes have been determined for *Sm*ChiB (Houston et al., 2002). *Af* ChiB1 and HCHT (Rao et al., 2005a). The structures reveal that cyclopeptide argifin binds to subsites -1, +1 and +2, interacting with residues Trp384, Trp137 and Phe251 that are conserved hydrophobic residues in family 18 chitinases (panel D, Fig. 4a). Cyclopeptide argifin binds in a similar fashion to the three different chitinases and itself contains one intramolecular hydrogen bond linking the carbonyl group of the D-Ala to the nitrogen of the first β-Asp. The *N*-methyl-carbamoyl moiety packs in the active site pocket so as to interact with the side chains of Tyr48 and Trp384; its nitrogen hydrogen bonds to the carboxyl groups of Asp175 and Glu177, whereas its oxygen hydrogen bonds to the hydroxyl group of Tyr245. The Arg residue also forms a salt-bridge-like interaction with the catalytic acid Glu177. Parts of the binding pattern of the *N*-methylcarbamoyl group resemble that seen for the natural substrate in which the *N*-acetyl group of the distorted -1 sugar in the *Sm*ChiB-GlcNAc5 structure overlaps with the *N*-methyl-carbamoyl group thereby retaining the hydrogen bonds to Asp175 and Tyr245. Likewise, one of the hydrogen bonds to the catalytic acid is preserved, while Asp175 is retained in the "up conformation" pointing towards the catalytic acid. An additional hydrogen bond conserved amongst chitinases is observed between the first β-L-Asp side chain and the Trp137 side chain. In addition, stacking interactions are formed between the L-Phe side chain of cyclopeptide argifin and the side chains of Phe251 and Trp137. The higher affinity of cyclopeptide argifin towards *Af* ChiB1 compared to *Sm*ChiB can be explained by a slight shift in the binding of cyclopeptide argifin to *Af* ChiB1 (maximum backbone coordinate shift of 1.9 A˚) (Rao et al., 2005a) that generates specific hydrogen bonds between the LArg side chain and the Asp246 carboxyl group and between the L-Arg carbonyl and the Arg301 side chain. In addition, a higher number of water-mediated hydrogen bonds linking cyclopeptide argifin with the protein are observed in the *Af* ChiB1 complex.

vi) The cyclopentapeptides argadin

Shortly after the isolation of cyclopeptide argifin was reported, a further cyclopentapeptide, argadin (Fig. 4b), was obtained from fungal strain *Clonostachys* sp. FO-7314 (Arai et al., 2000). Argadin consists of an acetylated L-Arg, a D-Pro, a backbone cyclised L-Asp-bsemialdehyde, an L-His and an L-aminoadipic acid residue. The published inhibition and binding constants for argadin against representative chitinases are generally lower compared to argifin, with IC_{50} values of 150 nM against *Lucilia cuprina* chitinase (Arai et al., 2000). 0.5 μM against *Af* ChiB1 (Rao et al., 2005a) and 13 nM against HCHT (Rao et al., 2005a). A *K*d of 0.81 μM was obtained against *Af* ChiB1 and a *K*i of 20 nM was obtained against *Sm*ChiB (Rao et al., 2005a). Compound argadin has also been shown to arrest the moulting of cockroach larvae upon injection into the ventral abdominal part (Arai et al., 2000). Compared to argifin, argadin has a smaller cyclic backbone, generating a more compact structure. The hemiaminal unit and the D-Pro restrict torsion involving the main chain, thus possibly contributing to a more rigid structure for argadin. Moreover, four conserved intramolecular hydrogen bonds (aminoadipic carbonyl to hemiaminal nitrogen, aminoadipic nitrogen to hemiaminal hydroxyl group and two bonds from the aminoadipic carboxyl group to the Arg side chain, panel E, Fig. 4a) are present in the binary *Sm*ChiB (Houston et al., 2002), *Af* ChiB1 and HCHT- argadin (Rao et al., 2005a) complexes to further stabilize the inhibitor conformation upon binding to chitinases. An additional intramolecular hydrogen bond between the aminoadipic carboxyl group and the backbone nitrogen of L-Arg is observed in the *Af* ChiB1 and HCHT complexes. While, like argifin, argadin is seen to bind to subsites -1, +1 and +2 in the complexes with *Sm*ChiB, *Af* ChiB1 and HCHT, this binding is surprisingly different compared to argifin with the His side chain instead of the Arg pointing inside the active site pocket. The binding pattern of the His residue of argadin mimics that of the natural substrate in a similar fashion to that observed for binding of argifin, with the L-His side chain hydrogen bonding the side chains of Asp175 and Tyr245; however the Asp175 is in the "down conformation" pointing towards Asp173. The peptide backbone of argadin binds noticeably deeper in the active site than that of argifin allowing hydrogen bonds between the hemiaminal carbonyl and the side chain of Asp246 whereas two hydrogen bonds are observed between the L-Arg carbonyl and the

side chain of Arg301. Mutation, crystallographic and kinetic studies have determined that the stacking interactions with Trp384, Trp137 and Phe251 (corresponding to the -1, +1 and +2 subsites) are the main contributors for cyclopentapeptide binding and specificity. Consequently, "plant-type" family 18 chitinases are believed to be poor targets for argifin or argadin, as these enzymes do not possess all of these conserved side chains. The published inhibition and binding constants of the cyclopentapeptides show that chitinases (except *Af* ChiB1) have a marked preference towards argadin over argifin. The difference can be explained by the more rigid structure of argadin, and a deeper binding in the active site that displaces more water molecules allowing a larger contact surface with the protein (130-148 A˚) compared to argifin (112-133 A˚) (Houston et al., 2002; Rao et al., 2005a). The stronger *Af* ChiB1 inhibition of argifin relative to argadin can be explained by Trp384 adopting a different conformation upon binding of a, thereby maximizing the stackingwith the guanylurea moiety. Moreover, a few enzyme-specific differences are observed in the hydrogen-bonding pattern.

vii) Methylxanthines

Methylxanthines have been found in as many as sixty different plant species and include the well known compounds caffeine (Fig. 4b), theophylline and theobromine (Fig. 10). Caffeine and theophylline have recently been identified as chitinase inhibitors, with theophylline previously having been shown to act as a bronchodilator, and to have several anti-inflammatory activities related to asthma (Weinberger and Hendeles, 1996). caffiene and theophylline were shown to be competitive *Af* ChiB1 inhibitors and crystallographically determined to bind in an identical fashion in the -1 subsite, mimicking the oxazolinium ion intermediate by hydrogen bonding the side chains of Asp175 (theophylline only) and Tyr245 as well as the main chain of Trp137 (panel F, Fig. 4a). Despite the loss of one hydrogen bond and a displacement of Asp175 to the "down conformation" pointing towards Asp173, caffiene was shown to be the more potent *Af* ChiB1 inhibitor compared to theophylline with IC_{50} values of 469 and 1500 μM, respectively. Inhibition of human acidic mammalian chitinase has also been reported by Rao et al., 2005. The preparation

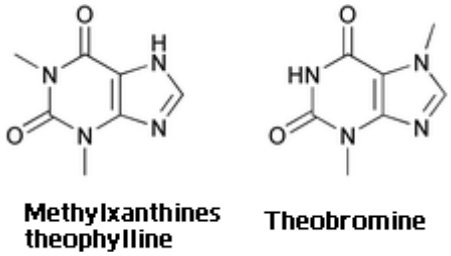

Fig. 10. Methylxanthines theophylline and theobromine.

of xanthine-type molecules related to caffeine, theophylline and theobromine are quite straight forward and there should therefore be considerable scope for the synthesis of a variety of analogues of this kind.

viii) Miscellaneous inhibitors

A few other reports of chitinase inhibitory activity have appeared for other natural products, but so far no crystallographic information have been reported for these molecules. Nitoda et al., 2003 have reported the identification ofa water-soluble polysaccharide from screening of fungal broths that is a potent inhibitor of a chitinase from *Spodoptera litura* (IC_{50} = 28 nM) (Nitoda et al., 2003). The isolated molecule, with an estimated molecular weight of 16 kDa, was partially characterised and shown to contain glucose, galactose, *N*-acetylglucosamine and a deoxysugar. Braun et al., 1995 isolated four α,β-Unsaturated γ-lactones A-D (Fig. 11) from *Streptomyces antibioticus* that were weak inhibitors of a chitinase from *S. marcescens*.

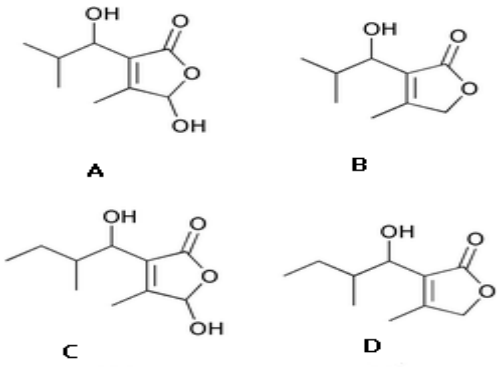

Fig. 11. α,β-Unsaturated γ-lactones isolated *Streptomyces antibioticus*.

The present chapter describes a slow-tight binding irreversible inhibition of Chitinase A from *Serratia marcescens* by API. API also reported to inhibit aspartic pepsin (Kumar and Rao, 2006). The steady-state kinetics reveals a two-step inhibition mechanism. The conformational modes observed during the binding of API to ChiA were conveniently monitored by fluorescence and CD-cpectra analysis. The mechanism of inactivation of ChiA by API was delineated by monitoring the isoindole fluorescence of the *o*-phthalaldehyde (OPTA)-labeled ChiA and a model for the probable interactions is proposed.

MATERIAL AND METHODS

Materials

Acetonitrile was purchased from E-Merck, Germany. Trifluoroacetate (TFA), *p*-nitrophenyl-*N,N'*-Diacetyl-β-chitobioside [*p*-NP-$(glcNAc)_2$] and OPTA were from sigma-Aldrich USA. All other chemicals were of analytical grade.

Purification and biochemical characterization of API

The inhibitor was purified and characterized from extra cellular culture filtrate of *Bacillus licheniformis* as described previously in part 2 of chapter 2 (Kumar and Rao 2006).

Assay for inhibitory activity towards ChiA for inhibition kinetics

ChiA was assayed in the presence of chromogenic substrate *p*-nitrophenyl-*N,N'*-diacetyl-β-chitobioside [*p*-NP-$(glcNAc)_2$] according to Vorgias, 1997 with some modifications. 250 µl of enzyme solution (0.5 nM) was incubated with 250 µl of 1mM [*p*-NP-$(glcNAc)_2$] solution dissolved in 100 mM macilvein buffer (pH 6.0) for 30 minutes at 50°C. The release of *p*-nitrophenol was monitored at 405 nm (E_{405} = 18.5 $mmol^{-1}.cm^{-1}$) using a 1cm path length cuvette. One unit of chiA activity was defined as the amount of enzyme that catalyzes the release of 1µM.min^{-1} of *p*-nitrophenol. For the kinetic analysis and rate constant determinations, the assays were carried out in triplicate, and the average value was considered throughout this work.

Initial kinetic analysis

The kinetic parameters for the substrate hydrolysis were determined by measuring the initial rate of enzymatic activity as described in materials and methods section of chapter 2 (part 2). ChiA was reported to have K_M value of 500µM for [*p*-NP-$(glcNAc)_2$] (Vorgias, 1997). For Dixon plot, hydrolytic activity of chiA (0.5 nM) was measured in the presence of 500 µM and 1000 µM [*p*-NP-$(glcNAc)_2$], incubated with 0.1 to 1 µM API concentrations at 50 °C for 30 min.

Demonstration of the time dependence of inhibition

API (0.1-1µM) was added from a 1 mM stock solution in milli Q water to 0.5 nM ChiA in 500µl macilvein buffer (pH 6.0). After 0-30 minutes of preincubation, 250 µl of

the chiA-API mixture was added into 250 µM of [*p*-NP-$(glcNAc)_2$] solution at 50°C. After 30 minutes, the release of *p*-nitrophenol was quantified as described above.

Determination of initial apparent inhibition constant

The apparent inhibition constant determination studies were performed by adding 250 µl of chiA (0.5nM) to 250 µl of 1 mM [*p*-NP-$(glcNAc)_2$] solution in macilvein buffer containing varying API concentrations (0.1-1 µM) at 50°C. After 30 minutes, the release of *p*-nitrophenol was quantified as described above. Please see materials and methods section of chapter 2 (part 2) for more detailes.

Time dependence of initial apparent inhibition constants

Experiments were conducted as described above, except that the ChiA was added to substrate sulution at varying API concentrations (0.1-1µM), and then assayed after preincubation for 0, 15, and 30 minutes.

Recovery of activity from inactivated ChiA

API was tested to determine if it was an irreversible inhibitor of ChiA. ChiA (0.5 nM) was preincubated with and without the equimolar concentration of API for 60 minutes in macilvein buffer. Further, the enzyme inhibitor mixture was diluted 100 fold into the assay mixture containing the substrate at 10 K_m. After preincubation for 60 minutes, 1.0 ml of sample was removed and diluted to 10.0 ml in macilvein buffer. At the specified time, aliquots were removed and assayed for the catalytic activity.

Inhibitor progress curve analysis

The inhibitor progress curves for the interaction between API and ChiA were analyzed as described in materials and methods section of chapter 2 (part 2).

Fluorescence analysis

Fluorescence measurements were performed according to Kumar and Rao 2006. For inhibitor binding studies, ChiA (0.5nM) was titrated with different API concentrations (0.1-1µM) each time to a new enzyme solution.

Effect of API on the isoindole fluorescence of OPTA-labeled ChiA

Fresh OPTA solution was prepared in methanol for each experiment. The enzyme modification was carried out by incubating ChiA (1 nM) in 1 ml macilvein buffer, pH 6, with 50 nM OPTA at 25 °C. Methanol had no effect on the activity of the enzyme and was always less than 2% (v/v). The formation of ChiA-isoindole derivative was followed

spectrofluorometrically by monitoring the increase in fluorescence with the excitation wavelength fixed at 338 nm. To monitor the effect of API on the isoindole fluorescence of ChiA, the enzyme was preincubated with API (1 μM) for 15 min, and then OPTA was added and the formation of isoindole derivative was monitored as described above.

Circular dichroism analysis

CD spectra were recorded in a Jasco-J715 spectropolarimeter at ambient temperature using a cell of 1-mm path length. Replicate scans were obtained at 0.1-nm resolution, 0.1-nm bandwidth, and a scan speed of 50 nm/min. Spectra were averages of six scans with the base line subtracted spanning from 200 to 260 nm in 0.1-nm increments. The CD spectrum of the ChiA (10 μM) was recorded in macilvein buffer (pH 6.0) in the absence and presence/absence of API (10-100 μM) and substrate (100 μM) at 4°C. Secondary structure content of the ChiA, the ChiA-substrate complex, and the ChiA-API complex was calculated using the algorithm of the K2d program (Andrade et al., 1993).

RESULTS

Biochemical characterization of API and determination K_i value

API, a peptidic inhibitor of aspartic proteases, produced extracellularly by thermo tolerant *Bacillus licheniformis* (Kumar and Rao, 2006) has an amino acid sequence of Asp-Leu-Tyr-Asp-Gly-Trp-Lys-His-Glu-Ala-Glu-Cys-Ile and a pI value of 4.3 (Part 2 of Chapter 2). The predominance of the charged amino acid residues in the inhibitor sequence indicates its hydrophilic nature. API inhibited ChiA with an IC_{50} value (50% inhibitory concentration) of 780±30 nM (Figure 12). The inhibition of ChiA followed a sigmoidal pattern with increasing concentrations of the inhibitor. However, non linearity of secondary plot (the slope of inhibition graph versus API concentration) suggests Michaelis-Menten inhibition kinetics is not appropriate in this study. The inhibition constant K_i, determined by Dixon plot was to be 510 nM (Fig. 13).

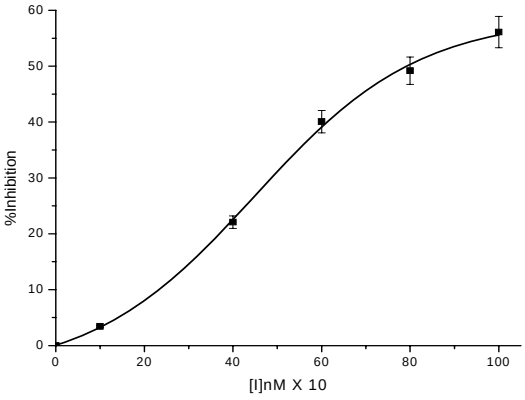

Figure 12 - The sigmoidal curve indicates the best fit for the percentage inhibition data obtained, and the IC_{50} value was calculated from the graph.

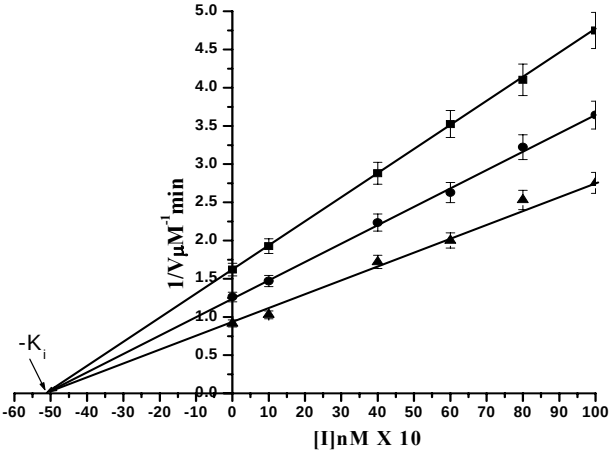

Figure 13- Enzymatic activity of the ChiA (0.5 nM) was estimated using the substrate [p-NP-(glcNAc)2] 0.5 mM (●) and 1.0 mM (■) at different API concentrations (0.1-1.0 µM). Reciprocals of the reaction velocity were plotted versus the [p-NP-(glcNAc)2] concentration. The straight lines indicated the best fit of the data obtained. The inhibition constant K_i was calculated from the point of the intersection of the plots.

Time dependent inhibition of ChiA by API and recovery of activity from inactivated ChiA

The concentration of [*p*-NP-$(glcNAc)_2$] was set to a value below the Michaelis constant (K_m) 500 μM (Vorgias, 1997), to make reactions approximately first-order. The results from the preincubation experiments with the API are presented in Table 1. The apparent inhibition constants decreased 41 fold over a 30 min period (Figure 14). When ChiA was preincubated with API for more than 60 minutes, recovered enzyme concentration was estimated very low as approximately 0.02 nM. Reduction of [*p*-NP-$(glcNAc)_2$] was observed at a steady-state velocity of approximately 7% relative to the control (Figure 15). This shows that API is an irreversible inhibitor of ChiA.

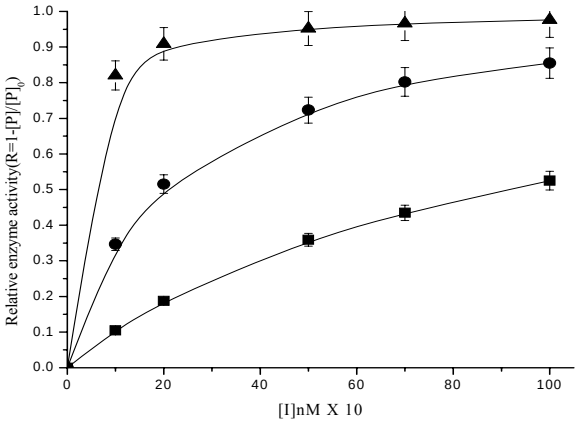

Figure 14. The preincubation kinetic studies. Apparent Inhibition Constants with or without Preincubation of API (0.1-1.0 μM) with chiA (0.5 nM). Results are described in table 1.

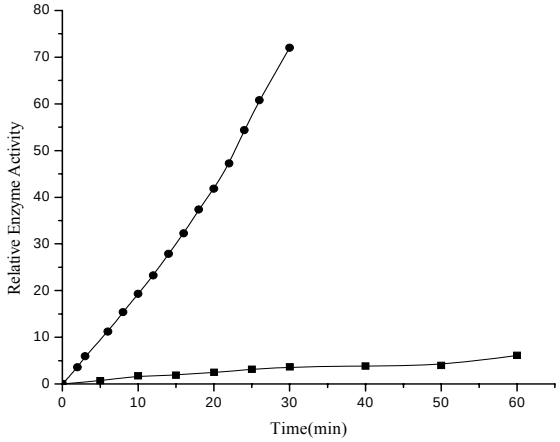

Figure 15- Loss of residual enzyme activity upon preincubation of 0.5 nM chiA with (●) and without (■) API. See Experimental Procedures for details.

Table 1- Apparent Inhibition Constants with or without Preincubation of Inhibitor (0.1-1.0 μM) with ChiA (0.5 nM).

K_{app} (μM)[a]		
t =0 min	t = 15 min	t = 30 min
949.5±56.4	185±11.4	21.7 ±3.2

[a]ChiA was preincubated with varying concentrations of inhibitor for 0, 15, or 30 min before the assay. Remaining residual enzyme activity was measured in a 30 min assay.

Simplified inhibition progress curve analysis for API

The reaction progress was analyzed by two different methods (Moss et al., 1996). The results of a preliminary analysis, based on the assumption of rapid equilibrium, are shown in Figure 16. The progress curves obtained at 100, 200, 400, 600 and 1000 nM API concentrations were fitted individually to eq. 2. The best-fit values of adjustable parameters, for each concentration of the API, are listed in Table 2. For a one-step inhibition mechanism, without an intermediate enzyme-inhibitor complex, the initial velocity V_0 should be constant, and the apparent rate constant k_{app} should increase linearly with the inhibition concentration $[I]_0$. These properties of the one-step mechanism are expressed in eq. 5a-c (Szedlacsek and Duggleby, 1995).

$$V_0 = V_{max}[S]_0/([S]_0 + K_M) \quad (5a)$$

$$V_S = V_{max}[S]_0/([S]_0 + K_M(1 + [I]_0/K_i)) \quad (5b)$$

$$k_{app} = k_7 + k_6[I]_0/(1 + [S]_0/K_M) \quad (5c)$$

On the other hand, for a two-step inhibition mechanism (Scheme 1 chapter 2, part 3) the initial velocity should decrease with the inhibitor concentration, by following a typical binding curve, and the apparent rate constant should depend on $[I]_0$ as a hyperbola, according to eq. 6a-c.

$$V_0 = V_{max}\,[S]_0/([S]_0 + K_M(1 + [I]_0/K_i)) \quad (6a)$$

$$V_S = V_{max}\,[S]_0/([S]_0 + K_M(1 + [I]_0/K_i^*)) \quad (6b)$$

$$K_{app} = k_7 + k_6([I]_0/K_i)/(1 + [S]_0/K_M + [I]_0/K_i) \quad (6c)$$

The parameters listed in Table 2 favor the two-step inhibition mechanism, because the initial velocity does decrease with the concentration of the inhibitor, as predicted by eq. 6a. Also, the increase of the apparent rate constant with $[I]_0$ is hyperbolic, instead of linear. The nonlinear least squares fit of V_0, V_S, and K_{app} to eq. 6a-c are shown in Figure 17. From fitting of V_0 to eq. 6a, the dissociation constant K_i of the initial complex was 830 nM; the fitted value of V_{max} was $9.7\pm 0.1\times10^{-2}$au s^{-1}. From fitting of V_S to eq. 6b, the overall dissociation constant K_i^* was 7.5±1 nM; the fitted value of V_{max} was 0.098 ±0.001 au s^{-1} in this case. From fitting of k_{app} to eq. 6c (fig. 17 *inset*), the initial inhibition constant K_i was 790 nM. The isomerization rate constants were k_6 $=8.74\pm0.1\times10^{-3}$ s^{-1} and k_7 $=7.3\pm0.6\times10^{-5}s^{-1}$, from which the total dissociation constant K_i^* $= K_ik_7/k_6$ was 6.6 nM.

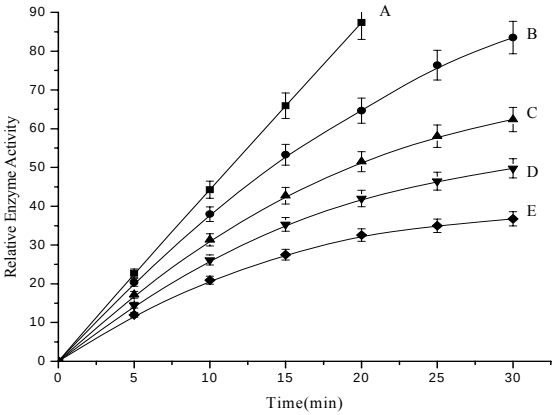

Figure 16- Least-squares fit of progress curves from the inhibition of ChiA (0.5 nM) by inhibitor to eq. 2. The initial substrate concentration was 1 mM. The API concentrations were 0.0, 0.2, 0.4, 0.6 and 1.0 μM for curves A-E, respectively. For experimental condition and the best-fit values of adjustable parameters see text.

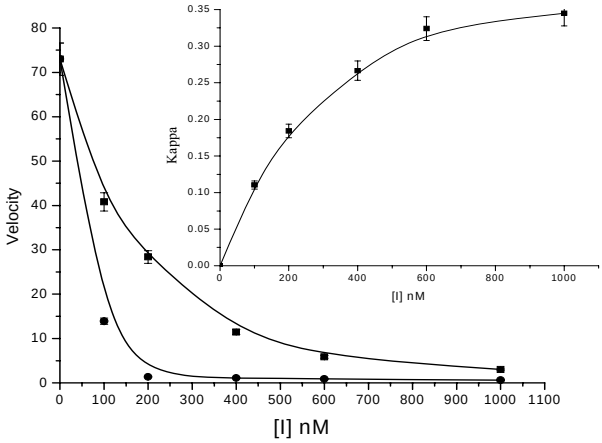

Figure 17- Least-squares fit of the initial velocities V_0 (■) from table 2 to eq. 6a, the steady-state velocity V_S (●) to eq. 6b, and the apparent first-order rate constant K_{app} to eq. 6c. The best fit values of adjustable parameters K_i, K_i*, k_6, and k_7 are listed in the text and summarized in table 3.

Table 2- Best fit values of adjustable parameters, obtained in fitting the progress curves shown in figure 16 (0.5 nM ChiA, 1 mM [p-NP-(glcNAc)2], pH 6.0, 37 ˚C) to eq. 2.

$[I]_0$ (nM)	V_S (REA)	V_0 (REA)	k_{app} (s^{-1})
0	73.00	73.00	0.00
100	13.91	49.88	0.11
200	1.36	29.36	0.18
400	1.11	12.03	0.26
600	0.86	5.66	0.32
1000	0.59	3.00	0.34

The inhibition progress curves for inhibitor were analyzed more thoroughly, by using a complete differential model where the rapid equilibrium assumption was not made Moss et al., 1996. The collections of progress curves in Figure 16 were fitted as a whole to the system of eqs. 3 and 4. The constant parameters were the initial concentration of the substrate ($[S]_0$ = 1 mM), API ($[I]_0$ = 0, 100, 200, 400, 600, and 1000 nM), initial concentration of the ChiA in the assay where inhibitor was absent ($[E]_0$=0.5 nM) and the bimolecular rate constant for the formation of the Michaelis complex (k_1 = 1000 μM^{-1} s^{-1}). The best-fit values of globally optimized parameters were k_2 = 9.92 ±

0.85 s^{-1}, k_3 = 8.8±0.95 μM^{-1} s^{-1}, k_4 =8.123 ± 1.0 s^{-1}, k_5 =6.31 ± 0.5 × 10^{-3} s^{-1}, k_6 = 5.47 ± 0.6 ×$10^{-5}s^{-1}$, k_7 = 2.68 ± 0.22 s^{-1} and r_P = .85 ± 0.02. From the best-fit values of rate constants k_3 and k_4, the dissociation constant of the initial complex, K_i, was calculated as k_5/k_4 =923 nM. Similarly, the overall dissociation constant of the final complex, K_i*, was calculated as k_5k_7/k_4k_6 =6.3 nM. The kinetic constants determined in this study are summarized in Table 3.

Effect of API binding on the fluorescence of chitA

The kinetic analysis has revealed a two-step inhibition mechanism, where the *E*I complex isomerizes to a tightly bound, slow dissociating *E*I* complex due to conformational changes in tertiary structure of ChiA induced by the binding of API. The tryptophanyl fluorescence of ChiA exhibited an emission maxima (λ_{max}) at 342 nm, as a result of the radioactive decay of the π-π* transition from the Trp residues (Figure 18). The binding of inhibitor resulted in a red shift in λ_{max} and concentration-dependent quenching of the fluorescence with saturation reaching at or above 1μM API concentration. The red shift in λ_{max} confirmed the conformational changes in the three-dimension structure of the enzyme due to API binding. Binding of API resulted in an exponential decay of the fluorescence intensity as indicated by a sharp decrease in the quantum yield of fluorescence followed by a slower decline to a stable value. Furthermore, titration of API against ChiA revealed that the magnitude of the initial rapid fluorescence loss (F_0-F) increases in a saturation-type manner (Figure 19) which corroborats the two-step slow-tight binding inhibition of ChiA by API. The value of K_i determined by fitting the data for the magnitude of the rapid fluorescence decrease (F_0-F) was 512 nM. The conformational changes induced during the isomerization of EI to EI* was monitored by analyzing the tryptophanyl fluorescence of the complexes as a function of time (Figure 20). The k_6 and K_i values were determined from the data derived from the slow decrease in fluorescence were 3.81 ± 0.25 × 10^{-3} s^{-1} and 867 nM respectively (Figure 21). These rate constants are in good agreement with that obtained from the kinetic analysis (table 3). A progressive quenching in the fluorescence of the ChiA at 342 nm was observed concomitant to the binding of substrate [*p*-NP-$(glcNAc)_2$]. The binding of the substrate lead to the quenching of the emission spectra of ChiA. The comparative analysis of the intensity changes in the fluorescence spectra of the ChiA upon binding of

the substrate was not found to be similar to that of API, suggesting that API does not bind in the active site of the enzyme. Therefore, the initial rapid fluorescence decrease and red shift in λ_{max} can be correlated to the formation of the irreversible complex EI**, whereas the slow, time-dependent decrease reflects the accumulation of the tight bound slow dissociating complex *E*I*.

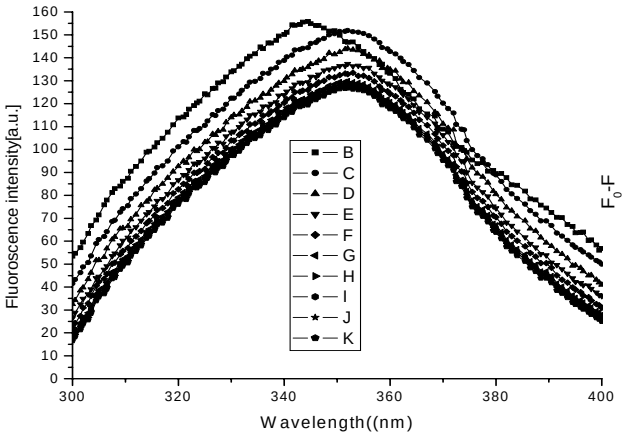

Figure 18- Steady-state fluorescence emission spectra of chiA as a function of inhibitor. Different concentrations of API, 0.1-1.0 μM (B-K) were added to a fixed concentration of ChiA and titration was performed.

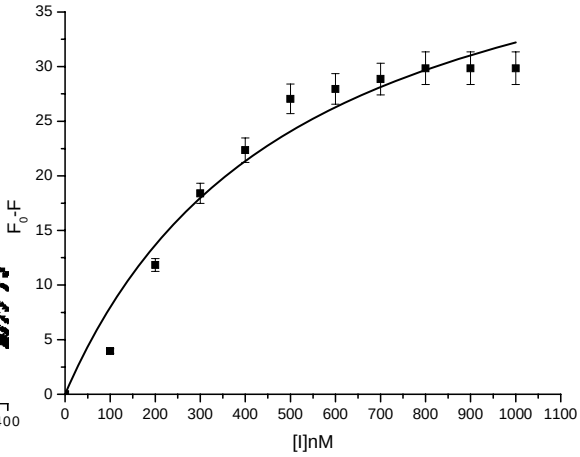

Figure 19- The fluorescence changes (F_0-F) were plotted against the API concentrations. The resulting hyperbola curve was fitted to the equation ((F_0 - F) = Δ F_{max} / (1 + (K_i/ [I])) to give the calculated value of K_i.

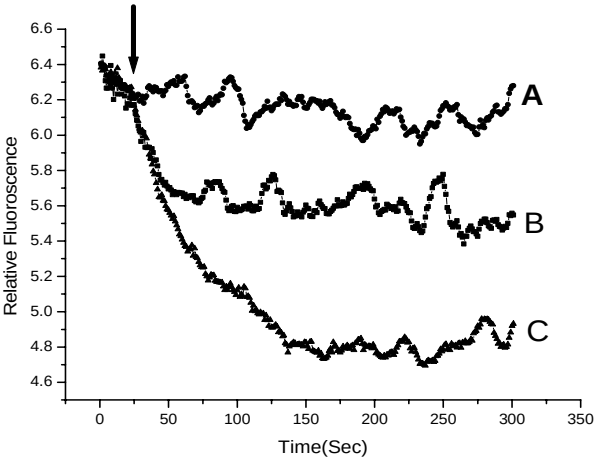

Figure 20- Time dependent effect of API on the fluorescence quenching of chiA. API in deferent concentrations, 0 μM (A), 0.5 μM (B) and 1.0 μM (C) was added to ChiA (0.5 nM) at the specified time (indicated by the *arrow*), and the fluorescence emission was monitored for 300 s, at a data acquisition time of 0.1 s. See methods for more details.

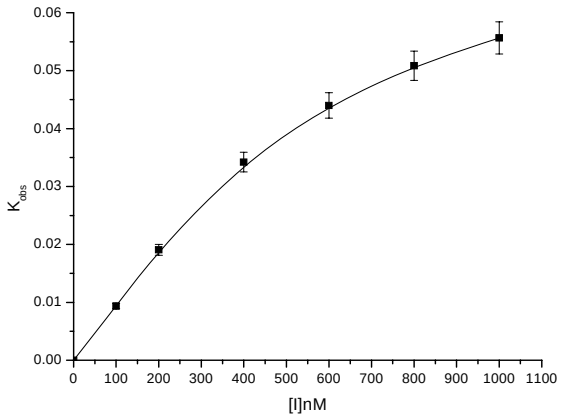

Figure 21- The slow decay of ChiA fluorescence at each concentration was fitted to a first order rate equation to obtain k_{obs} (see material and method). The k_{obs} values were then computer fitted to the equation $k_{obs}=k_6$ [I]/(K_i+[I]) to give calculated values of K_i and k_6.

Effect of API on the isoindole fluorescence of chiA-OPTA complex

The active site of ChiA has the residues like Asp 313, Glu 315, Trp 539 and Tyr 163, 390, which play a crucial role in catalysis [Yannis et al., 2003]. Lys 142, 267, 37 and His 263, 186, 137 are proximal residues to the catalytic site cleft of ChiA and have been exploited to probe the interaction of API with ChiA by chemo affinity labeling experiments using OPTA. To investigate the binding of API with ChiA and changes in the native intermolecular interactions, we have monitored the changes in the interaction of the lysine and histidine due to API binding, and their influence on the isoindole fluorescence of ChiA. The unbound enzyme did not show fluorescence when excited at 338 nm; however, incubation of ChiA with OPTA resulted in an increase in the fluorescence with a λ_{max} at 417 nm due to the formation of the isoindole derivative; however no loss was recorded in ChiA activity. ChiA pre-incubated with API was failed to react with OPTA, as revealed by the total loss of isoindole fluorescence (Fig. 22) and enzyme's catalytic activity which not only confirmed the binding of API near the active site of ChiA but also further revealed that the binding of API resulted in disruption of the native hydrogen bonding network of the lysine and histidine residues, which are essential for the formation of isoindole derivative as well as Asp 313, Glu 315, Trp 539 and Tyr 163, 390 residues which are essential for the catalytic activity of the enzyme.

Secondary structural analysis of enzyme substrate-inhibitor complexes

To evaluate the effects of API on the secondary structure of the enzyme, the CD spectra of the ChiA-API complex was analyzed. The secondary structure contents of the ChiA as determined from the crystallographic data are 31.1% α-helix, 26.6% β-sheet, and 42.3% of aperiodic conformation. The estimated secondary structure contents from the CD analysis are 32% α-helix, 28% β-sheet, and 40% aperiodic structure, which are in total agreement with the crystallographic data. The circular dichroism spectrum of the ChiA -API complex shows a pronounced shift in the negative band at 228 nm of the native enzyme to 234 nm at the 10 μM API concentration. This shift reveals gross conformational changes in the secondary structure of ChiA upon API binding at 100 μM concentration (Figure 23). To elucidate the changes in the secondary structure of the enzyme inhibitor complex, it was compared with that of the ChiA-substrate complex (data not shown). Interestingly, the ChiA-API and ChiA-substrate complexes did not

exhibited a similar pattern of negative ellipticity in the far-UV region, suggesting that the inhibitor does not cause similar structural changes and was distinctly different from that of the unliganded enzyme.

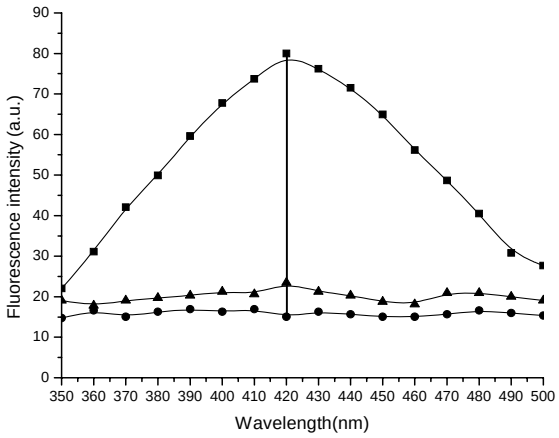

Figure 22- Effects of API binding on the OPTA fluorescence of ChiA. The lines represent the Isoindole fluorescence of ChiA (●), ChiA+OPTA (■), and ChiA+API (preincubated) and OPTA (▲) and are the average of six scans with corrections from buffer and respective controls.

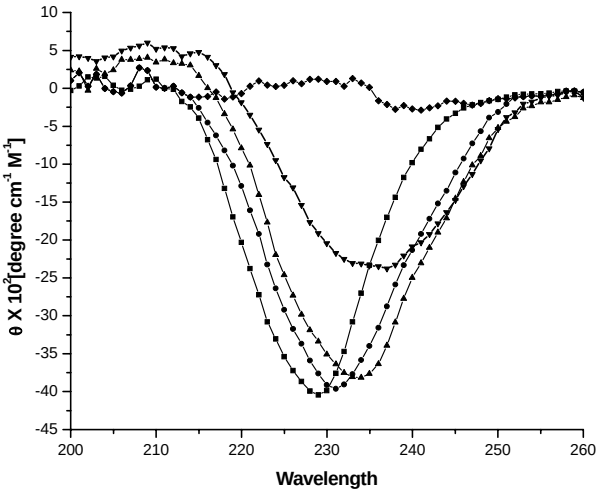

Figure 23- Effect on the secondary stucture of the ChiA upon binding of API. Far-UV circular dichroism spectra of the unliganded ChiA and its complexes were recorded in the absence (■) or in the presence of API, 10μM (●), 20μM (▲), 50μM (▼) and 100μM (♦) from 200 to 260 nm. Each spectrum represents the average of six scans.

Table 3- Summary of Kinetic Constants[a].

Method	K_i (nM)	K_i* (nM)	K_4($\mu M^{-1}s^{-1}$)	K_5(sec^{-1})	K_6 (sec^{-1})	K_7 (sec^{-1})
A[b]	830	7.5				
B[c]	790±50	6.6			$8.74\pm0.1\times10^{-3}$	$7.3\pm0.6\times10^{-5}$
C[d]	923 [e,]	6.3[e]	8.8±0.95	8.123±.5	$6.31\pm0.5\times10^{-3}$	$5.47\pm0.6\times10^{-5}$
D[f]	512±130					
E[g]	867±90				$3.81\pm0.25\times10^{-3}$	
F[h]	510±20					

[a]Uncertainties of parameters expressed with the "±" sign are standard errors from nonlinear regression. [b] From fitting initial velocities V_0 and pseudo-steady-state velocities V_S to eqs. 6a and 6b, respectively. [c] From fitting apparent first-order rate constants to eq. 6c. [d] From fitting progress curves to differential eqs. 4a-g. [e]Computed from rate constants. [f] From fitting progress curves to equation $(F_0 - F) = \Delta F_{max} / \{1 + (K_i/[I])\}$. [g]From fitting progress curves to equation $K_{obs} = k_6 [I] / (K_i + [I])$. [h] From initial kinetics with inhibitor (fig 13).

DISCUSSION

This chapter reports a bifunctional low molecular weight peptidic inhibitor API, from thermo tolerant *Bacillus licheniformis* exhibiting slow-tight binding inhibition against ChiA. The two step inhibition mechanism was corroborated by the equilibrium binding studies and also by the correlation of the kinetic data with the conformational changes induced in ChiA upon binding of the noncompetitive inhibitor API. The failure of substrate protection against ChiA inhibition by API and the non dissociative nature of the ChiA-API complex with multiple dilutions led us to apply tight binding inhibition kinetics. The noncompetitive nature of API may be addressed due to the binding affinity of the inhibitor other than the active site of ChiA. This, however, does not exclude the possibility of the differential binding pockets for the inhibitor in the active site of the enzyme. From the available crystallographic data, it is deduced that binding of substrate or transition state analogue inhibitors in the substrate-binding site of ChiA do not induces conformational changes in the enzyme (Yannis et al., 2003). Enzymatic hydrolysis of the glycosidic bond takes place by binding the substrate into the eight stranded $(\alpha\beta)_8$ barrel of the catalytic domain via general acid-base catalysis which is initiated by protonation of the glycosidic oxygen by an acidic Glu residue (Yannis et al., 2003).

It is proposed here that API behaves as a slow tight binding inhibitor in accordance with Scheme Ib (chapter 2, part 3) until the formation of the *E*I*, however, as a function of time it acts like an irreversible suicidal type inhibitor (Scheme II), essentially because of the conformational modes attended by the enzyme-inhibitor complex. These conformational changes are mainly induced because of extended secondary interactions between API and ChiA. Scheme II describes the kinetics and conformational modes of the proposed mechanism of inhibition of ChiA by API, where the rate constant k_{con} is associated with the irreversible conformational change in the *E*I*.

$$E + I \underset{k_5}{\overset{k_4}{\rightleftharpoons}} EI \underset{k_7}{\overset{k_6}{\rightleftharpoons}} EI^* \xrightarrow{k_{con}} EI^{**}$$

----------Scheme II

The two-step inhibition mechanism of ChiA by API was reflected in the fluorescence analysis of the enzyme-inhibitor complexes. The rate constants derived from

the fluorescence analysis of the complexes corroborated the values derived from the kinetic analysis. Therefore, it is proposed that the initial rapid fluorescence loss reflected the formation of the reversible complex *E*I, whereas the subsequent slower decrease was correlated to the accumulation of the tightly bound complex *E*I*. Presence of red shift in the tryptophanyl fluorescence of the complexes reflect the major alteration in the three-dimensional structure of ChiA because of the binding of API at the *E*I* stage. The agreement of the rate constants concomitant with the fluorescence changes observed during the time-dependent inhibition lead us to correlate the localized conformational changes in the enzyme-inhibitor complex to the isomeriation of the *E*I to *E*I*. The shift in the emission maxima as a function of time in the *E*I* indicated induction of gross conformational changes in the complex because of the secondary interactions within protein and peptide molecules (Fig. 18). These interactions are strong enough to form an irreversible complex of the enzyme-inhibitor from which the inhibitor failed to dissociate. This is the first report with ChiA that a peptidic slow tight binding inhibitor behaving as an irreversible suicidal type inhibitor as a function of time.

The crystal structure of ChiA-allosamidin complex has revealed that allosamidin binds to ChiA via several covalent bonds. The most significant of these are mediated via the three critical residues namely Asp313, Glu315 and Tyr390 (Yannis et al., 2003). We have used the ChiA-allosamidin complex as model system to interpret the interactions of ChiA with API at the molecular level. OPTA has been utilized as a fluorescent probe to investigate the microenvironment of active site tunnel of ChiA where the substrate enters inside. OPTA reacts with NH_2 group of Lys residue and SH group of cysteine residue to form a fluorescent isoindole derivative (Palczewski et al., 1983). Moreover, Yoshimura et al. have elucidated the mechanism for isoindole formation between Lys, His and OPTA. OPTA contains two aldehyde groups; one of these aldehyde groups reacts with the primary amine in Lys and other residual aldehyde group reacts with the secondary amine in the imidazole ring of His (Yoshimura et al., 1990; George and Rao, 2001). The crystallographic data of ChiA (PDB code 1EDQ) reveals that Lys-142, 267, 37 and His-263, 186, 137 residues, respectively are in the position to form an isoindole derivative with OPTA. The experimental data shows that ChiA labeled with OPTA resulted in an increase in the fluorescence at 417 nm which confirms the formation of isoindole

derivative in ChiA-OPTA complex. Based on our results, we propose that one aldehyde group of OPTA reacts with the primary amine Lys-142, 267, 37 residues of ChiA resulting in the release of a water molecule. The another residual aldehyde group of OPTA reacts with the secondary amine in the imidazole ring of His-263, 186, 137 residues of ChiA resulting in the release of another water molecule and forms a fluorescent isoindole derivative (Fig. 24A). ChiA pre-incubated with API failed to form an isoindole derivative as there was no fluorescence observed at 417 nm. The possible explanation for the quenching of fluorescence is that Asp 1 residue of API has one free -COOH group and one free -NH_2 group. Based on our results, we propose that the free -COOH group of Asp-1 residue of API forms covalent bond with the free amine groups of the Lys-142,267,37 residues and the free NH_2 group of Aps-1 of API forms covalent bond with secondary amine of the imidazole ring of His-263,186,137 residues (Fig. 24B). The quenching of the ChiA-OPTA complex fluorescence may be the consequence of the stacking effect of the π-π electrons of the Asp1 residue of API which proves API binds near the active site tunnel of ChiA in the *E*I complex. The other residues near the reactive site and π-π stacking interaction of the Trp residue of API may interfere with the hydrogen bonding network and electronic environment of the catalytic site of the enzyme due to which the active site may get disturbed.

The formation of a tight complex between the enzyme and inhibitor can be attributed to the secondary interactions between API and ChiA as analysed by the CD-spectra analysis (Fig. 23). CD-spectra analysis has revealed the presence of β-sheet structures in API (Kumar and rao, 2006). β-sheet structures are known to play a critical role during secondary contacts between the other reported inhibitors and the target enzymes. These secondary β-sheet interactions along with the network of hydrogen bonding, non-ionic and other weak interactions between the proximal active site and reactive site residues probably are sufficient to induce substantial conformational changes in the *E*I* complex leading toward the formation of the irreversible *E*I** complex. These extensive interactions between the active site proximal residues of ChiA and the reactive site residues of API are probably responsible to convert a slow tight binding inhibitor into an irreversible suicidal inhibitor of ChiA.

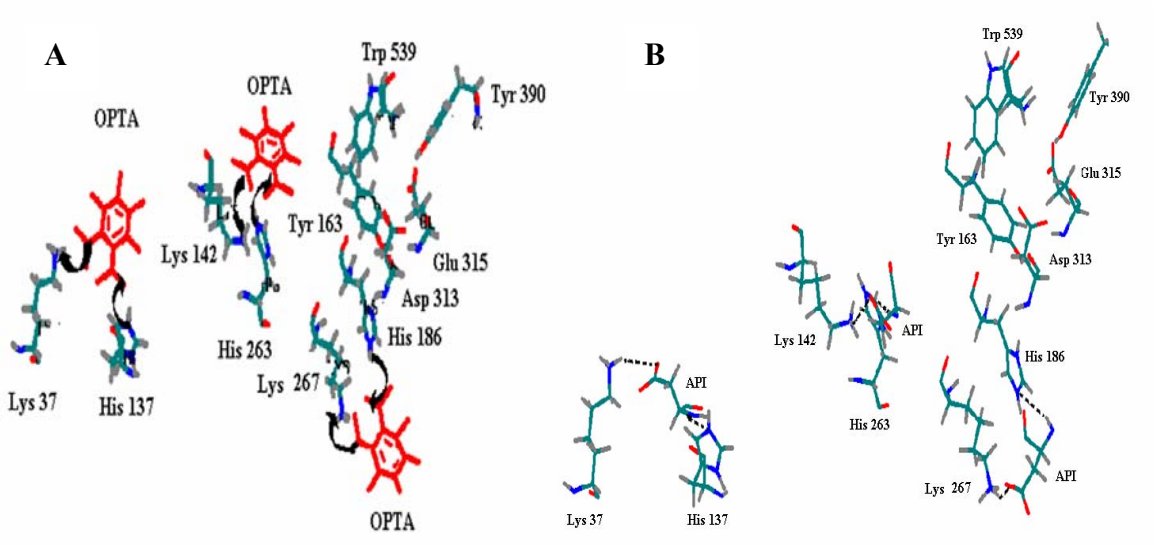

Figure 24- Hypothetical schematic representation of the model depicting the probable mechanism of API binding to ChiA. The active site and proximal residues of the ChiA have been modeled based on the x-ray crystallographic structure of ChiA from *Serratia marcescens* (Yannis et al., 2003) (PDB code 1EDQ) using the software Hyperchem 7.5 (evaluation version). The active site of ChiA includes the essential Asp313, Glu315, Tyr163-390 and Trp539 residues. **(A)** The chemoaffinity label OPTA (shown in *red color*) contains two aldehyde groups, one of which binds to the primary amine of the Lys 142, 267, 37 residues and the other group reacts with the secondary amine of the imidazole ring of His 263, 186, 137 residues of ChiA resulting in the release of water molecules (not shown). These chemical reactions result in the formation a fluorescent isoindole derivative. **(B)** Pre-incubation of ChiA with API resulted in the binding of free -COOH group of Asp-1 residue of API form covalent bond with the amine group of the Lys-142, 267, 37 residues. The free NH_2 group of Aps-1 of API form covalent bond with secondary amine of the imidazole ring of His 263, 186, 137 residues of ChiA (*dashed lines*). These interactions in conjunction with the tight binding nature of API probably prevent the binding of OPTA to the Lys and His residues, thus an isoindole derivative failed to be formed with the ChiA pre-incubated with API.

CHAPTER 5

ASPARTIC PROTEASE INHIBITOR FROM ALKALO-THERMOPHILIC *BACILLUS SP.*: IN *VIVO* AND IN *VITRO* EFFECTS ON CUTICLE MOULTING FLUID ENZYMES OF *HELICOVERPA ARMIGERA*

SUMMARY

The inhibition of moulting fluid enzymes from *Helicoverpa armigera* by an aspartic protease inhibitor ATBI (Alkalo-Thermoplic Bacillus Inhibitor) is reported in the present chapter. In vivo and in vitro experiments were carried out to evaluate the effects of ATBI against the development of *H. armigera.* ATBI showed 75% proteolytic and 95% of chitinase enzyme inhibition with the IC_{50} values of 48 μM and 35 μM respectively. The inhibition studies of proteases with the help of specific protease inhibitors and ATBI suggest that one or more aspartic proteases have important roles in insect development. Also, laboratory experiments in vitro showed significant inhibition towards the growth and development of *H. armigera*. The effect of ATBI on insect metamorphosis can be correlated through the inhibition of proteases and chitinase from moulting fluid. The results provide the basis for the selection of non-host inhibitors and present an optimized combination for developing *H. armigera* resistant transgenic plants. It will be a new area of making transgenic plants targeting the insect moulting fluid enzymes.

INTRODUCTION

Pod borer, Helicoverpa armigera (Lepidoptera: Noctuidae) is a polyphagous pest, which infests important crops like cotton, tomato, sunflower, pigeon pea, chickpea, okra and corn throughout the world. It was recorded feeding on 182 plant species belonging to 47 botanical families in Indian subcontinent. Of late, an annual crop loss due to Helicoverpa in India has been estimated at around Rs.2, 000 Crores despite the use if insecticides worth Rs.500 Crores. Hazardous implications of these insecticides and their residue at various trophic levels have also caused incalculable damage to every aspect of environment, globally (Manjunath et al., 1989). For the control of this pest, a variety of methods such as physical methods, chemical pesticides and biological methods based on microorganisms are employed (Forrester, 1993). The most important of the latter is Bacillus thuringiensis (Bt), a bacterium which produces endotoxins that are toxic to larvae of different species of Lepidoptera and other insects. The pyrethroids and organophosphates (OPs) have commonly been mixed since mid 1980s to manage pest complex of cotton and other crops but pests have developed resistance to endosulfan, pyrethroids, organophosphates and carbamates (Ahmad, 1998, 1999). Therefore, search for Safer & effective alternative to chemical control are desirable as a part of an integrated interdisciplinary approach to pest management.

I. An insite in to insect moulting fluid proteases

Insect cuticle is composed mainly of crystalline microfibres of chitin embedded in a protein matrix (Peters, 1992). As the insect grows, the degradation of the old cuticle is accomplished by enzymes present in the moulting fluid, a liquid secreted between the old and new cuticles during moulting (Kramer et al., 1985). Proteolytic enzymes are thought to attack the cuticle before chitinolytic enzymes as protein masks the chitin micro fibers (Kramer and Koga, 1986). The proteolytic enzymes from insect moulting fluid have received more attention due to showing the main role in the development of the insect. Studies of proteolytic activity in the moulting fluid of silk moths showed the presence of enzymes with trypsin-like specificity, which were presumed to be cuticle degrading. A cuticle degrading protease from the molting fluid of Menduca sexta has been purified and classified as trypsin-like from its substrate specificity and inhibition by SBTI. (Samuels

and Reynolds, 1993a; Samuels et al., 1993a). Allosamidin and other chitinase inhibitors were isolated and synthesized from different sources (Sakuda et al., 1987a, 1987b).

It has been now proved that degradation of the old cuticle is accomplished by enzymes present in the moulting fluid, a liquid secreted between the old and new cuticles during moulting (Jungries, 1979). Bade and Shoukimas, 1974 described a serine protease and a neutral metal chelator sensitive protease from the moulting fluid of the tobacco hornworm Manduca sexm. The moulting fluid of silkmoths showed the presence of enzymes with trypsin-like specificity, which were presumed to be cuticle degrading (Katzenellenbogen and Kafatos, 1970, 1971a). Samuels et al. (1993a) purified and characterized a trypsin-like moulting fluid protease 1 (MFP-I) from the moulting fluid of Manduca. MFP-1 showed a primary specificity for elongated substrates with arginine at the P~ position and the substitution of lysine at this position resulted in a 86% reduction in activity. This type of specificity was also found in a serine proteinase isolated from Drosophila melanogaster embryos (Medina and Vallejo, 1989) and trypsin-like enzymes from silkmoth moulting fluid (Katzenellenbogen and Kafatos, 1971a). Active site classification of MFP-I was not straightforward. Although MFP-I was inhibited by the classical active site serine inhibitors DFP and PMSF, it was also inhibited by the diagnostic inhibitor of cysteine proteinases, E-64 (Samuels et al., 1993a). Classical trypsin-like enzymes have been isolated from insects, for example, the midgut of M. sexta larvae (Miller et al., 1974) and Vespa spp. (Jany et al., 1978). These enzymes have normal trypsin-like specificities and are inhibited by diagnostic inhibitors of serine proteinases and the normal range of substrate inhibitors (e.g. SBTI, leupeptin, TLCK). Crude moulting fluid from pharate adult Manduca had no activity against chymotrypsin substrates (Samuels et al., 1993a). However, chymotrypsin-like activity was detected by Brookhart and Kramer, 1990 in semi-purified fractions of Manduca pharate pupal moulting fluid. They found that the activity of chymotrypsin-like enzymes was ten-fold lower than that of trypsin-like enzymes. A similar ratio of chymotrypsin to trypsin activity was also found in the midgut of the grass grub, Costelytra zealandica (Christeller et al., 1989). MFP-I was the major cuticle degrading enzyme found in the moulting fluid of pharate adult M. sexta. MFP-I was shown to degrade Manduca cuticle proteins in vitro, producing fragments in the size range 200-2000Da (Samuels et al., 1993b). In the

silkmoth, when the pharate adult epidermis retracts from the overlying pupal cuticle, a colourless gel fills the exuvial space. Once the new adult cuticle has formed, the moulting gel becomes a less viscous "moulting fluid" and cuticle degradation begins (Katzenellenbogen and Kafatos, 1970). Katzenellenbogen and Kafatos, 1971b have shown that silkmoth moulting gel contains inactive proteolytic enzymes which become active in vitro by dilution. The timing of appearance of cuticle degrading activity in the moulting fluid of Manduca (Samuels and Reynolds, 1993a) may support the theory of enzyme activation or removal of an inhibitor. In the case of regulation of chitinolytic enzymes, Kimura, 1973 showed that, in Bombyx, activation of chitinase by ecdysterone was not a result of de novo synthesis of the enzyme and it has more recently been demonstrated that high levels of 20-hydroxyecdysone induced chitinase through activation of a zymogen (Koga et al., 1991). However, Kramer et al., 1993 found no evidence of chitinase zymogens in Manduca sexta. Proteinase inhibitors have been found in the moulting fluid of pharate adult Manduca, although their role remains uncertain. Trypsin and chymotrypsin inhibitors were separated from MFP-I by passage of moulting fluid through a Heparin affinity column. Preliminary results showed that trypsin inhibitor titre fell during the later stages of ecdysis, indicating a possible regulatory role. An additional role for proteinase inhibitors in the moulting fluid may be as a defence mechanism against entomopathogenic fungi. An inhibitor has also been isolated from the haemolymph of Bombyx mori, which had a high affinity for fungal proteinases (Eguchi et al., 1993). A proteinase inhibitor was present in crayfish cuticle, which may provide some protection against penetration by invading microorganisms (Hall and Soderhall, 1983).

II. An insite in to Insect chitinases

Insect chitinases belong to family 18 of the glycohydrolase superfamily and share a high degree of amino acid similarity. A characteristic of the family 18 chitinases is their multidomain structure, which is consistently found in all primary structures deduced from insect genes encoding these enzymes. Substantial biochemical and kinetic data are available, and primary structures of different enzymes have been determined by nucleotide sequencing. Insect chitinases have theoretical molecular masses ranging between 40kDa and 85kDa and also vary with respect to their pH optima (pH 4-8) and

isoelectric points (pH 5–7) (Table 1). The basic structure consists of three domains that include (1) the catalytic region, (2) a PEST-like region, enriched in the amino acids proline, glutamate, serine and threonine, and (3) a cysteine-rich region (Kramer and Muthukrishnan, 1997). The last two domains, however, do not seem to be necessary for chitinase activity because naturally occurring chitinases that lack these regions are still enzymatically active (Girard and Jouanin, 1999; Feix et al., 2000; Yan et al., 2002). In agreement with these observations, C-terminus-truncated versions of the recombinant Manduca chitinase still exhibit catalytic activity (Wang et al., 1996; Zhu et al., 2001). In all insect chitinases sequenced so far, a hydrophobic signal peptide is predicted to precede the N-terminal region of the mature protein (Kramer et al., 1993; Koga et al., 1997; Choi et al., 1997; Nielsen et al., 1997; Shen and Jacobs-Lorena, 1997; Kim et al., 1998; Mikitani et al., 2000; Royer et al., 2002). The signal peptide presumably mediates secretion of the enzyme into the endoplasmic reticulum and it is cleaved off by signal peptidases after the protein has been transported across the membrane (von Heijne, 1990; Müller, 1992).

So far, no crystal structure of an insect chitinase is available, but homology modeling using crystal structures of bacterial and plant chitinases has revealed three-dimensional models of the catalytic domain from the Manduca chitinase showing striking similarities with the α/β barrel structure described above (Kramer and Muthukrishnan, 1997; Huang et al., 1999). Although the models lack a well defined $(\alpha/\beta)_8$ folding, they predict eight β-sheets and four complete and several incomplete α-helices. In some insects, the catalytic region is followed by a less conserved domain containing a putative PEST-like region that is also found near the C-terminus of the yeast chitinase (Kim et al., 1998; Kuranda and Robbins, 1991; Kramer et al., 1993; Royer et al., 2002). As already mentioned, insect chitinases without a PEST-like region have also been described in the literature (Girard and Jouanin, 1999; Feix et al., 2000; Yan et al., 2002). PEST-like regions presumably increase the susceptibility of the enzyme to proteolysis by a calcium-dependent protease or to degradation via the 26S proteasome (Rogers et al., 1986; Rechsteiner and Rogers, 1996). Therefore, these regions could play a role in enzyme turnover or activation of zymogenic chitinases.

Like some fungal chitinases, the chitinases found in insect molting fluids are extensively glycosylated. Thus, insect chitinases can be easily detected by carbohydrate staining after sodium dodecyl sulfate polyacrylamide gel electrophoresis (SDS-PAGE) and blotting. Several putative N-linked glycosylation sites that may be necessary for the secretion of the protein and maintenance of its stability are found within the deduced amino acid sequences of insect chitinases (Gopalakrishnan et al., 1995; Kramer and Muthukrishnan, 1997; Kim et al., 1998). Moreover, the serine/threonine-rich PEST-like region of the Manduca chitinase is extensively modified by O-glycosylation (Kramer et al., 1993; Arakane et al., 2003). Previous determination of the carbohydrate composition of the Manduca chitinases revealed N-acetylglucosamine and several neutral hexoses as part of the sugar portion (Koga et al., 1983, 1997).

The attachment of oligosaccharides probably increases solubility and protects the peptide backbone against proteases. Insect chitinases are anchored to their substrate through the C-terminal chitin-binding domain, which is characterized by a six-cysteine motif that is also found in nematode chitinases (Venegas et al., 1996). It functions in targeting of the enzyme to its substrate and thereby facilitates catalysis. The six cysteine motif is also found in several peritrophic matrix proteins, as well as in receptors and other proteins that are involved in cellular adhesion (Tellam et al., 1992; Tellam, 1996; Kramer and Muthukrishnan, 1997; Shen and Jacobs- Lorena, 1999). Individual chitinases possess different combinations of these three basic domains. While the chitinases from Manduca, Bombyx and fall webworm moth Hyphantria cunea exhibit the typical tripartite domain structure (Kramer et al., 1993; Kim et al., 1998), some other chitinases lack PEST-like or the typical chitin-binding regions (Girard and Jouanin, 1999; Feix et al., 2000; Yan et al., 2002). Other insects, in turn, may express multi-modular enzymes. In Aedes, for example, chitinases are encoded by two different genes. Nucleotide sequencing has revealed that one of the genes contains tandemly arranged open reading frames that encode three separate chitinases, each containing a catalytic and also a chitin-binding domain. The gene arrangement suggests co-regulated transcription resembling bacterial operons (Niehrs and Pollet, 1999). Posttranscriptional splicing, however, may also lead to a single, multi-modular protein with three catalytic- and chitin-binding domains each (de la Vega et al., 1998; Henrissat, 1999). TmChit5, the gene that encodes chitinase 5 of the

beetle Tenebrio molitor, also exhibits an unusual structure, since it contains five chitinase units of approximately 480 amino acids that are separated by putative PEST-like, chitin-binding and mucin-like domains (Royer et al., 2002). It is speculated that multi-modular chitinases may be expressed as zymogens that are subsequently cleaved by proteolysis to reveal multiple active enzymes. The highly conserved sequence YDFDGLDLDWEYP found in insect chitinases is consistent with the family 18 chitinase signature (Terwisscha van Scheltinga et al., 1994; Choi et al., 1997; de la Vega et al., 1998).

Table 1. Characteristics of some insect chitinases. (Hans and Lars, 2003)

	MsCHT-1	*BmCHT-1*	*AaCHT-1*
Organism	*M. sexta*	*B. mori*	*A. aegypti*
Accession no.	A56596	AAB47538	AAB81849
Molecular mass (kDa)			
Deduced from cDNA	62.20	63.39	64.27
Zymogenic forms*	119	215	
Active forms	50, 62, 75, 97	54, 65, 88	33, 40
pI (isoelectric point)	5.32	5.15	4.83
PEST sites	404—437	417—440	394—408
	474—508	471—499	413—436
			451—471
Total number of *N*-glycosylation sites	3	3	2
Total number of *O*-glycosylation sites	24	23	25

Prediction of putative PEST sites and *N*- and *O*-glycosylation sites was performed with the programs PESTfind, PROSCAN and NetOGlyc 2.0, respectively (Rogers et al., 1986; Bairoch et al., 1997; Hansen et al., 1997).

*Putative zymogenic forms were suggested based on their immunoreactivity with anti-chitinase antibodies after SDS-PAGE and western blots (Koga et al., 1989, 1992)

Consequently, site-directed mutagenesis of the essential glutamate of the insect chitinase active site results in a loss of enzymatic activity (Huang et al., 2000; Lu et al., 2002; Royer et al., 2002). The functional importance of active site residues has also been demonstrated for an insect chitinase (Lu et al., 2002). Site-directed mutagenesis of the *Manduca* chitinase revealed that E146 may function as an acid/base catalyst while D142 may influence the pKa values of the catalytic residue E146 but also that of D144; the latter residue may be an electrostatic stabilizer of the positively charged transition state. Moreover, W145, which is also present in all family 18 chitinases, might extend the alkaline pH range in which the enzyme is active and may increase affinity to the substrate (Huang et al., 2000).

The present chapter describes the partial purification of *Helicoverpa armigera* moulting fluid enzymes and their interaction with an alkalo-thermophilic aspartic protease inhibitor, ATBI reported from our laboratory (Dash and Rao, 2001). ATBI purified from *Bacillus sp.* is well known to have inhibitory effects on different aspartic proteases (Dash and Rao, 2001; Dash et al., 2001a, 2001b; Dash et al., 2002). Therefore, to achieve a novel effective pest control strategy it is very important to study the proteases and chitinases from insect moulting fluid and their inhibitors from different sources. This study was undertaken to determine the *in vivo* and *in vitro* effects of an aspartic protease inhibitor, ATBI on cuticle moulting fluid enzymes of Pod borer, *H. armigera.* These efforts will be helpful to establish an idea of inhibiting cuticle moulting fluid enzymes to exploit protein and chitin metabolism of insect cuticle for insect management programs.

MATERIALS AND METHODS

Materials

All the materials used are described in chapter 3 materials section.

Purification of ATBI

The extremophilic *Bacillus* sp. was grown in a liquid medium containing soya meal (2%) and other nutrients at 50°C for 48 hours as described by Dash and Rao, 2001. Briefly, about 1,000 ml of the extracellular culture filtrate was treated with 65 g of activated charcoal and the supernatant was subjected to membrane filtration using Amicon UM10 (*M*r cutoff, 10,000) and UM2 (*M*r cutoff, 2,000) membranes. The resulting clear filtrate was concentrated by lyophilization and loaded onto a prepacked Ultropac Lichrosorb RP-18 (LKB) column. The fractions detected at 210 nm were eluted on a linear gradient of 0 to 50% acetonitrile and water containing 0.01% trifluoroacetate. The fractions showing inhibitory activity were pooled and found to be homogenous by reverse phase high-performance liquid chromatography.

Rearing and bioassays with H. armigera

H. armigera larvae were reared on an artificial diet. The composition for 1 L of the artificial diet was as follows: 140 g chickpea flour, 14 g yeast extract, 0.4 g Bavistin (BASF, Mumbai, India), 0.2 ml formalin, 4.3 g ascorbic acid, 1.3 g sorbic acid, 2.6 g methyl benzoate, 0.5 g tetracycline, one tablet of vitamin B-complex, two drops of vitamin E and 17 g of agar. Cubes of this composition (2 g each) were used for feeding. Newly hatched larvae were reared on this artificial diet for all instars. The bioassays were carried out with fifth instar larvae of *H. armigera* by treating each larva with 100 µl water suspensions containing 10 µg ATBI and 0.1% Tween20 as a surfactant in potter tower. Larvae treated with distilled water containing 0.1% Tween20 were used as control. The experiments were carried out in Completely Randomized Block Design with four replication containing 30 larvae in each replication. All the experiments were carried out at 25^{o}C temperature and 70% relative humidity with photoperiod 16:8 (L: D).

Effect of ATBI on various growth parameters

To study the effect of ATBI on growth parameters such as percent pupation, pupal weight and emergence of adults, the surviving larvae were transferred to vials containing

semi artificial diet. 5 male and 5 female from each replicate and treatment were weighed separately after 3 days of beginning of pupation. Thereafter, pupae were kept in glass vials containing thin layer of sand at bottom to collect the data on the pupation and emergence of adults.

Effect of ATBI on various reproductive parameters

To measure the reproductive parameters such as fecundity and fertility of eggs, 6 pairs of newly emerged adults (male and female) from each replicate were transferred to plastic jars (7.5-cm diameter, 9.5 cm high) lined with a layer of paper for egg laying. The adults were fed with 10 % (w/v) aqueous solution of honey. The eggs laid on the filter paper were harvested daily. To study the percent of egg hatching, the eggs were kept in petri plates with moist filter paper and incubated in BOD incubator at 25±1°C temperature and 70±10 % relative humidity.

Extraction of cuticle moulting fluid and partial purification of enzymes from moulting fluid of H. armigera

H. armigera cuticle moulting fluid was obtained by puncturing the pupal cuticle at the base of the proboscis and collecting liquid in to a glass capillary (25 µL from each insect) containing 50mM phosphate buffer, pH 7.0. The moulting fluid was centrifuged at 15000g for 20 minutes at 4^{o}C and the supernatant was kept under refrigeration and used for enzyme assays. 500 µl of moulting fluid was saturated with 40-60% ammonium sulphate at 4^{o}C and centrifuged at 15000g for 10 minutes. The precipitates were dissolved in 50mM phosphate buffer, pH 7.0 and dialyzed against double distilled water for further use. The dialyzed fraction was then loaded on a sephadex G-75 gelfiltration column (100 cm X 1cm) pre-equilibrated with 50mM phosphate buffer, pH 7.0. The fractions showing protease activity and chitinase activity were collected, pulled together and lyophilized. Protein concentration was determined according to the method of Bradford, using Bovine Serum Albumin as standard (Bradford, 1976).

Protease activity assay

The total protease activity from moulting fluid was measured by hemoglobinolytic assays. The principle of the method was that used originally by Anson, 1938 and Kunitz, 1947. The reaction mixture (2ml) contained a 200µl (from 100µg/ml stock solution) of enzyme solution, 1 ml of substrate and 800 µl of buffers of different

pH. Enzyme reaction was carried out at 37^{o}C for 30 min and terminated by the addition of 2 ml of acidified trichloroacetic acid (TCA). The absorbance of the TCA soluble fraction was measured at 280 nm. The following inhibitors, EDTA (ethylene diamine tetraacetic acid), E-64 (L-*trans*-epoxysuccinyl-leucyl-amido (4-guanidino)-butane), pepstatin, pHMB (p-hydroxymercutybenzoic acid), BBTI (Bowman-Birk trypsin inhibitor), TPCK (tosyl-phenylalanyl-chloromethyl-keton, TLCK (tosyl-lysyl-chloromethyl-keton) were utilized for inhibition studies (Hanada, 1978; Barret, 1977; Fersht, 1977; North, 1982). The concentrations used for each inhibitor is given in table 1. For inhibition assays with ATBI, The enzyme of suitable concentration (2μg/ml) was incubated with 0-100 μM of ATBI and the remaining enzyme activity was determined at different pH as described above.

Chitinase assay using colloidal chitin and Ramazol Brilliant Violet dyed chitin extracted from H. armigera cuticle

Chitinase activity from moulting fluid was estimated using acid-swollen chitin as the substrate (Nahar et al., 2004). To prepare acid-swollen chitin, the chitin (10 g, purified powder from crab shells, Sigma) was suspended in chilled O-phosphoric acid (88%, w/v) and stirred at 0^{o}C for 1 h. The acid-swollen chitin was repeatedly washed with chilled distilled water, followed with a 1% (w/v) $NaHCO_3$ wash, and then dialyzed against cold distilled water. After homogenization in a Waring blender (1 min), 50mM acetate buffer, pH 5.0, was added to the suspension so that 1ml of suspension contained 7mg of chitin. The reaction mixture for chitinase assay contained 1 ml of 0.7% swollen chitin, 1ml of 50mM acetate buffer, pH 6.0, and 1ml enzyme solution that was incubated at 50°C for 1 hour. The *N*-acetylglucosamine residues (GlcNAc) produced was estimated colorimetrically with *p*-dimethyl amino benzaldehyde (DMAB). One international unit of chitinase was defined as the catalytic activity that produced 1 μmol of GlcNAc per minute under assays conditions. For inhibition assays, the enzyme of suitable concentration (2μg/ml) were incubated with 0-100 μM of ATBI and the remaining enzymes activity was determined as described above.

The chitinase activity was also determined by using *H. armigera* cuticle chitin dyed with Ramazol Brilliant Violet (RBV). Chitin was obtained from the insect larvae and pupae by extraction of soft tissue from homogenized insects with potassium

tetraborate (Leger et al., 1998). The chitin was dyed with RBV according to M. Gomez Ramirez et al., 2004. 2.5 grams of chitin was homogeneously mixed with 10 ml of aqueous solution of RBV at 0.84%. The resulting suspension was heated in a boiling water bath for one hour with gentle stirring. The colloidal material was removed by filtration and, to fix the RBV- colour, the obtained material as such was suspended in 25 ml of aqueous solution of 1.5% sodium dichromate and 1.5% sodium potassium tartrate, without any pH adjustment, followed by heating with gentle stirring in a boiling water bath for 10 minutes. The dye material was then separated by filtration and washed with hot water until the filtrate was colorless. The gelatinous blue material obtained was sterilized by autoclaving and stored at 5^{o}C. The plate assays to detect Chitinase activity in moulting fluid was performed according to Draborg et.al., 1997. The chitinolytic activity was measured in agar gels containing cuticle chitin dyed with RBV (RBV-chitin). Plate assays contained 0.2% (w/v) RBV-chitin in 1.5% agar, 0.1M citrate buffer pH 6 for the detection of chitinases activity in moulting fluid. Clearing zones were formed around the chitinase loaded in plates. The inhibition assays in plates were performed by loading chitinse preincubated with different concentrations of ATBI.

RESULTS

Purification and biochemical characterization of ATBI

ATBI produced by extracellularly by an extremophilic *Bacillus* sp. was a low molecular peptidic inhibitor and has characterized with the amino acid sequence of Ala-Gly-Lys-Lys-Asp-Asp-Asp-Asp-Pro-Pro-Glu. The predominance of the charged amino acid residues in the inhibitor sequence indicated its hydrophilic nature. The molecular mass of ATBI as determined from electrospray mass spectrometry was 1147 Da. Previously it has been evaluated the antifungal potential of ATBI, against phytopathogenic fungi in vitro. The kinetic studies had revealed the bifunctional characteristics of ATBI, as it was found to inhibit aspartic proteases and xylanase (Dash and Rao, 2001; Dash et al., 2001a, 2001b; Dash et al., 2002).

In vivo effect of ATBI on Helicoverpa armegera development

The fifth instar larvae of *H. armigera* treated with ATBI showed significant abnormal changes during larval to pupae (Figure 1A) and pupae to adult (Figure 1D) transformation. Figure 1B and 1C shows the normal Pupae and normal adult respectively. About 40% abnormal pupae and 30% abnormal adults emergence was observed from inhibitor treated larval populations.

In vivo effect of ATBI on various physiological parameters of Helicoverpa armegera

A significant effect of inhibitor was recorded on growth parameters such as pupation and adult emergence. Inhibitor treated larvae showed 82% pupation, which is 98% in control. The adult emergence was observed 75% as compared to 100% in control (Figure 2A). The significant reduction in the mean pupae weight of inhibitor treated larvae was also observed as compared to the control (Figure 2B).

In vivo effect of ATBI on various reproductive parameters of H. armigera

ATBI showed significant effect on various reproductive parameters of *H. armigera* like fecundity, fertility and percentage of egg hatching. The average number of eggs laid by the female hatched from the pupae converted from larvae treated with ATBI were observed as 1220.22 as compared to control 1601.66. The effect of ATBI on the fertility of eggs laid by the adult female was considerably reduced as 736.33 as compared

with control 1277.00 (Figure3A). The egg hatching was 75% in treatment with ATBI as against 100% in control (Figure3B).

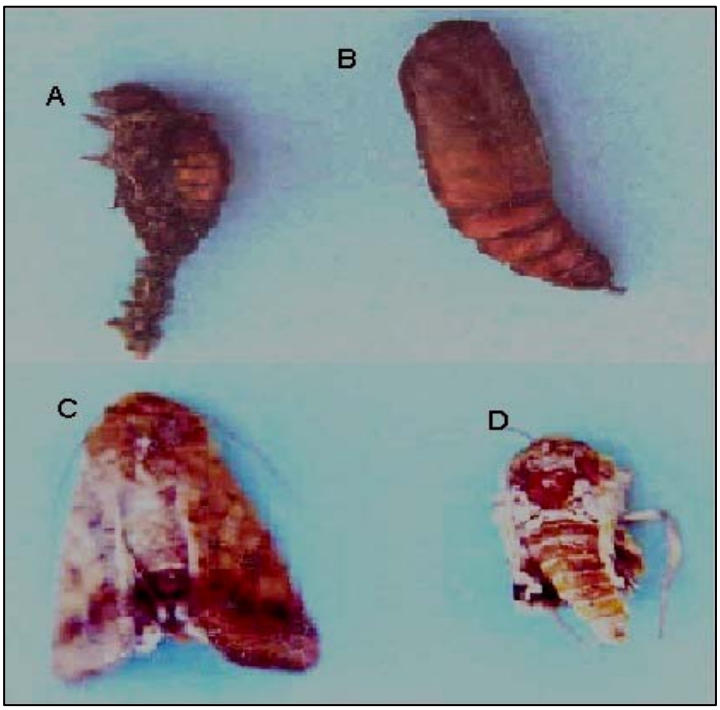

Figure 1. The effect of ATBI on growth and development of *H. armigera*
(A) Abnormal pupa treated with of ATBI (B) Normal pupa in control treatment (C) Adults emerged from the control treatment and (D) Adults emerged from the abnormal pupa treated with ATBI

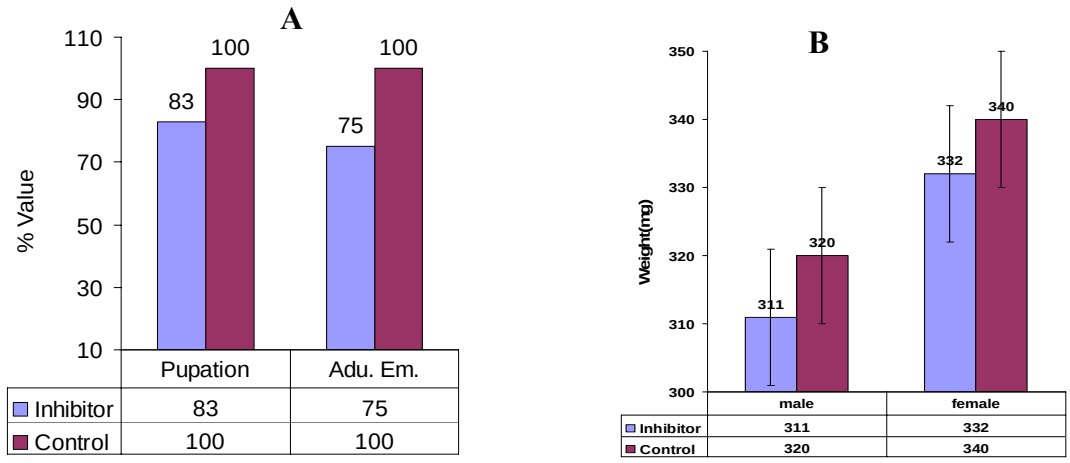

Figure 2. The effect of ATBI on (A) percent pupation and adult emergence and (B) mean pupal weight. The inhibitor treated larvae changed to pupae and the adult emergence from the pupae were counted.

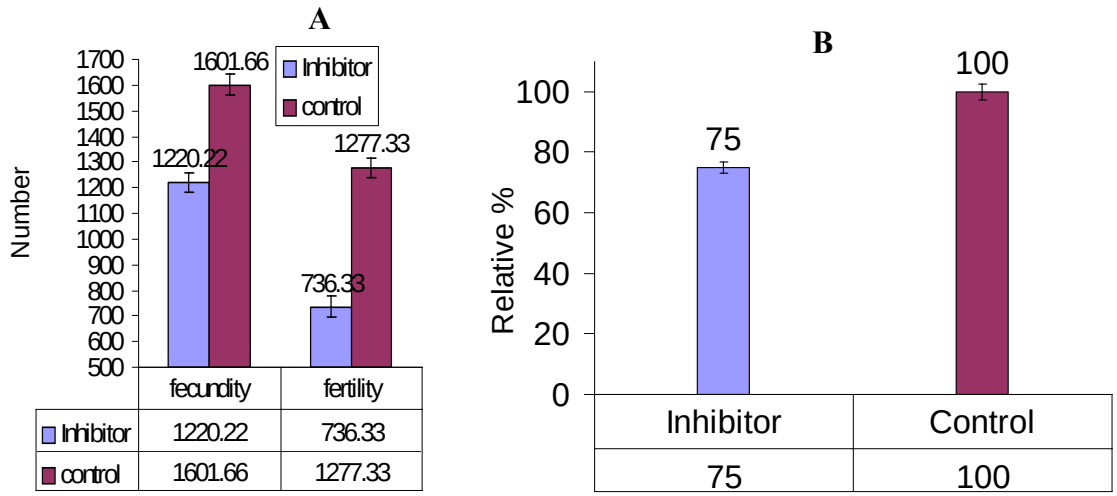

Figure 3. The effect of ATBI on fecundity, fertility and percent egg hatching. (A) The normal and abnormal *Helicoverpa* adults were reared. The eggs laid by females and larvae hatched from the eggs counted. There was a significant decrease in the egg laid and eggs hatched. (B) Effect of ATBI on percent egg hatching by *H. armigera* adult.

Extraction and partial purification of enzymes of H. armigera Larvae cuticle

Ammonium sulphate precipitation and Sephadex G-75 gel filtration chromatography resulted in partial purification of the *H. armigera* cuticle moulting fluid enzymes. Fractions 20-100 from gel filtration chromatography showed acidic proteolytic activity while fractions 30-49 showed chitinase activity (Figure 4). The fractions collected, lyophilized and used for further studies.

Inhibition of moulting fluid proteases activity by specific inhibitors

The inhibition of moulting fluid proteases by specific inhibitors indicates the presence of different proteases in *H. armigera* cuticle. EDTA, a metal ion chelator, had very low effect on the proteolytic activity of *H. armigera* cuticle proteases. E-64, a specific inhibitor of thiol proteases, was a potent inhibitor, causing 42.5% at 1mM concentration. Pepstatin A, an inhibitor of aspartic proteases, showed a modest inhibitory effect (27.5%). The effects of additional inhibitors were studied at pH 7.8, which is the pH range for optimum activity of serine like proteases. Results presented in table1 indicated that 1mM pHMB abolishes nearly 35% proteolytic activity. In contrast, BBTI from soyabean abolishes about 37% activity. TPCK and TLCK were both equally effective in blocking the moulting fluid protease activity. Both TPCK and TLCK are known to inhibit thiol proteases.

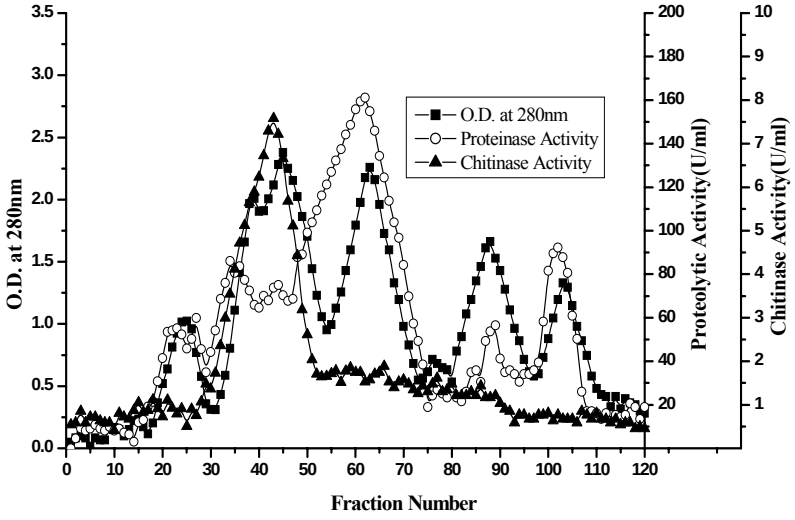

Figure 4. Partial purification of *H. armigera* moulting fluid enzymes by gel filtration.40-60% ammonium sulphate precipitated cuticle moulting fluid was dialyzed and loaded on a Sephadex G-75 gel-filtration column. See experimental procedures for details.

Plate assay for the detection of chitinase activity from moulting fluid

Chitinase assay based on the hydrolysis of RBV dyed *H. armigera* cuticle chitin is used to detect the chitinase enzyme present in the *H. armigera* cuticle moulting fluid. When the moulting fluid was loaded in the increasing concentrations (0 μM, 50 μM and 100 μM) on the sterilized paper discs in the agar plates containing RBV-Chitin, the substrate was hydrolyzed and clearing zones appear after 24 hour of incubation (Figure 6, discs 2A, 2B and 2C). The increasing enzyme concentration showed the increased clearance zone on plates around the paper discs. Chitinase enzyme pre-incubated with different ATBI concentrations showed less clearance zone around paper discs in agar plates containing RBV-Chitin as a substrate (Figure 6, discs 1A, 1B and 1C).

Inhibition of moulting fluid Proteases and chitinase by ATBI

ATBI shows 67% inhibition of moulting fluid proteolytic activity at pH 3.0 (Acidic proteases), 4% at pH 6.0 (acidic and serine proteases), 7% at pH 7.8 (serine proteases) and 2% at pH 9.5 (cystein proteases) while using hemoglobin as a substrate. ATBI shows 80 % inhibition of protease from crude moulting fluid with an IC_{50} value of 48 μM. The inhibition assay at pH 6.0 using Colloidal Chitin (for chitinase) as a substrate has shown 90% inhibition with a IC_{50} value of 35 μM of ATBI. The inhibition of the

crude enzyme was observed increasing as the inhibitor concentration was increased. The increased (0-100 µg) inhibitor concentration shows the increased relative inhibitory activity to 100 units/ml for proteases and 1 unit/ml in case of chitinase (Figure 7).

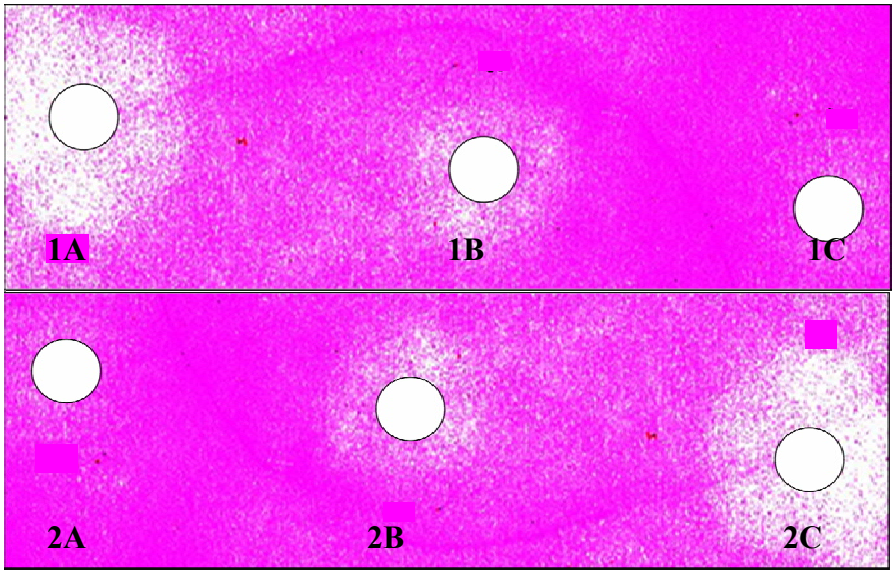

Figure 6. The chitinase plate assay containing 0.2% Ramazol dyed chitin. Discs 1A, 1B and 1C indicate the clearing zones by 100 µM chitinase enzyme preincubated with increasing concentration of ATBI (0, 50 and 100 µM respectively). Discs 2A, 2B and 2C indicate the clearing zones by chitinase in increasing concentrations (0, 50 and 100 µM respectively).

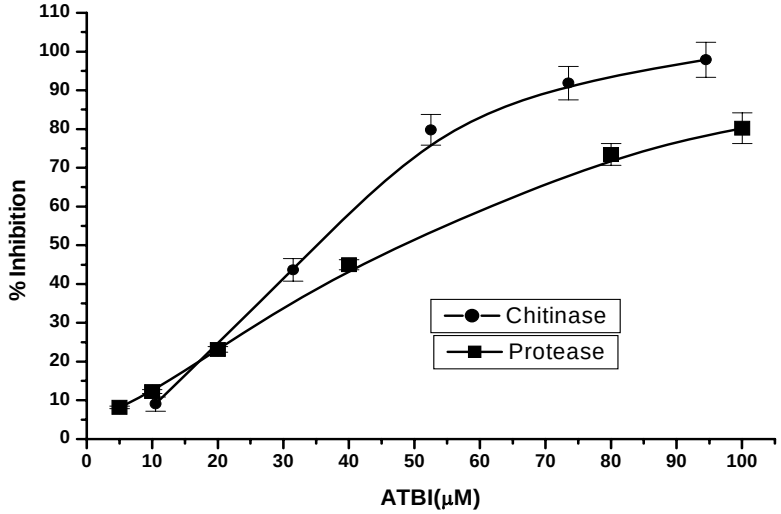

Figure 7. Effect of ATBI on Proteases and Chitinase Activity in vitro. The fractions from gel filtration showing proteolytic and chitinase activity were incubated with ATBI for 30 minutes and the remaining enzyme activity was calculated. There is 80% loss in proteolytic activity with an IC_{50} value of 47µM and 100% loss in chitinase activity with an IC_{50} value of 37µM of ATBI.

DISCUSSION

The studies in this chapter indicate that the inhibition of proteases and chitinases by ATBI is the basis of reduced growth and development *H. armigera*. The inhibition of moulting fluid proteases and chitinase activity in invitro system could corroborate the involvement of these enzymes. The abnormality in pupal stage is very evident in related study. The requirement of lower concentration of ATBI for maximum effect on *H. armigera* growth retardation indicates its high specificity towards *Helicoverpa* moulting fluid proteases and chitinases.

The essence of insect moulting is the laying down of new cuticle followed by shedding of the old cuticle and the degradation is brought about by the enzymes present in the moulting fluid, a liquid which lies between the new and old cuticles, and which is apparently secreted by epidermis. However, comparatively little is known about cuticle degradation or regulation by its inhibitors and hormones. This is a significant omission as inhibition of cuticle degrading enzymes is known to prevent moulting, resulting in mortality. The interference with the inhibitors and hormonal regulation of moulting is a proven method in pest control (Menn et al., 1989).

Knowledge on the role of proteases and their inhibitors in insect metamorphosis is limited than that of digestion process. The active chitinase and β-*N*-acetylglucoseaminidase are present in moulting fluid before cuticle thinning commences and is further evidence that chitinolytic enzymes are unlikely to be responsible for initiating the process of cuticle thinning during ecdysis (Samuels and Reynolds, 1993b). MFP-1 a trypsin like protease is likely to be the prime cause of cuticle thinning in *M. sexta* because of the timing of its increase in the titre during pre-ecdysial development (Samuals et al., 1993b). Mechanistic studies on the enzymatic degradation of chitin using semi-purified chitin and pure chitinolytic enzymes from *M. sexta* reveal that the ratio of chitinases to β-*N*-acetylglucosaaminidase in situ was very similar to the ratio which provided the largest possible synergism in vitro. It was likely not fortuitous because that ratio allowed the insect to depolymerize chitin in the most efficient manner (Fukamizo and Kramer, 1985).

Based on the inhibition studies with the help of specific inhibitors, it is concluded that ATBI inhibits aspartic proteases present in the moulting fluid. It is also suggested

that some aspartic proteases have very significant role in *H. armigera* development. This is to our knowledge, one of the first reports on the characterization of homogeneous chitinase from insect integument. The three chitinases were purified and characterized from moulting fluid of pharate pupae haemolymph in tobacco hornworm that exhibit normal kinetic behavior and had similar kinetic properties (Koga et al., 1983). The chitinase are also present in the silkworm, *Bombix mori* L. during larval and pupal development. These chitinases were detected in integument, moulting fluid and several other tissues. (Kimura, 1974, 1976). Two peaks of activity were separated from *Bombix mori* moulting fluid by gel filteration while only one peak was detected in case of *H. armigera* in this study. Chitinolytic enzymes have also been partially charaterized from integument of *Drosophila hydei* (Spindler, 1976) and *Locusta migatoria* (Zielkowski and Spindler, 1978). The expression of a chitinase cDNA gene from the integument of *H. armigera* was 2870 bp in length and contains an open reading frame of 1767 bp that encodes a polypeptide of 588 residues with a predicted molecular weight of 66 kDa (Ahmad et al., 2003). Inhibition of chitinase would be detrimental to moulting, digestion and certainly other metabolic processes. A determination of how this enzyme is regulated in vivo and in vitro and also of how they can be inhibited or activated may lead to new developments in insect control. Based on this information in the present study, ATBI can be considered as a suitable candidate for developing insect resistant transgenic plants.

REFERENCES

REFERENCES

Abad-Zapatero C., Goldman R. et al., 1996. Protein Sci. 5, 640–652.

Abad-Zapatero C., Goldman R. et al., 1998. Adv. Exp. Med. Biol. 436, 297–313.

Ackermann W.W. and Potter V.R., 1949. Proc. Soc. Exp. Biol. Med. 72, 1-9.

Adkins J. and Faulds D., 1998. Drugs 55, 837–842.

Ahmad M., Arif M.I. and Ahmad Z. 1998. In: Proceedings of the 2nd World Cotton Research Conference, Athens, Greece, pp. 697–700.

Ahmad M., Arif M.I. and Ahmad Z. 1999. Pesticide Science 55, 626–632.

Ahmad T., Rajagopal R. and Bhatnagar R.K. 2003. BBRC 310, 188-195.

Aloise P.A., Lumme M. and Haynes C.A., 1996. In: Muzzarelli R.A.A., (ed), Chitin Enzymology, 2. Grottammare, Eur. Chitin Soc. 581-94.

Ancillo G., Witte B., Schmelzer E. and Kombrink E., 1999. Plant Mol. Biol. 39, 1137-51.

Andersen O.A., Mark J.D. et al., 2005. Nat.Prod.Rep. 22,563-579.

Andrade M.A., Chacon, P. et al., 1993. Protein Eng. 6, 383-390.

Anson M.L. 1938. J.Gen. Physiol. 22, 79.

Anson M.L., 1940. J. Gen. Physiol. 23, 695-704.

Antonov V.K., Ginodman L.M. et al., 1978. FEBS Lett. 88, 87-90.

Arabshahi L. and Schmitz F.J., 1987. J. Org. Chem. 52, 3584-3586.

Arai N., Shiomi K., Iwai Y. and Omura S., 2000. J. Antibiot. 53, 609-614.

Arakane Y., Zhu Q. et al., 2003. Insect Biochem. Mol. Biol. 33, 631-648.

Armand S., Tomita H. et al., 1994. FEBS Letters. 343, 177-180.

Arnon R., 1970. In: Perlmann G.E. and Lorand L. (eds.), Methods in Enzymology, Academic Press, New York, 19, pp. 226-244.

Asakura T., Watanabe H., Abe K., and Arai S., 1995. Eur. J. Biochem. 232, 77–83.

Atzori C., Angeli E. et al., 2000. J. Infect. Dis 181, 1629.

Bade M.L. and Shoukimas J.J., 1974. J. Insect Physiol. 20, 281-290.

Bairoch A., Bucher P. et al., 1997. Nucleic Acids Res. 25, 217-221.

Baldwin E., Bhat T. et al., 1993. Proc. Natl. Acad. Sci. USA 90, 6796–6800.

Barett A., Rawlings N. and Woessner, J. 1998. In, Handbook of Proteolytic Enzymes Academic Press Inc., London.

Barret, A.J. 1977. In: Barret A.J. (ed.), proteinases from mammalian cells and tissues. North-Holland, Amsterdam 2, pp181-208.

Barret, A.J., 1977. In: Barret A.J. (ed.), proteinases from mammalian cells and tissues, North-Holland, Amsterdam 2, pp. 209-248.

Becker M., Harrop S. et al., 1995. J. Biol. Chem. 270, 24496–24501.

Beckett R., Davidson A. et al., 1996. Drug Discover. Today 1, 16–26.

Benedetti F., Berti F. and Norbedo S.J., 2002. Org. Chem. 67, 8635.

Benedetti F., Magnan M. et al., 1999. Bioorg. Med. Chem. Lett. 20, 3027.

Benedetti F., Miertus S. et al., 1997. Org. Chem. 62, 9348.

Benhamou N., Asselin A., 1989. Biol. Cell 67, 341-50.

Bennett B., Babu-Khan S., et al., 2000. J. Biol. Chem. 275, 20647–20651.

Blaak H., Schnellmann J. et al., 1993. Eur. J. Biochem. 214, 659-69.

Blattner R., Furneaux R.H. et al., 1994. J. Chem. Soc., Perkin Trans. 1, 3411-3421.

Blundell T., Cooper J., Sali A. and Zhu, Z. 1991. In, Structure and Function of the Aspartic Proteases, B. N. Dunn, Eds., pp. 443, Plenum Press, New York.

Bokma E., Rozeboom H.J. et al., 2002. Eur. J. Biochem. 269, 893-901.

Bold G., Fassler A., Capraro H. et al., 1998. J. Med. Chem. 41, 3387–3401.

Boller T., 1985. In: Key J.L. and Kosuge T., (Eds.) Cellular and Molecular Biology of Plant Stress pp. 247-262, New York.

Boot R.G., Blommaart E.F.C. et al., 2001. J. Biol. Chem. 276, 6770-6778.

Borg-von Zeppelin M., Meyer I. et al., 1999. Invest. Dermatol.113, 747.

Bortone K., Monzingo A.F. et al., 2002. J. Mol. Biol. 320, 293-302.

Bradford M.M., 1976. Anal. Biochem. 72, 248-254.

Brameld K.A. and Goddard W.A., 1998. Proc. Natl. Acad. Sci. USA 95, 4276-4281.

Brameld K.A., Shrader W.D.et al., 1998. J. Mol. Biol. 280, 913-923.

Braun D., Pauli N., S´equin U. and Zahner H., 1995. FEMS Microbiol. Lett. 126, 37-42.

Brik A. and Wong C.H., 2003. Org. Biomol. Chem. 1,5.

Brindley P., Kalinna B. et al., 1997. Mol. Biochem. Parasitol. 89, 1–9.

Brookhart G.L. and Kramer K.J., 1990. Insect Biochem. 20, 467 477.

Brunelle F., Girard C. et al., 2005. Archi. Insect Biochem. Physiol. 60, 20-31.

Buchanan R.H. and Gibbons N.E., 1974. Bergey's manual of determinative bacteriology. 8th ed., William and Wilkins Co., Baltimore, pp. 529-550.

Buhlmayer P., Caselli, A. et al., 1988. J. Med. Chem. 31, 1839–1846.

Cabib E., Silverman S.J. and Shaw J.A., 1992. J. Gen. Microbiol. 138, 97-102.

Cai H., Wang Y., et al., 2001. Nature Neuroscience 4(3), 233–234.

Carrillo A., Stewart K., Sham H., et al. 1998. J. Virol. 72, 7532–7541.

Cassone A., Bernardis F., Torosantucci A. et al., 1999. J. Infect. Dis. 180, 448–453.

Cha S., 1975. Biochem. Pharmacol. 24, 2177-2185.

Cha S., 1976. Biochem. Pharmacol. 25, 1561-1569.

Chatfield D. and Brooks B., 1995. J. Am. Chem. Soc. 117, 5561–5572.

Chet I. And Inbar J., 1994. Appl. Biochem. Biotechnol. 48, 37-43.

Cheung H.C., 1991. In: Lakowiez J.R. (Ed.), Topics in fluorescence spectroscopy, Vol.2: principles, Plenum press, New York, pp. 127-176.

Cho W.L., Dhadialla T.S. and Raikhel A.S. 1991. Insect Biochem. 21, 165-175.

Choi H.K., Choi K.H. et al., 1997. Insect Biochem. Mol. Biol. 27, 37-47.

Christeller J.T., Farley P.C., Ramsay R.J. et al., 1998. Eur. J. Biochem. 254, 160–167.

Christeller J.T., Laing W.A. et al., 1992. Insect Biochem. Molec. Biol. 22, 735–746.

Christeller J.T., Shaw B.D. et al., 1989. Insect Biochem.19, 221-231.

Clarke P.H. and Tracey M.V., 1956. J. Gen. Microbiol. 14, 188-196.

Collinge D.B., Kragh K.M. et al., 1993. Plant J. 3, 31-40.

Coombs G.H., Goldberg D.E. et al., 2001. Trend Parasitol. 17 (11), 532–537.

Cooper J.B., Khan G. et al., 1990. J. Mol. Biol. 214, 199-222.

Cornish-Bowden A.J. and Knowles J.R., 1969. Biochem. J. 113, 353-362.

Craik M. and Debouck C., 1995. In, McKerrow J.H. and James M.N.G. (Eds.), ESCOM, Leiden, Vol. 2, pp. 1–125.

Cutfield S., Dodson E., Anderson B. et al., 1995. Structure 3, 1261–1271.

D'Arcy-Lameta A., Zuily-Fodil Y. et al., 1996. Complete cds, accession no. U61396.

Dales N., Bohacek R., Satyshur K. and Rich D., 2001. Organic Letters 3, 2313–2316.

Dame J., Reddy G., Yowell C. et al., 1994. Mol. Biochem. Parasitol. 64(2), 177–90.

Darke P. and Huff J., 1994. Adv. Pharmacol. 25, 399–454.

Dash C. and Rao M., 2001. J. Biol. Chem. 276, 2487–2493.

Dash C., Ahmad A. et al., 2001b. Antimicrob. Agents. Chemother 45, 2008–2017.

Dash C., Phadtare S., Deshpande V. and Rao M. 2001a. Biochemistry 40, 11525–11532.

Dash C., Vathipadiekal V. et al., 2002. J. Biol. Chem. 277, 17978–17986.

De Bernardis F., Arancia S. et al., 1999. Infect. Dise.179, 201.

De Bernardis F., Arancia S. et al., 1999. J. Infect. Dis.179, 201–208.

De Jong A.J., Heidstra R. et al., 1993. Plant Cell. 5, 615-620.

de la Vega H., Specht C.A., Liu Y. and Robbins P.W. 1998. Insect Mol. Biol. 7, 233-239.

Deane E.E., Whipps J.M. et al., 1999. Enzyme Microb. Technol. 24, 419-24.

Debouck C., and Metcalf B.W. 1990. Drug. Dev. Res. 21, 1-17.

De-Clercq E., 2002. Nat. Drug Discov. 1, 13.

Deising H. and Siegrist J., 1995. FEMS Microbiol. Lett. 127,207-12.

Deshpande M.V., 1998. In, proceeding of biotechnology- a challenge for 2005. New Delhi, All India Biotech Association 1-4.

Devaux C., Menard J., Sicard P., and Corvol P. 1976. Eur. J. Biochem. 64, 621-627.

Dickinson K., Keer V. et al., 1989. J. Gen. Microbiol. 135, 1417-1421.

Diekmann H., Tschech A. and Plattner H., 1989. In: Skjar-Braek G., Anthonsen T. and Sandford P., (Eds.), Chitin and Chitosan. pp. 207-214. Elsevier Science, London.

Dittmer N.T. and Raikhel A.S., 1997. Insect. Biochem. Molec. Biol. 27, 323-335.

Dixon M., 1953. Biochem. J. 55, 170-171.

Doi E., Shibata, D. Matoba et al., 1980. Agric. Biol. Chem. 44(4), 741-7.

Dorsey B., Levin R., McDaniel S., et al., 1994. J. Med. Chem. 37, 3443-3451.

Draborg H., Kauppinen S. et al., 1997. In: Muzzarlliand R.A., Peter A.M.G. (eds.), chitin handbook., pp 261-266, Europian Chitin Society.

Duggleby R.G., 1986. Biochem. J. 235, 613-616.

Dunn B., 1991. In, Structure and function of the aspartic peptidases, Plenum Press, New York.

Dunn B., 1992. In, Coxon, J., (Eds.), 2, JA1 Press, Greenwich, Connecticut, pp. 213-241.

Dunn B., 2002. Chem. Rev. 102, 4431–4458.

Dunn B., Scarborough P. et al.,1995. In, Takahashi, K., Eds., Plenum Press, pp. 1-9.

Eason L.H. and Stedman E., 1936. Proc. R. Soc. London, Ser B. 121, 142-165.

Eguchi M., Itoh M.et al., 1993. Comp. Biochem. Physiol. 104B, 537-543.

Erickson J., 1995. Nat. Struct. Biol. 2(7), 523–529.

Erikson J., Neidhart D.J. et al., 1990. Science 249, 527.

Faro C., Ramalho-Santos M. et al., 1999. J. Biol. Chem. 274, 28724-28729.

Fath M., Wu X. et al., 1998. J. Biol. Chem. 273, 13563–13569.

Favilla R., Parisoli A. and Mazzini A., 1997. Biophys. Chem. 67, 75-83.

Feix M., Gloggler S. et al., 2000. Arch. Insect Biochem. Physiol. 45, 24-36.

Ferron P., 1985. Vol. 12. Oxford, Pergamon Press 313-46.

Fersht A. 1977. In: enzyme structure and mechanism. Freeman W.H. and Co. Reading and San Francisco, p-18.

Fitzgerald P., 1993. Curr. Opin. Struct. Biol. 3, 868.

Fitzgerald P., McKeever B. et al., 1990. J. Biol. Chem. 265, 14209–14219.

Flach J., Pilet P.E. and Jolles P., 1992. Experientia. 48, 701-716.

Forrester N.W., Cahill M. et al., 1993. Bull. Entomol. Res. 1,1–132.

Francis S., Gluzman I.O. et al., 1994. EMBO J. 13, 306–317.

Francis S., Sullivan D. Jr. and Goldberg D., 1997. Annu. Rev. Microbiol., 51, 97-123.

Frazão C., Bento I. et al., 1999. J. Biol. Chem. 274, 27694–27701.

Frecer V., Miertus S., Tossi A. and Romeo D., 1998. Drug Design Discov. 15, 211.

Friedman L.S. and Peterson W.L., 1998. In: Fauci A.S., Braunwald E., Isselbacheret K.J. et. al.,(Eds), 14th ed. McGraw Hill, pp.1596-1616.

Friedman S.J. and Skehan P., 1980. Proc. Natl. Acad. Sci. USA 77, 1172-6.

Fruton J., 2002. Quart. Rev. Biol. 77(2), 127–147.

Fuetterer J. and Hohn T., 1987. Trends Biochem. Sci. 12(3), 92–95.

Fukamizo T. and Kramer K.J. 1985. Insect Biochem. 15, 141-145.

Fung H., Kirschenbaum H. and Hameed R., 2000. Clin. Ther. 22, 549–572.

Fusek et al., 1995. In, Aspartic Peptidases Physiology and Pathology, CRC Press, Boca Raton.

Garfinkel D., Hedge A., Youngren S. et al., 1991. Ty1. Virology 65(9), 4573–4581.

Gelb M., Svaren J. and Abeles R., 1985. Biochemistry 24, 1813-1817.

George S.P. and Rao M.B., 2001. Eur. J. Biochem. 268, 2881-2888.

Ghosh A., Shin D. et al., 2000. J. Am. Chem. Soc. 122(14), 3522–3523.

Gibson W. and Hall M., 1997. Drug Des. Discovery 15(1), 39–47.

Girard C. and Jouanin L., 1999. Insect Biochem. Mol. Biol. 29, 549-556.

Girdwood K., Perler F.B., and Berry C., 1998. In, Aspartic Proteinases, Retroviral and Cellular Enzymes, Advances in Experimental Medicine and Biology, Plenum Press, New York, pp. 419.

Gleave A.P., Taylor R.K et al., 1995. FEMS Microbiol. Lett. 131, 279-288.

Glenner G.C. and Wong C.W., 1984. Biochem. Biophys. Res. Commun. 120, 885–890.

Glick D.M., Auer H.E. et al., 1986. Biochemistry 25, 1858-1864.

Gokhale D.V., 1992. J. Sci. Ind. Res. 51,497-506.

Goldstein A.J., 1944. Gen. Physiol. 27, 529-580.

Gooday G.W., 1995. In: Zakaria M.B., Wan Muda W.M., Abdullah M.P., (eds). Chitin and Chitosan. Malaysia, Penerbit Universiti Kebangsaan. 191–202.

Gooday G.W., Humphreys A.M. and McIntosh W.H., 1986. In: Muzzarelli R., Jeuniaux C. and Gooday G.W., (Eds.), Chitin in Nature and Technology pp. 83-91. Plenum Press, New York.

Gopalakrishnan B., Muthukrishnan S. and Kramer K.J., 1995. Insect Biochem. Mol. Biol. 25, 255-265.

Goschke R., Cohen N., Wood J. and Maibaum J., 1997. Bioorg. Med. Chem. Lett. 7(21), 2735–2740.

Grant G.A., Eisen A.Z. and Bradshaw R.A., 1981. In: Lorand L. (ed.), Methods in Enzymology, Academic Press, New York, 80, pp. 722-734.

Gruber A., Speth C. et al., 1999. Immuno-pharmacology 41(3), 227–234.

Gustchina A., Li M. et al., 2005. J. Mol. Biol. 348, 433–444.

GyoÈrgy P. and Rose C.S., 1955. Proc. Soc. Exp. Biol. Med. 90,219-223.

Hadwiger L.A. and Beckman J.M., 1980. Plant Physiol. 66, 205-11.

Hall L. and Soderhall K., 1983. Comp. Biochem. Physiol. 76B, 699-702.

Hamamura Y. and Kanehara Y., 1940. J. Agric. Chem. Soc. Jpn. 16, 907-909.

Hansen J.E., Lund O. et al., 1997. Nucleic Acids Res. 25, 278-282.

Hanada K., Tamai M.et al., 1978. Agric Biol Chem 42, 523.

Hans M. and Lars Z., 2003. The J. Exp. Biol. 206, 4393-4412.

Hart P.J., Monzingo A.F. et al., J.D., 1993. J. Mol. Biol. 229, 189-193.

Hart P.J., Pfluger H.D. et al., 1995. J. Mol. Biol., 248, 402-413.

Hawtin R.E., Zarkowska T. et al., 1997. Virology. 238, 243-253.

Hellen C.U.T. and Wimmer E., 1992. Experientia. 48(2), 201–215.

Henderson P., 1972. Biochem. J. 127, 321-333.

Henrissat B. and Bairoch A., 1993. Biochem. J. 293,781-788.

Henrissat B. and Bairoch A., 1996. Biochem. J. 316,695-696.

Henrissat B., 1991. Biochem. J. 280,309-316.

Henrissat B., Callebaut I. et al., 1995. Proc. Natl. Acad. Sci. 92, 7090-7094.

Hermova M., Selitrennikoff C.D., 1987. Curr. Microbiol. 16, 33-38.

Higuchi T., Okubo K., Saiga T. and Senda S., 1998. Jpn. Kokai Tokkyo Koho JP 10067613 A2 10 Mar 1998 Heisei. (CA 1998, 128, Patent 254077).

Hill J. and Phylip L., 1997. FEBS Lett. 409(3), 357–360.

Hindmarsh A.C., 1983. In: Stepleman R S., Ed. North Holland, Amsterdam, pp 55-64.

Hiraiwa N., Kondo M. et al., 1997. Eur. J. Biochem. 246, 133–141.

Hirschmann R., 1991. Angew. Chem., Int. Ed. Engl. 30, 1278.

Hoegl L., Korting H.C. and Klebe G., 1999. Pharmazie 54, 319.

Hollis T., Honda Y., Fukamizo T., Marcotte E., Day P.J. and Robertus J.D., 1997. Arch. Biochem. Biophys. 344, 335-342.

Hollis T., Monzingo A.F., Bortone K., Ernst S., Cox R. and Robertus J.D., 2000. Protein Sci. 9, 544-551.

Honda Y., Kitaoka M. and Hayashi K., 2004. FEBS Lett. 567, 307-310.

Hong L., Turner RT et al., 2002. Biochemistry. 41, 10963–10967.

Hoover D., Lefker B. et al., 1995. Adv. Exp. Med. Biol. 362, 167–80.

Hopwood D.A., Bibb M.J. et al., 1985. In: Genetic Manipulation of Streptomyces-A laboratory manual. The John Innes Foundation. Norwich, England.

Houseman J.G., MacNaughton W.K. and Downe A.E.R 1984. Can. Ent.116,1393-1396.

Houston D.R., Eggleston I. et al., 2002 Biochem. J. 368, 23-27.

Houston D.R., Shiomi K et al., 2002a. Proc. Natl. Acad. Sci. USA99, 9127-9132.

Houston D.R., Synstad B. et al., 2004. J. Med. Chem. 47, 5713-5720.

Houtzager V., Oullet M. et al., 1996. Biochemistry 35, 10974-10984.

Howlett D., Simmons D. et al., 2000. Trend. Neurosci. 23, 565–570.

Hruby V.J., 2001. Acc. Chem. Res., 34, 389.

Huang F., Higgins R.A. and Buschman L.L., 1999. ACPC conference, Pestology, 2–29.

Huang X., Zhang H. et al., 2000. Insect Biochem. Mol. Biol. 30, 107-117.

Hube B., Sanglard D. et al., 1997. Infect. Immun. 65(9), 3529–3538.

Hugli T., 1996. Trend. Biotechnol. 14,409–412.

Hurst M. and Faulds D., 2000. Drugs 60, 1371–1379.

Hussain I., Powell D.J. et al., 1999. Mol. Cell. Neurosci. 14, 419–427.

Hussain I., Powell D.J. et al., 2000. Mol. Cell. Neurosci. 16, 609–619.

Inoue H., Kimura T. et al., 1991. J. Biol. Chem. 266, 19484–19489.

Inouye S., Yuki, S. and Saigo K., 1986. Eur. J. Biochem. 154, 417–425.

Inouye Y., Onodera K. et al., 1956. J. Am. Chem. Soc. 78, 4722-4724.

Iseli B., Armand S. et al., 1996b. FEBS Lett. 382, 186-188.

Iseli B., Boller T. and Neuhaus J.M., 1996a. In, Muzzarelli R.A.A., (ed), Chitin Enzymology, 2. Atec Edizioni-Grottammare 136-42.

Ishikawa F. and Oishi K., 1985. J. Gen. Microbiol. 131, 3311-3316.

Isogai A., Sato M. et al., 1989. Agric. Biol. Chem. 53, 2825-2826.

Izumida H., Imamura N. And Sano H., 1996a. J. Antibiot. 49, 76-80.

Izumida H., Nishijima M. et al., 1996. J. Antibiot. 49, 829-831.

James M., 1998. In, Structure and Function of Aspartic Protease, Retroviral and Cellular Enzymes, Plenum Press, New York, pp. 1–481.

James M.N.G. and Sielecki A.R., 1986. Nature 319, 33-38.

James M.N.G. and Sielecki A.R., 1987. In, Jurnak FA. and McPherson A (Eds.), John Wiley & Sons, New York, Vol. 3, p. 413.

Jany K.D., Haug H. and Ishay J., 1978. Insect Biochem. 8, 221-230.

Jencks W.C., 1975. Adv. Enzymol. Relat. Areas Mol. Biol. 43, 219-411.

Jimenez C. and Crews P., 1991. Tetrahedron 47, 2097-2102.

Johns M., Babcock M. et al., 1989. Plant Mol. Biol. 12(6), 633–42.

Johnson E.A., Villa T.G. et al., 1979. J. Appl. Biochem. 1, 273-282

Johnson L., Dyer R. and Hupe D, 1998. Curr. Opin. Chem. Biol. 379,113–123.

Jungreis A.M., 1979. In: Treherne J.E., Berridge M.J. and Wigglesworth V.B. (eds.), Advances in Insect Physiology, pp. 103-183. London, Academic Press.

Kageyama T., 1998. Eur. J. Biochem. 253, 804–809.

Kakuda T.N., Struble K.A. and Piscitelli S.C., 1998. Am. J. Health-Syst. Pharm. 55, 233.

Kaldor S., Kalish V., Davies J. et al., 1997. J. Med. Chem. 40, 3979–3985.

Kang S.C., Park S. and Lee Dg., 1998. FEMS Microbiol. Lett. 165, 267-71.

Kati W.M., Saldivar A.S. et al., 1998. Biochem. Biophys. Res. Com. 244, 408-413.

Kato T., Shizuri Y. et al., 1995. Tetrahedron Lett. 36, 2133-136.

Katzenellenbogen B.S. and Kafatos F.C., 1970. J. Insect Physiol. 16, 2241-2256.

Katzenellenbogen B.S. and Kafatos F.C., 1971a. J. Insect Physiol. 17, 775-800.

Katzenellenbogen B.S. and Kafatos F.C., 1971b. J. Insect Physiol. 17, 823-832.

Kay J., 1985. In, Kostka V. (Eds.), Walter de Gruyter, Berlin, pp.1–17.

Kay J., Valle M.J. and Dunn B.N., 1983. In, Katunuma N., Umezawa H. and Holzer H. (Eds.), Japan Scientific Societies Press, Tokyo, pp. 201–210.

Kelkar H.S., Shankar V. and Deshpande M.V.,1990. Enzyme Microb.Technol. 12, 510-4.

Kempf D. and Sham H., 1996. Disease 2(2), 225–246.

Kempf D., Marsh K. et al., 1997. Antimicrob. Agents Chemother. 41(3), 654–660.

Kempf D.J., 1994. Methods Enzymol. 241, 334.

Kervinen J., Tobin G., et al., 1999. EMBO J. 18, 3947–3955.

Kim C.Y., Al S.W., Choe M.S. et al., 1998. Plant Mol. Biol. 37,523-34.

Kim E., Baker C. et al., 1995. J. Am. Chem. Soc. 117, 1181–1182.

Kim J., Morgenstern K. et al., 1996. 87(2), 343–355.

Kim M.G., Shin S.W. et al., 1998. Insect Biochem. Mol. Biol. 28, 163-171.

Kimura S., 1973. J. Insect Physiol.19, 115-123.

Kimura S., 1974. Comp. Biochem. Physiol. 49B, 345-351.

Kimura S., 1976. Insect Biochem. 6, 479-482.

Kinnel R.B., Gehrken H.P. and Scheuer P.J., 1993. J. Am. Chem. Soc. 115, 3376-3377.

Kinnel R.B., Gehrken H.P. et al.,1998. J. Org. Chem. 63, 3281-3286.

Kitamoto Y., Mori N. et al., 1988. Appl. Microbiol. Biotechnol. 28, 445-450.

Kitch L.W. and Murdock L.L., 1986. Archi. Insect Biochem. Physiol. 3, 561-576.

Kleinert H., Stein H. et al., 1992. Hypertension 20(6), 768–75.

Kobayashi S., Kiyosada T. and Shoda S., 1997. Tetrahedron Lett. 38, 2111-2.

Koga D., Funakoshi T. et al., 1991. Insect Biochem. 21, 277-284.

Koga D., Jilka J. and Kramer K.J., 1983. Insect Biochem. 13, 295-305.

Koga D., Sasaki Y. et al., 1997. Insect Biochem. Mol. Biol. 27, 757-767.

Kombrink E. and Somssich I.E., 1995. Adv. Bot. Res. 21, 2-34.

Konno T., Kamatari Y.O. et al., 2000. Biochemistry 39, 4182-4190.

Kotani1 N., Kitazume S. et al., 2005. J. Biochem. 137, 315–322.

Kramer K.J. and Koga D., 1986. Insect Biochem. 16, 851–877.

Kramer K.J. and Muthukrishnan S., 1997. Insect Biochem. Mol. Biol. 27, 887-900.

Kramer K.J., Corpuz L. et al., 1993. Insect Biochem. Mol. Biol. 23, 691-701.

Kramer K.J., Turner C.D. and Koga D., 1985. In: Kerkut G.A. and Gilbert L.I. (eds.), by Pergamon Press, Inc. New York, 3, p. 75.

Kreft S., Ravnikar M. et al., 1997. Phytochemistry 44(6), 1001–1006.

Kumar A. and Rao M., 2006. Biochimica et Biophysica Acta 1760, 1845–1856.

Kumari J.A. and Panda T., 1992. Enzyme Microb. Technol. 14, 241-248.

Kunitz M., 1947. J. Gen. Physiol. 30, 291.

Kuranda M.J. and Robbins P.W., 1991. J. Biol. Chem. 266, 19758-19767.

Lacy M. and Abriola K., 1996. Conn. Med. 60, 723–727.

Laemmli U.K., 1970. Nature 227, 680–685.

Laine R.A. and Lo W.C.J., 1998. PCT Int Appl WO 9802742 Al 22, 1998 CA,128,86184.

Lakowicz J.R., 1983. Principles of Fluorescence Spectroscopy, Plenum Press, New York.

Lam P., Jadhav P., Eyermann C. et al., 1994. Science 263, 380–384.

Lamarre D., Croteau G. et al., 1997. Antimicrob. Agents Chemother. 41(5), 965–971.

Le Q.T. and Katunuma N., 2004. Anal. Biochem. 324, 237–240.

Lea A. and Faulds D., 1996. Drugs 52(4), 541–546.

Lee S.Y., Jung S.W., Kim S.H. and Lee Y.N., 1993. Misaengmul Hakhoechi.31, 218-23.

Leger R.J., Lokesh J. And Donald R., 1998. Appl. Environ. Microbiol. 64, 709-713.

Lemos F.J.A., Campos F.A.P. et al.,1990. Entomol. Exp. Appl. 56, 219-227.

Lenarcic B. and Turk V., 1999. J. Biol. Chem. 274, 563–566.

Lenney J.F., 1975. J. Bacteriol. 122, 1265-1273.

Leung D., Abbenante G. and Fairlie D.P.J., 2000. Med. Chem. 43, 305.

Li Z., Chen X. et al., 1994. Chem. Biol. 1(1), 31–7.

Lin J.H., 1997. Adv. Drug Deliv. Rev. 27, 215.

Lin X., Koelsch G. et al., 2000. Proc. Natl. Acad. Sci. USA 97, 1456–1460.

Lin X., Loy J.A., Sussman F. and Tang J., 1993. Protein Sci. 2, 1383-1390.

Lin Y., Fusek M., Lin X. et al., 1992. J. Biol. Chem. 267, 18413-18418.

Lorito M., Harman G.E. et al., 1993. Phytopathology 83, 302-7.

Love R., Parge H. et al., 1996. Cell 87(2), 331–342.

Lu Y.M., Zen K.C. et al., 2002. Insect Biochem. Mol. Biol. 32, 1369-1382.

Lunt M.R. and Kent P.W., 1960. Biochim. Biophys. Acta 44, 371-373.

Luo Y., Bolon B. et al., 2001. Nature Neurosci. 4(3), 231–232.

MacKay V., Welch S. et al., 1988. Proc. Natl. Acad. Sci. USA, 85(1), 55–9.

Majer P., Collins J., Gulnik S. and Erickson J., 1997. Protein Sci. 6, 1458–1466.

Manjunath T.M., Bhatnagar V.S. et al., 1989. In: King E.G., Jackson, R.D. (Eds.), Proceedings of the workshop on biological control of Heliothis: increasing the effectiveness of natural enemies, Far Eastern Regional Office, U.S. Department of Agriculture, New Delhi, India, pp. 197–228.

Marciniszyn Jr. J., Huang J.S. et al., 1976. J. Biol. Chem. 251, 7095-7102.

Masters C.L., Simms G. et al., 1985. Proc. Natl. Acad. Sci. USA 82, 4245–4249.

Mathivanan N., Kabilan V. and Murugesan K., 1998. Can. J. Microbiol. 44, 646-51.

McNab R. and Glover L.A., 1991. FEMS Microbiol. Lett. 82, 79-82.

McPhie P., 1972. J. Biol. Chem. 247, 4277-4281.

McPhie P., 1989. Biochem. Biophys. Res. Commun. 158, 115-119.

Medina M. and Vallejo C.G., 1989. Insect Biochem. 19, 687 691.

Mendonsa E.S., Vartak P.H. et al., 1996. Biotechnol. Lett. 18, 373-6.

Menn J.J., Raina A.K. and Edwards J.P., 1989. In: McFarlane N.R. (Ed.), progress and prospects in insect control, pp. 89-106. BCPC Monograph No. 43, British Crop Proection Council, Farnham, Surrey.

Menon A. and Goldberg A., 1987. J. Biol. Chem. 262, 14929–14934.

Merker D.J., Brenowitz M. and Schramm V.L., 1990. Biochemistry 29, 8358-8364.

Miertus S., Furlan M., Tossi A. and Romeo D., 1996. Chem. Phys. 204, 173.

Mikitani K., Sugasaki T. et al., 2000. J. Biol. Chem. 275, 37725-37732.

Miller J.W., Kramer K.J. and Law J.H., 1974. Comp. Biochem. Physiol. 40B, 117 129.

Miller M., Jaskolski M. et al., 1989. Nature (London). 337(6207), 576–9.

Miller M., Palojarvi A., et al., 1998. Appl. Environ. Microbiol. 64, 613-7.

Mohan M. and Gujar G.T., 2002. Bull. Ent. Res. 92, 489–498.

Mohan M. and Gujar G.T., 2003. Journal of Invertebrate Pathology 82, 1-11.

Monod M., Hube B., Hess D. and Sanglard D., 1998. Microbiology 144, 2731–2737.

Monzingo A.F., Marcotte E.M.et al., 1996. Nature Struct. Biol. 3, 155-162.

Morgavi D.P., Sakurada M. et al., 1994.Microbiology. 40, 631-636.

Moriguchi M. and Kotegawa S., 1985. Agri. Biol. Chem. 49, 2791-2793.

Moringa T., Kikuchi M. and Nomi R., 1985. Agri. Biol. Chem. 49, 523-524.

Morisson J.F. and Walsh C.T., 1988. Adv. Enzymol. Relat. Areas Mol. Biol. 61, 201-301.

Morrison J.F., 1969. Biochim. Biophys. Acta 185, 269.

Morrison J.F., 1982. Trends Biochem. Sci. 7, 102-105.

Moss M.L., Kuzmic P. et al., 1996. Biochemistry 3511, 3457-3464.

Müller M., 1992. EXS 48, 118-129.

Murao S., Kawada T. et al., 1992. Biosci. Biotech. Biochem. 56, 368-9.

Mutlu A., Pfeil J. and Gal S., 1998. Phytochemistry 47(8), 1453–1459

Naglik J., Newport G. et al., 1999. Infect. Immun. 67(5), 2482–2490.

Nahar P., Ghormade V. and Deshpande M.V., 2004. J. invertebrate pathology 85, 80–88.

Nanjo F., Sakai K. et al., 1989. Agric. Biol. Chem. 53, 2189 -95.

Nezami A., Luque I. et al., 2002. Biochemistry 41, 2273–2280.

Ng K.K.S., Peterson J. et al., 2000. Natur. Struct. Biol. 7 (8), 653–657.

Niehrs C. and Pollet N., 1999. Nature 402, 483-487.

Nielsen H., Engelbrecht J., Brunak S. and von Heijne G., 1997. Protein Eng. 10, 1-6.

Nishimoto Y., Sakuda S., Takayama S. and Yamada Y., 1991. J. Antibiot. 44, 716-722.

Nitoda T., Usuki H. and Kanzaki H., 2003. Z. Naturforsch. C, 58, 891-894.

Noble S. and Goa K. 2000. Drugs 60, 1383–1410.

North M.J., 1982. Microbiol Rev 46, 308.

Northrop D., 2001. Accounts Chem. Res., 34(10), 790–797.

Northrop J.H., 1930. J. Gen. Physiol. 13, 739.

Oda K., Takahashi T. et al., 1994. J. Biol. Chem. 269, 26518–26524.

Oefner C., Binggeli A. et al., 1999. Chem. Biol. 6, 127–131.

Ohtakara A., 1961. Agric. Biol. Chem. 25, 54-60.

Ordentlich A., Elad Y. and Chet I., 1988. Phytopathol. 78, 84-8.

Overdijk B., Van S.G., Odds F., 1994. Glycobiology. 6, 627-634.

Pakyz A. and Israel D., 1997. J. Am. Pharm. Assoc. (Washington) NS37, 543–551.

Palczewski K., Hargrave P.A. and Kochman M., 1983. Eur. J. Biochem. 137,429- 435.

Papanikolau Y., Prag G. et al., 2001. Biochemistry 40, 11338-11343.

Papanikolau Y., Tavlas G. et al., 2003. Acta Crystallogr. Sect. D, Biol. Crystallogr. 59, 400-403.

Papassotiropoulos A., Bagli M. et al., 1999. Neurosci. Lett. 262,171–174.

Patick A. and Potts K., 1998. Clin. Microbiol. Rev. 11, 614–627.

Pawagi A.B. and Deber C.M., 1990. Biochemistry 294, 950-955.

Pearl L.H. and Taylor W.R., 1987. Nature 329, 351-354.

Peberdy J.F., 1989. Mycol. Res. 93, 1-20.

Pegg M.S. and Vonitzstein M., 1994. Biochem. Mol. Biol. Int. 32, 851-858.

Perrakis A., Tews I. et al., 1994. Structure, 2, 1169-1180.

Perrakis A., Wilson K.S. et al., 1993. In: Muzzarelli R.A.A., (ed), Chitin enzymology. Ancona, Eur Chitin Soc. 217-32.

Peters W., 1992. In: Bradshaw S.D., Burggeren W., Heller H.C., Ishii S., Langer H., Neuweiler G., Randall D.J., (Eds.), Zooephysiology: Perotrophic Membranes, 130, Chemical Composition. Springer-Verlag, Berlin.

Phylip L.H., Lees W.E. et al., 2001. J. Biol. Chem. 276, 2023-2030.

Pina I.C., Gautschi J.T. et al., 2003. J. Org. Chem. 68, 3866-3873.

Pishko E.J., Kirkland T.N. and Cole G.T., 1995. Gene 167,173-7.

Ploux O., Breyne O., Carillon S. and Marquet A., 1999. Eur. J. Biochem. 259, 63-70.

Powning R.F. and Irzykiewez H., 1965. Comp. Biochem. Physiol. 14, 27-133.

Purchase E.R. and Braun C.E., 1946.Org. Syn. 26, 36-37.

Quinoa E. and Crews P., 1987. Tetrahedron Lett. 28, 3229-3232.

Rabossi A., Stoka V. et al., 2004. Arch. Insect Biochem. Physiol. 57, 51–67.

Ramaguero A., Tschech A et al., 1993. Enzyme Microb. Technol. 15,412-417.

Rao F.V., Andersen O.A. et al., 2005. Chem. Biol. 12, 973-980.

Rao F.V., Houston D.R., Boot R.G., Aerts J., Hodkinson M., Adams D.J., Shiomi K., Omura S. and van Aalten D.M.F., 2005. Chem. Biol. 12, 65-76.

Rao F.V., Houston D.R., Boot R.G., Aerts J., Sakuda S. and van Aalten D.M.F., 2003 J. Biol. Chem. 278, 20110-20116.

Rao M., et al. 1998. Microbiol. Mol. Biol. Rev. 62(3), 597–635.

Rechsteiner M. and Rogers S.W., 1996. Trends Biochem. Sci. 21, 267-271.

Reich J.G., 1992. Curve Fitting and Modelling for Scientists and Engineers, Graw-Hill, New York .

Reid W.A., Vongsorasak L. et al., 1984. J. Cell Tissue Res. 236(3), 597–600.

Reiner J.M., 1959. In "Behavor of Enzyme Systems" Burgess, Minneappolis, Minnesota.

Remirez M.G., Avelizapa L.I.R. et al., 2004. J. Micro. Methods 56, 213-219.

Revah-Moiseev S. and Carroad P.A., 1981. Biotechnol. Bioeng. 23, 1067-1078.

Rich D. and Sun E., 1980. Biochem. Pharmacol. 29, 2205-2212.

Rich D., 1985. J. Med. Chem. 28(3), 263–73.

Richman D.D., 2001. Nature 410, 995.

Ripka A., Satyshur K., Bohacek R. and Rich D., 2001. Organic Letters 3, 2309–2312.

Ripka A.S. and Rich D.H., 1998. Curr. Opin. Chem. Biol. 2, 441.

Roberts N., Martin J., Kinchington D. et al., 1990. Science 248, 358–361.

Roberts R.L. and Cabib E., 1982. Anal. Biochem. 127, 402-412.

Roberts W.A. and Selitrennikoff C.P., 1988. J. Gen. Microbiol. 134, 169-76.

Rochefort H. and Liaudet-Coopman E., 1999.APMIS 107(1), 86–95.

Rodriguez A.D., Akee R.K. and Scheuer P.J., 1987. Tetrahedron Lett. 28, 4989-4992.

Rogers S., Wells R. and Rechsteiner M., 1986. Science 234, 364-368.

Romaguera A., Menge U. et al., 1992. J. Bacteriol. 174, 3450-3454.

Rosenberg S.H., 1995. In: Ellis G.P. and Loscombe D.K. (Eds.), Elsevier Science, New York, Vol. 32, pp. 37–115.

Rosenthal P.J., 1998. Emerging Infect. Dis. 4, 49-57.

Royer V., Fraichard S. and Bouhin H., 2002. Biochem. J. 366, 921-928.

Runeberg-Roos P., Kervinen J. et al., 1994. Plant Physiol. 105(1), 321–329.

Runeberg-Roos P., Tormakangas K. et al., 1991. Eur. J. Biochem. 202, 1021–1027.

Rusconi S., La Seta C. et al., 2000. Antimicrob. Agents. Chemother. 44, 1328–1332.

Ryle A.P., 1970. Methods Enzymol. 19, 316-336.

Saftig P., Hetman M. et al., 1995. EMBO J. 14, 3599–3608.

Sahai A.S. and Manocha M.S., 1993. FEMS Microbiol Rev. 11,317-38.

Sakuda S., 1996. In: Muzzarelli R.A.A, editor. Chitin Enzymology, Vol. 2. Grottammare, Eur. Chitin Soc. p. 203-12.

Sakuda S., 1996. In: Muzzarelli R.A.A., (ed), Chitin Enzymology, Atec Edizioni, Ancona Italy.

Sakuda S., Isogai A. et al.,1986. Tetrahedron Lett. 27, 2475-2478.

Sakuda S., Isogai A., Matsumoto S. and Suzuki A., 1987. J. Antibiot., 40, 296-300.

Sakuda S., Isogei A. et al., 1987a. Agric. Biol. Chem. 51, 3251-3259.

Sakuda S., Isogei A. et al., 1987b. SJ. Antibiot. 40, 296-300.

Sakuda S., Nishimoto Y. et al.,1990. Agric. Biol. Chem. 54, 1333-335.

Samuels R.I. and Reynolds S.E., 1993a. Journal of Insect Physiology 39, 633-637.

Samuals R.I. and Reynolds S.E., 1993b. Archs Insect Phys. Biochem. 24, 33-44.

Samuels R.I., Charnley A.K. and Reynolds S.E., 1993a. Insect. Biochem. Mol. Biol. 23, 607-614.

Samuals R.I., Charnley A.K. and Reynolds S.E., 1993b. Insect Biochem. Molec Biol. 23, 615-620.

Sandhu D.K., Wadhwa V. and Bagga P.S., 1989. Enzyme. Microb. Technol. 11, 21-25.

Sandor E., Pusztahelyi T. et al., 1998. FEMS Microbiol. Lett. 164, 231-236.

Sanglard D., Hube B. et al., 1997. Infect. Immun. 65, 3539–3546.

Sathivel C., Lachke A. and Radhakrishnan S., 1995. J. Chromatogr. 705, 400-402.

Scarborough P.E., Guruprasad K. et al., 1993. Protein Science 2, 264-276.

Sculley M.J. Morrison J.F. and Cleland W.W., 1996. Bio. Biophys. Acta. 1298, 78-86.

Seife C., 1997. Science 277, 1602–1603.

Semenov A., Olson J. and Rosenthal P., 1998. Antimicrob. Agents Chemother. 42(9), 2254–2258.

Shahabuddin M., Toyoshima T. et al., 1993. Proc. Natl. Acad. Sci. USA90, 4266-4270.

Shaikh S.A. and Deshpande M.V., 1993. World J. Microbiol. Biotechnol. 9, 468-75.

Sham H., Kempf D., Molla A. et al., 1998. Antimic. Agents Chemother. 42, 3218–3224.

Shapira R., Ordentlich A., Chet I. and Oppenheim A.B., 1989. Phytopathol.79, 1246-9.

Shaw E., 1990. Adv. Enzymol. Relat. Areas Mol. Biol. 63, 271–347.

Shen Z. and Jacobs-Lorena M., 1999. J. Mol. Evol. 48, 341-347.

Shen Z.C. and Jacobs-Lorena M., 1997. J. Biol. Chem. 272, 28895-28900.

Shetty B., Kosa M., Khalil D. et al., 1996. Antimicrob. Agents Chemother. 40, 110–114.

Shieh S., Kurumbail R. et al., 1996. Nature 383, 279–282.

Shinshi H., Mohnen D. and Meins F., 1987. Proc. Natl. Acad. Sci. USA 84, 89-93.

Shiomi K., Arai N. et al., 2000. Tetrahedron Lett. 41, 2141-2143.

Sielecki R, Fujinanga M., Read R.J. and James M.N.G., 1991. J. Mol. Biol. 219,671–692.

Silva A.M., Lee A.Y. et al., 1996. Proc. Natl. Acad. Sci. USA 93, 10034–10039.

Silva C.P. and Xevier-filho J., 1991. Comp. Biochem. Physiol. 99B, 529-533.

Simoneau B., Lavallee P. et al., 1999. Bioorg. Med. Chem. 7, 489–508.

Skrbec D. and Romeo D., 2002. Biochem. Biophys. Res. Commun. 297, 1350–1353.

Skujins J.J., Potgieter H.J. and Alexander M., 1965. Arch. Bioch. Biophys. 111, 358-364

Somers P.J.B., Yao R.C. et al., 1987. J. Antibiot. 40, 1751-1756.

Song M., Rajesh S., Hayashi Y. et al., 2001. Bioorg. Med. Chem. Lett. 11, 2465–2468.

Soto-Gil R.W. and Zyskind J.W., 1984. In, Zikakis J.P., (Ed.), Chitin, Chitosan, and related enzymes pp. 209-223. Academic Press, New York.

Southworth M.W., Fuhrman J.A. et al., 1996. Gene 177, 55-8.

Spindler K., 1976. Insect Biochem. 6, 663-667.

Staib P., Kretschmar M. et al., 2000. Proc. Natl. Acad. Sci. U.S.A. 97, 6102.

Stewart K. and Abad-Zapatero C., 2001. Curr. Med. Chem., 4726.

Stintzi A., Heitz T. et al.,1993. Biochimie. 75, 687-706.

Stoyachenko I.A., Varlamov V.P. and Davankov V.A., 1994. Carbohyd. Polym.24,47-54.

Strauss O.H., and Goldstein A.J., 1943. Gen. Physiol. 26, 559-585.

Stubbs M.T. and Bode W., 1993. Thromb. Res. 69, 1–53.

Suguna K., Padlan E.A. et al., 1987. Proc. Natl. Acad. Sci. U.S.A. 84, 7009-7013.

Symersky J., Monod M. and Foundling S.I., 1997. Biochemistry 36, 12700–12710.

Szedlacsek S.E. and Duggleby R.G., 1995. Methods Enzymol. 249, 144-180.

Szelke M., Leckie B. et al., 1982. Nature 299, 555–557.

Tabudravu J.N., Eijsink V.G.H. et al., 2002. Bioorg. Med. Chem. 10, 1123-1128.

Takahashi K., 1995. In, Aspartic Peptidases Structure, Function, Biology and Biomedical Implications, Plenum Press, New York.

Takayanagi T., Ajisaka K. et al., 1991. Biochim. Biophys. Acta 1078, 404-410.

Talekar N.S., 1992. Proceedings of the Second International Workshop, Asian Vegetable Research and Development Center, Taiwan, 603.

Tanaka R.D., Clark J.M. et al., 1995. Int. Arch. Allergy Immunol. 107, 408–409.

Tang J., 1977. In, Acid Proteases, Structure, Function, and Biology, New York, Plenum Press.

Tang J., 1979. Mol. Cell Biochem. 26, 93–109.

Tantimavanich S., Pantuwatana S. et al.,1997. J. Gen. Appl. Microbiol. 43, 341-7.

Tarentino A.L. and Maley F., 1974. J. Biol. Chem. 249, 811-817.

Tellam R.L., 1996. In: Lehane M.J. and Billingsley P.F. (eds.), Biology of the Insect Midgut, pp. 86-114. Cambridge, Chapman and Hall.

Tellam R.L., Smith D.H. and Willadsen P., 1992. In: Yong W.K., (ed.), Animal Parasite Control Utilizing Biotechnology, 303-331. Boca Raton, CRC Press.

Terayama H., Takahashi S. and Kuzuhara H., 1993. J. Carbohyd. Chem. 12, 81-93.

Terwisha van Scheltinga A.C. et al., 1994. Structure, 2, 1181-1189.

Tews I., Perrakis A. et al., 1996. Nat. Struct. Biol. 3, 638-648.

Tews I., van Scheltinga A.C.T. et al., 1997. J. Am. Chem. Soc. 119, 7954-7959.

Tews I., Vincentelli R. et al., 1996. Gene 170, 63-7.

Thaisrivongs S. and Strobach J., 1999. Biopolymers 51, 51–58.

Thaisrivongs S., 1989. Drug News Prospect. 1, 11-16.

Thaisrivongs S., 1994. Ann. Rep. Med. Chem. 29, 133.

Thompson P., Higgins D. and Gibson T., 1994. Nucelic Acids. Res. 22, 4673–4680.

Tom R.A. and Carroad P.A., 1981. J. Food. Sci. 46, 646-647.

Tomasselli A.G. and Heinrikson R.L., 2000. Biochim. Biophys. Acta 1477, 189.

Torruella M., Gordon K. and Hohn T., 1989. EMBO J. 8, 2819–2825.

Tossi A., Antcheva N. et al., 1999. Prot. Pep. Lett. 6, 145.

Tossi A., Antcheva N., Romeo D. and Miertus S., 1995. Peptide Res. 8, 328.

Tossi A., Bonin I. et al., 2000. Eur. J. Biochem. 267, 1715.

Trejo-Estrada S.R., Paszczynski A. et al., 1998. J. Ind. Microbiol. Biotechnol.21, 81-90.

Tsujibo H., Orikoshi H. et al., 1993. J. Bacteriol. 175, 176-181.

Turner R.T., Koelsch G. et al., 2001. Biochemistry 40(34), 10001–10006 .

Turner S., Strohbach J., Tommasi R. et al., 1998. J. Med. Chem. 41, 3467–3476.

Umezawa H., Aoyagi T. et al., 1970. J. Antibiot. (Tokyo) 23, 259-262.

Umezawa H., Takita T. and Shiba T., 1978. "Bioactive Peptides Produced by Microorganisms" Halsted, New York.

Usui T., Matsui H. and Isobe K., 1990. Carbohydr. Res. 203, 65-77.

Vaaje-Kolstad G., Houston D.R. et al., 2004. BBA-Proteins Proteomics 1696, 103-111.

Vacca J., Dorsey B. et al., 1994. Proc. Natl. Acad. Sci. USA 91, 4096–4100.

Vacca J.P. and Condra J.H., 1997. Drug Discov. Today 2, 261.

van Aalten D.M.F., Komander D. et al., 2001. Proc. Natl. Acad. Sci. USA 98, 8979-8984.

van Scheltinga T.A., Armand S. et al., 1995. Biochemistry 34, 15619-15623.

Vassar R., Bennet B.D. et al., 1999. Science 286, 735–741.

Veerapandian B., Cooper J. et al., 1992. Protein Sci. 1(3), 322–328.

Velazquez-Campoy A., Luque I. et al., 2000. Protein Sci. 9, 1801-1909.

Venegas A., Goldstein J.C. et al., 1996. Mol. Biochem. Parasitol. 78, 149-159.

Verissimo P., Faro C. et al., 1996. Eur. J. Biochem. 235, 762–768.

Villagomez–Castro J.C., Pedraza–Reyes M. et al., 1993. In: Muzzarelli R.A.A., (ed), Chitin Enzymology. Ancona, Eur Chitin Soc. 311-22.

Vinetz J.M., Dave S.K. et al., 1999. Proc. Natl. Acad. Sci. USA 96, 14061-14066.

Vinetz J.M., Valenzuela J.G. et al., 2000. J. Biol. Chem. 275, 10331-10341.

von Heijne G., 1990. J. Membr. Biol. 115, 195-201.

Vorgias C.E., 1997. In: Muzzarlli R.A.A. and Peter M.G (eds.), chitin handbook, pp 353-358, Europian Chitin Society.

Vyas P.R. and Deshpande M.V., 1989. J. Appl. Gen. Microbiol. 35, 343-50.

Vyas P.R. and Deshpande M.V., 1991. J. Appl. Gen. Microbiol. 37, 267-75.

Vyas P.R., 1991. Pune, submitted to University of Pune,. Ph.D. thesis.

Wacher V.J., Silverman J.A. et al., 1998. J. Pharm. Sci. 87, 1322–30.

Walsh K.A., 1970. In: Perlmann G.E. and Lorand L. (eds.), Methods in Enzymology, Academic Press, New York, 19, pp. 41-63.

Wang J.L. and Edelman G.M., 1971. J. Biol. Chem. 246, 1185.

Wang X., Ding X. et al., 1996. Insect Biochem. Mol. Biol. 26, 1055-1064.

Ward M. and Kodama K.H., 1991. In: Dunn B.M. (Ed.), Plenum Press, New York, pp. 149-160,

Watanabe T., Kobori K. et al., 1993. In, Muzzarelli R.A.A., (ed). Chitin Enzymology. Ancona, Eur. Chitin. Soc. 329-36.

Watanabe T., Oyanagi W., Suzuki K. and Tanaka H., 1990. J. Bacteriol. 172, 4017-4022.

Watanabe T., Suzuki K. et al., 1990. J. Biol. Chem. 265, 15659-15665.

Watanalai P., Srisurang T. et al., 1997. Biotechnol Sustainable Util Biol Resource Trop.11, 252-8. (CA 1999, 130:181532).

Weinberger M. and Hendeles L., 1996. N. Engl. J. Med. 334, 1380-1388.

West M.L. and Fairlei D.P., 1995. Trend. Pharmacol. Sci. 16, 67–75.

Westling J., Cipullo P. et al., 1999. Protein Science 8 (10), 2001-2009.

White P., Cordeiro M. et al., 1999. J. Biol. Chem. 274, 16685–16693.

Whitten J.M., 1964. J. Insect Physiol.10, 447-469.

Wieman K.F.S. and Nielsen S.S., 1987. Comp. Biochem. Physiol. 89B, 419-426.

Williams J.W. and Morrison J.F., 1979. Methods Enzymol. 63, 437-467.

Wiwat C., Lertcanawanichakul M. et al., 1996. Gene 179,119-26.

Wlodawer A. and Erickson J.W., 1993. Annu. Rev. Biochem. 62, 543–585.

Wlodawer A., 2002. Annu. Rev. Med. 53, 595–614.

Wolfe M.S., Xia W. et al., 1999. Biochemistry 38, 4720–4727.

Wolfenden R., 1976. Annu. Rev. Biophys. Bioeng. 5, 271-306.

Wortman A.T., Somerville C.C. and Colwell R.R., 1986. Appl. Env. Micro.52, 142-145.

Wrighta M.K., Brandta S.L. et al., 2006. J. Insect Physiol. 52, 717–728.

Yan J., Cheng Q., et al., 2002. Insect Biochem. Mol. Biol. 32, 979-989.

Yan S., Sameni M. and Sloane B.F., 1998. Biol. Chem. 379, 113–23.

Yanagi S.O., Takabe I., 1984. Appl. Microbiol. Biotechnol. 19, 58-60.

Yiallouros I., Vassiliou S. et al., 1998. Biochem. J. 331, 375-379.

Yoshimura T., Kamataki T. and Miura T., 1990. Anal. Biochem. 188, 132-135.

Yoshioka K., Honma H. et al., 1990. EMBO J. 9, 535–541.

Yu M.Y. and Chang S.T., 1987. Appl. Microbiol. Biotechnol. 3,161-167.

Yuasa Y., Shimojo H. et al., 1975. J. Natl. Cancer Inst. 54, 1255–1256.

Zechel D.L. and Withers S.G., 2001. Curr. Opin. Chem. Biol. 5, 643-649.

Zhang Z., ElSohly H. et al., 2002. J. Natural Prod. 65, 979–985.

Zhou Z.Y., Sakuda S. and Yamada Y., 1992. J. Chem. Soc., Perkin Trans. 1, 1649-1652.

Zhou Z.Y., Sakuda S., Kinoshita M. and Yamada Y., 1993. J. Antibiot. 46, 1582-1588.

Zhu X., Zhang H. et al., 2001. Insect Biochem. Mol. Biol. 31, 1221-1230.

Zhu Z., Zheng T. et al., 2004. Science, 304, 1678-1682.

Zielkowski R. and Spindler K., 1978. Insect Biochem. 8, 67-71.

Zikakis J.P., 1989. In: Whitaker J.R., Sonnet P.E., (eds). Biocatalysts in Agricultural Biotechnology, ACS Symposium Series 389. Washington, DC, Am. Chem. Soc. p. 116-26.